MTI-70TR15

EVAPORATIVE PROCESSES IN SUPERHEATED FORCED CONVECTIVE BOILING

by

J. H. Vohr

December 1970

NO. MTI-70TR15

DATE: December 31, 1970

TECHNICAL REPORT

EVAPORATIVE PROCESSES IN SUPERHEATED FORCED CONVECTIVE BOILING

by

J. H. Vohr

Author(s)

Approved

Approved

Prepared for

NASA Headquarters
Washington, D. C.

Prepared under

Contract No. NASw-1705

MTI
MECHANICAL TECHNOLOGY INCORPORATED

968 ALBANY - SHAKER ROAD — LATHAM, NEW YORK — PHONE 785-0922

FOREWORD

The work described in this report was performed by Mechanical Technology Incorporated under NASA Contract NASw-1705. The overall objective of this contract was to develop a comprehensive dynamical theory of forced-convection boiling in liquid metals. This report covers the second aspect of this study; namely, the evaporation rates for various thermo-hydraulic processes in forced convective boiling with superheat.

The work was done under the technical management of Mr. S. V. Manson, NASA Headquarters, Nuclear Power Systems.

TABLE OF CONTENTS

INTRODUCTION

The combination of excellent thermal conductivity, high vaporization temperature and moderate vapor pressure possessed by alkali metals makes them very attractive for use as working fluids for Rankine cycle space power systems. Consequently, considerable effort has been devoted recently toward development of once-through alkali metal boilers in which the liquid metal enters subcooled, is vaporized and departs as saturated or superheated vapor. Much of the work to date has concentrated on boilers for potassium and sodium, and considerable attention has been paid to the problem of achieving stability of operation of such boilers.

A number of traditional instability mechanisms for boiling flow have been recognized for some time, e.g. "Ledinegg Excursions," and liquid metal boilers are subject to these instabilities as well as are water boilers. The problem of the stability of liquid metal boilers, however, is further complicated by the fact that liquid metals can exhibit very large degrees of superheating before inception of boiling. This makes dynamic analysis of boiling liquid metal flow quite difficult because one can no longer assume that the flow is in thermodynamic equilibrium. Moreover, the superheating of liquid metals appear to give rise to a unique type of flow instability associated with drastic flow regime changes in the boiling channel. This instability is of the following nature.

When power input to the heated length of a liquid metal boiler is steadily increased from zero, a point is reached when the flow temperature at the exit of the heated length reaches saturation temperature. Due to the tendency of liquid metals to superheat in the liquid phase, further increase in power often does not result in inception of boiling, but rather leads to the condition that superheated flow exits from the heated length. As power is further increased, however, a point is reached where the degree of superheat at the exit is sufficiently large such that nucleation of vapor bubbles will occur and boiling will commence. The boiling will then tend to propagate upstream into superheated liquid, causing a sudden change of flow regimes and resulting in undesirable rapid temperature fluctuations in the boiling channel. The vapor liquid interface then can (a) reach a stable position, (b) oscillate within a finite zone, or (c) be swept back

out of the boiler to reenter later as superheating again accumulates. The latter two modes are, of course, deemed unstable and are to be avoided if possible. Which mode occurs is governed by the thermo-hydraulic characteristics of the boiler and its associated flow loop.

Because of the technological importance of liquid metal boilers, an analytical program was undertaken at M.T.I. under NASA Contract Number NASw-1705 directed toward obtaining solutions for the thermo-hydraulic liquid metal boiler stability problem. The crux of this study is the problem of the nonequilibrium behavior of liquid metal flows.

The program was carried out in two phases. The first phase is concerned with the prediction of incipient boiling, and the corresponding study has been documented in a topical report, MTI-69TR45, "A Review of Criteria for Predicting Incipient Nucleation in Liquid Metals and Ordinary Fluids," by J.H. Vohr and T. Chiang [Ref. 41].

This document is the second topical report of the subject contract and is concerned with the various vaporization processes subsequent to incipient boiling in the forced convective flow of a superheated liquid. In particular, approximate derivations in closed form for the growth of a submerged single vapor bubble and for the propagation of a large central void in a forced convective flow are carried out. In addition, general expressions for the vapor generation rate are constructed not only for above two processes but also for the annular and the dispersed flow regimes.

VOID DYNAMICS

GROWTH RATE OF BUBBLE IN SUPERHEATED LIQUID

Background

The growth rate of a vapor bubble in an infinite, superheated liquid is a basic physical phenomenon which plays a role in many fluid mechanical and heat transfer processes. As such, it has been the object of a considerable amount of analytical study. Solutions for bubble growth rate have been obtained which consider that this growth is controlled solely by hydrodynamic forces, by heat transfer, by mass transfer, or, more generally, by a combination of these effects. These solutions will be cited below in the course of a general discussion of the physical problem of the growth of a vapor bubble.

Consider a vapor bubble of radius R_v in an infinite liquid medium as shown in Figure 1. Let us assume that P_v, the pressure inside the bubble, is due entirely to the vapor pressure of the liquid surrounding the bubble i.e. no noncondensible gases are present in the bubble. Let us also assume that the bubble is in a condition of static equilibrium at $R_v = R_o$ such that the vapor pressure inside the bubble is sufficiently greater than the liquid pressure P_∞ so as to just balance the surface tension force $2\sigma/R_o$ i.e.

$$P_v = P_\infty + 2\sigma/R_o \tag{1}$$

For P_v to be greater than P_∞ requires that the liquid at the bubble surface be superheated by an appropriate amount

$$\Delta T_s = T_\infty - T_{sat} \tag{2}$$

where T_∞ is the temperature of the liquid and T_{sat} is the saturation temperature corresponding to P_∞.

Let us denote the temperature in the liquid just at the bubble surface as T_L. Let us further denote P_L^* as the saturation vapor pressure corresponding to T_L. At the initial condition of the static equilibrium we have

$$T_L = T_\infty \; ; \quad P_v = P_L^* \tag{3}$$

This equilibrium condition is, however, unstable because if the bubble radius is increased slightly i.e. R_v becomes slightly greater than R_o, then the pressure inside the bubble will be greater than that required to maintain equilibrium against surface tension forces and the bubble will commence to expand. As this occurs, three distinct mechanisms come into play to control the growth rate of the bubble. These are: 1. Inertia forces associated with acceleration of the liquid radially outward from the expanding bubble surface, 2. Heat transfer associated with the necessity of vaporizing liquid to fill the growing vapor bubble, and 3. Mass transfer, also associated with the necessity of vaporizing liquid into the bubble. Let us see how each of these mechanisms acts.

First, if the liquid had infinite thermal conductivity and a very high coefficient of vaporization, then T_L would remain equal to T_∞ and no significant difference between P_v and P_L^* would be required to produce vaporization into the bubble. Hence, P_v would remain constant at the saturation vapor pressure corresponding to T_∞ throughout the growth of the bubble and growth rate would be controlled entirely by the force required to accelerate liquid radially outward by the expanding bubble surface. The solution for bubble growth rate under these conditions was obtained by Rayleigh (Ref. 2) and will be described in the next section.

If the thermal conductivity of the liquid is finite, then the necessity of providing heat transfer to the growing bubble to maintain vaporization will require that T_L decrease below T_∞. If thermal conductivity of the liquid is sufficiently low, then the bubble growth rate will be substantially controlled by this heat transfer process. Under these conditions, P_v will be maintained at a value very near to that required to just overcome P_∞ and surface tension forces i.e.

$$P_v \cong P_\infty + \frac{2\sigma}{R_v} \tag{4}$$

and T_L will be the value of saturation temperature corresponding to P_v. The problem of calculating bubble growth under this thermally controlled condition becomes, essentially, a problem of calculating the rate of heat transfer to a growing spherical surface with boundary temperature T_L given by the condition cited above. Rate of bubble growth is governed, of course, by the rate of liquid vaporized by this heat transfer.

Solutions to bubble growth rate where growth is limited by the heat conduction in the liquid have been obtained by a number of investigators [Refs. 3,4,5,6,7,8]. The solutions obtained are valid for what is referred to as the asymptotic later stages of growth where surface tension effects are no longer significant. Under these condtions, P_v can be set approximately equal to P_∞ (see Eq. (4)).

As has been pointed out by Theofanous, et al [Ref. 9], the growth rate of a vapor bubble tends to be governed more by inertia forces during its early stages of growth and more by heat transfer during its later stages. For liquid metals, however, vapor bubble growth tends to remain dominated by inertia forces or mass transfer resistance throughout all of the significant growth period of the bubble. Hence, analyses which consider that the growth rate is controlled solely by heat transfer are not applicable to liquid metals.

A third possibility exists wherein the growth of a vapor bubble could be controlled solely by mass transfer considerations. The net evaporation rate from the inner surface of the bubble can be expressed approximately by the relationship**

$$\dot{m} = \frac{4\pi R_v^2 C}{\left(\frac{2\pi R}{g_c}\right)^{\frac{1}{2}}} \left[\frac{P_L^*}{\sqrt{T_L}} - \frac{P_v}{\sqrt{T_v}}\right] \tag{5}$$

where R = gas constant, C = vaporization coefficient, and T_v is the temperature of the vapor within the bubble. The assumptions involved in this relationship are that the coefficients for evaporation and for condensation are numerically equal, that the vapor molecules have a Maxwellian distribution, and that the absolute rate of vaporization is the same in a vacuum as it is at pressure P_v. This equation is based on a model which considers vaporization to be the net result of molecules diffusing toward the interface at a statistical mass rate per unit area given by $\rho_v\sqrt{\frac{R\,T_v\,g_c}{2\pi}}$, and molecules diffusing away from the interface at a statistical mass rate per unit area given by $\rho_v^*\sqrt{\frac{R\,T_L\,g_c}{2\pi}}$, where $\rho_v^* = \frac{P_L^*}{R\,T_L}$. A value of C = 1 implies that all molecules which drift toward the interface are absorbed there (condensed) while new molecules are freely supplied (vaporized) at the interface to diffuse away at rate $\rho_v^*\sqrt{\frac{R\,T_L\,g_c}{2\pi}}$. A value of C < 1 implies that these mechanisms of condensation and vaporization are equally suppressed.

**This is the relationship used in reference 9.

From Eq. (5) we see that if the vaporization coefficient is appreciably less than 1, a significant difference between P_L^* and P_v must be maintained in order to produce mass flux into the growing bubble. For C very small, bubble growth rate will be controlled by mass transfer rather than by heat transfer or by hydrodynamic forces. Under these circumstances, T_L will approach T_∞ and P_v will be given by Eq. (4). Substitution of these values for T_L and P_v into Eq. (5) above will then yield an expression appropriate for bubble growth rate controlled entirely by mass transfer considerations.

In physically real situations, bubble growth rate is affected by all three mechanisms: liquid inertia, heat transfer, and mass transfer. Analyses of bubble growth rate in which all of these effects are taken into account have been performed by Theofanous, et al [Ref. 9], by Bornhorst and Hatsopoulas [Ref. 10], and by Waldman and Houghton [Ref. 11]. In each of these analyses, however, solutions for growth rate were obtained only by numerical integration of nonlinear differential equations using a digital computer. Hence none of these analyses provide a very convenient means for the engineer to calculate bubble growth rates for particular situations of interest.

In this present report there is developed an analysis which, by dint of a few reasonable simplifying assumptions, allows one to obtain a closed form algebraic solution for bubble growth rate including effects of liquid inertia, heat transfer and mass transfer. The solution is valid for all phases of bubble growth rate from initial phase to final phase, and is found to agree well with more exact analyses of other investigators. A description of this analysis follows below.

Analysis

The present analysis of bubble growth rate follows, in some basic respects, the analysis of Theofanous, et al in that it employs the same physical assumptions concerning mass transfer relationships and liquid temperature profiles that these authors used. In the Theofanous approach, however, there are obtained five nonlinear ordinary differential equations in time which must be integrated simultaneously from an initial condition to obtain bubble radius as a function of time. In the present analysis, approximate algebraic equations rather than differential equations are written which must be satisfied at each instant of bubble growth. A simultaneous solution to these algebraic relationships provides a closed form algebraic expression for $\dot{R}_v$, the rate of change of bubble radius, which may be solved for any particular instant in the growth cycle of a bubble. The analysis proceeds as follows:

A first condition which must be satisfied at any instant in the growth cycle of a vapor bubble is that, due to conservation of energy, the work done by the bubble on the surrounding liquid as the bubble expands from its initial condition of equilibrium ($R_v = R_o$) must equal the kinetic energy imparted to the liquid. According to Rayleigh [Ref. 2], the kinetic energy of an infinite body of liquid surrounding an expanding bubble of radius R_v and surface velocity $\dot{R}_v$ is given by

$$K.E = \frac{2\pi\rho_L \dot{R}_v^2 R_v^3}{g_c} \tag{6}$$

The net work done by the bubble on the liquid in expanding from initial radius R_o is

$$\text{Work} = 4\pi \int_{R_o}^{R_v} R_v^2 \left(P_v - \frac{2\sigma}{R_v} - P_\infty\right) dR_v \tag{7}$$

In the Rayleigh solution for growth rate, heat transfer resistance in the fluid is neglected and it is assumed that the vapor pressure P_v inside the bubble is constant and in thermodynamic equilibrium with the liquid at temperature T_∞ i.e. P_v is the saturation vapor pressure corresponding to T_∞. Let us denote this value of vapor pressure as $P_{L\infty}^*$. With P_v constant at $P_{L\infty}^*$, Eq. (7) integrates to give

$$\text{Work} = \frac{4\pi}{3} R_v^3 \left\{ \left[P_{L\infty}^* - P_\infty\right] \left(1 - \frac{R_o^3}{R_v^3}\right) - \frac{3\sigma}{R_v} \left(1 - \frac{R_o^2}{R_v^2}\right) \right\} \tag{8}$$

Equating (6) to (8), and solving for $\dot{R}_v$, we obtain

$$\dot{R}_v = \sqrt{\frac{2g_c}{3\rho_L} \left\{ \left(P_{L\infty}^* - P_\infty\right) \left(1 - \frac{R_o^3}{R_v^3}\right) - \frac{3\sigma}{R_v} \left(1 - \frac{R_o^2}{R_v^2}\right) \right\}} \tag{9}$$

which is the so-called "extended"**Rayleigh solution for bubble growth rate.

**Rayleigh did not consider surface tension in his original analysis.

This solution is not used in the present analysis. Instead, a more general but approximate form for Eq. (9) is obtained below which permits taking account of heat and mass transfer.

If heat and mass transfer resistance is considered, then one finds that as R_v increases from R_o, P_v will not remain constant but will decrease monotonically from $P_{L\infty}^*$.

In particular, from the results obtained in Ref. 9, we expect P_v to decrease rapidly at first as R_v increases from R_o, but then to decrease much less rapidly with R_v as R_v/R_o becomes on the order of 3 or 4. This behavior of P_v is shown schematically in Fig. 2.

Examining Eq. (7), we note that the factor R_v^2 in the integrand gives heavy weighting to values of P_v taken at larger values of R_v i.e. at values of R_v near the end of the range of integration rather than at values of R_v near R_o. Considering this, plus the anticipated behavior of P_v with R_v as shown in Fig. 2, it seems reasonable to treat the variable P_v in Eq. (7) as a constant having the value that P_v obtains at the end of the range of integration. Making this approximation in evaluating Eq. (7) we obtain

$$\text{Work} \simeq \frac{4\pi}{3} R_v^3 \left\{ [P_v - P_\infty] \left(1 - \frac{R_o^3}{R_v^3}\right) - \frac{3\sigma}{R_v} \left(1 - \frac{R_o^2}{R_v^2}\right) \right\} \tag{10}$$

and our resultant expression for $\dot{R}_v$ is

$$\dot{R}_v \simeq \sqrt{\frac{2g_c}{3\rho_L} \left\{ (P_v - P_\infty) \left(1 - \frac{R_o^3}{R_v^3}\right) - \frac{3\sigma}{R_v} \left(1 - \frac{R_o^2}{R_v^2}\right) \right\}} \tag{11}$$

In Eqs. (10) and (11), P_v is the as yet unknown vapor pressure in the bubble at the time when the bubble radius is R_v.

We next consider the thermal relations that must be satisfied during the growth process of the bubble. The energy equation for the growing vapor bubble is derived in Appendix III where it is obtained that

$$\frac{dU_v}{dt} + \frac{P_v}{J}\frac{dV}{dt} = \frac{dQ}{dt} + u_L \dot{m} + \frac{1}{J}\frac{P_L}{\rho_L}\dot{m} \tag{12}$$

where $\frac{dU_v}{dt}$ is the time rate of change of the total internal energy inside the bubble, V is the volume of the bubble, $\frac{dQ}{dt}$ is the rate of heat transfer into the bubble, u_L is the specific internal energy, P_L is the pressure of the liquid just at the bubble surface, and J is the conversion factor to change Btu's to ft-lb_f. In this present analysis, we will use the following approximate expression for this energy equation

$$\frac{dQ}{dt} \cong h_{fg}\, 4\pi\rho_v\, R_v^2\, \dot{R}_v . \tag{13}$$

In essence, Eq. (13) states that the heat flux into the bubble can be predominately accounted for by considering the heat of vaporization associated with the increase in mass of the bubble, neglecting the changes in mass associated with changes in vapor density. The specific terms that are neglected in going from Eq. (12) to Eq. (13) are indicated in Appendix III where Eq. (13) is derived.

In order to express the heat flux $\frac{dQ}{dt}$, we shall assume a quadratic form for the temperature profile in the liquid surrounding the bubble as was done in Ref. 9.*

$$T = T_\infty + (T_L - T_\infty)\left(\frac{R_L - r}{R_L - R_v}\right)^2 \tag{14}$$

where $R_L - R_v$ is the thickness of the thermal boundary layer surrounding the growing bubble. R_L is an unknown variable yet to be determined. Using Eq. (14)

*The significance of this assumption for the form of the temperature profile is discussed fully in Ref. 9. The conclusion reached there is that this assumed form is quite adequate for the purpose of determining bubble growth rate.

the rate of heat transfer into the bubble can be written as

$$\frac{dQ}{dt} = 4\pi R_v^2 K_L \left.\frac{dT}{dr}\right|_{r = R_v} = -8\pi R_v^2 K_L \frac{(T_L - T_\infty)}{(R_L - R_v)} \tag{15}$$

Substituting Eq. (15) into Eq. (13) one obtains

$$2K_L \frac{(T_\infty - T_L)}{(R_L - R_v)} \cong h_{fg} \rho_v \dot{R}_v. \tag{16}$$

A further thermal relation that must be satisfied during the growth rate of a bubble in an infinite medium is that the total heat transferred to the growing bubble must come from the cooling of the superheated liquid surrounding the bubble. Expressed mathematically, this condition is

$$\int_0^t \frac{dQ}{dt}\, dt = \int_{R_v(t)}^{R_L(t)} (C_p)_L \rho_L 4\pi r^2 (T_\infty - T)\, dr \tag{17}$$

where T is given by Eq. (14). In general, the quantity $(R_L - R_v)/R_v$ is much less than unity.* Therefore, we can make the approximation that $r \cong R_v$ in the integral on the right hand side of Eq. (17). Making this approximation, and substituting for dQ/dt by means of Eq. (13) and for T by means of Eq. (14) one obtains

$$h_{fg} 4\pi \int_0^t \rho_v R_v^2 \dot{R}_v\, dt = C_p \rho_L 4\pi R_v^2 \frac{(T_\infty - T_L)}{(R_L - R_v)^2} \int_{R_L}^{R_v} (R_L - r)^2\, dr \tag{18}$$

*This assumption is based on data from Ref. 9.

One should note that in obtaining Eq. (18) we make use of the fact that the integral on the right hand side of Eq. (17) is to be evaluated with t held constant at the value corresponding to the upper limit of the integral on the left hand side of Eq. (17). Hence R_v is a constant in the expression on the right hand side of Eq. (18) and could be brought outside the integral.

Neglecting the variation of ρ_v with time, which is consistent with the assumptions involved in obtaining Eq. (13), we can integrate Eq. (18) to obtain

$$h_{fg}\ \rho_v\ R_v \left(1 - \frac{R_o^3}{R_v^3}\right) = C_P\ \rho_L\ (T_\infty - T_L)\ (R_L - R_v) \tag{19}$$

where R_o is the radius of the vapor bubble at t = 0 and R_v is the radius of the bubble at time t.

A fourth condition to be satisfied during bubble growth pertains to the rate of vaporization mass transfer. As noted earlier, the net mass evaporation rate from the inner surface of the bubble was expressed approximately by Eq. (5). In our present analysis, we make the further approximation that the temperatures T_L and T_v can be replaced in Eq. (5) by the temperature T_∞. With this approximation we obtain

$$\dot{m} \cong \frac{4\pi\ R_v^2 C}{\left[2\pi \frac{R}{g_c}\ T_\infty\right]^{\frac{1}{2}}}\ (P_L^* - P_v) \tag{20}$$

Consistent with the approximations made in obtaining Eq. (13), $\dot{m}$ may be written as

$$\dot{m} \cong \rho_v\ 4\pi R_v^2\ \dot{R}_v \tag{21}$$

Equating Eqs. (21) and (20) we obtain

$$\dot{R}_v = \frac{C}{\rho_v}\sqrt{\frac{g_c}{2\pi R T_\infty}}\ (P_L^* - P_v) \tag{22}$$

A further relationship required to solve our system of equations for $\dot{R}_v$ is a relationship between the difference in saturation vapor pressures, $P_{L\infty}^* - P_L^*$, and the difference in temperatures $T_\infty - T_L$. In general, this relationship can be approximated quite well over a narrow temperature range by writing

$$P_{L\infty}^* - P_L^* \cong \kappa\ (T_\infty - T_L) \tag{23}$$

where $P_{L\infty}^*$ denotes the saturation vapor pressure corresponding to T_∞ and where κ is the <u>average</u> slope of the curve of vapor pressure versus temperature over the range from T_{sat} to T_∞, i.e.

$$\kappa \equiv \frac{P_{L\infty}^* - P_\infty}{T_\infty - T_{sat}} \tag{24}$$

Equations (11), (16), (19), (22), and (23) constitute a sufficient number of algebraic equations for us to obtain solutions for the unknown variables $\dot{R}_v$, P_v, P_L^*, T_L, and R_L. The algebraic work required to achieve this is as follows:

First by eliminating $(R_L - R_v)$ between Eqs. (16) and (19) we obtain

$$(T_\infty - T_L)^2 = \frac{h_{fg}^2 \rho_v^2 R_v \dot{R}_v \left(1 - \frac{R_o^3}{R_v^3}\right)}{2C_V \rho_L K_L} \tag{25}$$

Substituting for $T_\infty - T_L$ in Eq. (23) from Eq. (25) yields

$$P_{L\infty}^* - P_L^* = \kappa h_{fg} \rho_v \left[\frac{R_v \dot{R}_v \left(1 - \frac{R_o^3}{R_v^3}\right)}{2C_V \rho_L K_L}\right]^{1/2} \tag{26}$$

Solve Eq. (26) for $\dot{R}_v$

$$\dot{R}_v = \frac{2(P_{L\infty}^* - P_L^*)^2 C_V \rho_L K_L}{\kappa^2 h_{fg}^2 \rho_v^2 R_v \left(1 - \frac{R_o^3}{R_v^3}\right)} \tag{27}$$

Set Eq. (27) equal to Eq. (22)

$$\frac{2(P_{L\infty}^* - P_L^*)^2 C_V \rho_L K_L}{\kappa^2 h_{fg}^2 \rho_v^2 R_v \left(1 - \frac{R_o^3}{R_v^3}\right)} = \frac{C}{\rho_v}\sqrt{\frac{g_c}{2\pi R T_\infty}}\,(P_L^* - P_v) \tag{28}$$

The density ρ_v in Eq. (28) can be expressed in terms of the pressure P_v by means of the perfect gas law

$$\rho_v = \frac{P_v}{RT_v} \tag{29}$$

Unfortunately, this substitution introduces a new unknown variable T_v, the temperature of the vapor inside the bubble. Theofanous et al solved this problem by considering simultaneously the mechanisms for mass and heat transfer kinetics. Here we shall simply use the approximation

$$\rho_v \simeq \frac{P_v}{RT_{sat}} \tag{30}$$

where T_{sat} is the saturation temperature corresponding to P_∞. T_{sat} is chosen as a temperature for evaluating ρ_v because an accurate evaluation of ρ_v is important only when growth rate is controlled by heat or mass transfer; and according to Ref. 9, if the growth rate is completely controlled by heat transfer then $T_v \rightarrow T_{sat}$.

Eq. (28) is a quadratic equation in P_L^*. Solving for P_L^* and substituting for ρ_v by means of Eq. (30) we obtain

$$P_L^* = P_{L\infty}^* + \frac{P_v\varphi}{2} - \sqrt{(P_{L\infty}^* - P_v)\,P_v\varphi + P_v^2\left(\frac{\varphi}{2}\right)^2} \tag{31}$$

where

$$\varphi = \frac{C\kappa^2 \quad h_{fg}^2 \quad R_v \left(1 - \frac{R_o^3}{R_v^3}\right)}{R^{3/2} T_{sat} T_\infty^{1/2} \left(\frac{8\pi}{g_c}\right)^{1/2} K_L C_V \rho_L} \tag{32}$$

Substituting Eq. (31) and (30) into Eq. (22) yields

$$\dot{R}_v = \frac{CRT_{sat}}{P_v}\sqrt{\frac{g_c}{2\pi RT_\infty}}\left[P_{L\infty}^* - P_v + \frac{P_v\varphi}{2} - \sqrt{(P_{L\infty}^* - P_v)P_v\varphi + P_v^2\left(\frac{\varphi}{2}\right)^2}\right] \tag{33}$$

Equating Eq. (33) to Eq. (11) to eliminate $\dot{R}_v$, we obtain, finally, after some rearranging

$$\frac{CRT_{sat}}{P_v}\left[P_{L\infty}^{*} - P_v + \frac{P_v\varphi}{2} - \sqrt{(P_{L\infty}^{*} - P_v)P_v\varphi + P_v^2\left(\frac{\varphi}{2}\right)^2} \right]$$

$$-\sqrt{\frac{4\pi RT_\infty}{3\rho_L}}\left\{(P_v - P_\infty)\left(1 - \frac{R_o^3}{R_v^3}\right) - \frac{3\sigma}{R_v}\left(1 - \frac{R_o^2}{R_v^2}\right)\right\} = 0 \qquad (34)$$

Eq. (34) is an algebraic equation implicitly relating the unknown bubble vapor pressure P_v to other known physical variables. It may be solved for P_v, and the resulting value for P_v substituted into either Eq. (33) or Eq. (11) to obtain the bubble growth rate $\dot{R}_v$.

A convenient means for solving Eq. (34) is by Newton-Raphson iteration. The solution scheme is described in Appendix I. The solution scheme is implemented by means of a simple computer program, a listing for which is also provided in Appendix I.

In addition to P_v and $\dot{R}_v$, two other quantities which are of interest to calculate are $T_\infty - T_L$, the temperature difference across the thermal boundary layer surrounding the growing vapor bubble, and $(R_L - R_v)$, the thickness of the thermal boundary layer. The first of these quantities may be obtained by combining Eq. (25) and (30)

$$T_\infty - T_L = \frac{h_{fg}\, P_v}{RT_{sat}}\sqrt{\frac{R_v \dot{R}_v}{2C_V\, \rho_L\, K_L}\left(1 - \frac{R_o^3}{R_v^3}\right)} \qquad (35)$$

The second of these quantities may be obtained by substituting Eq. (35) above in Eq. (19)

$$R_L - R_v = R_v\sqrt{\frac{2K_L}{C_V\, \rho_L\, R_v\, \dot{R}_v}\left(1 - \frac{R_o^3}{R_v^3}\right)} \qquad (36)$$

Results

Curves of bubble growth rate $\dot{R}_v$ versus dimensionless bubble radius ratio R_v/R_o as obtained from the present simplified closed form analysis are compared in Figs. 3 and 4 with corresponding curves obtained from the more exact numerical integration analysis of Theofanous et al [Ref. 9]. Figure 3 is for sodium at 14.7 psia with a superheat of 273 F while Fig. 4 is for water at 1.47 psia with a superheat of 4.81 F. In the case of sodium, agreement between the present analysis and that of [Ref. 9] is very good. For sodium, the initial bubble growth rate is controlled by fluid inertia forces for values of vaporization coefficient C = 1 and C = ∞*. This is evidenced by the close agreement of the curves labeled C = ∞ and C = 1 with the curve shown for the "extended" Rayleigh solution (Eq. (9)). At higher values of R_v/R_o, i.e., later in time in the growth cycle, heat transfer begins to exert an increasing important influence on growth rate resulting in a reduction in growth rate below that predicted by the "extended" Rayleigh solution.

For low values of the vaporization coefficient C, ($C < 10^{-1}$) the bubble growth rate begins to be increasingly limited by mass transfer considerations. However, even for values of C as low as 10^{-2}, agreement between the present analysis and that of Theofanous remains quite good. This indicates that the simplifying assumptions employed in arriving at Eqs. (10) and (20) of the present analysis are quite reasonable for this situation.

In Fig. 4, for low pressure water, there is a greater discrepency (up to ≃ 16 percent) between the bubble growth rates predicted by the present analysis and those predicted by the Theofanous analysis than was obtained in the case of sodium. Curves for the extended Rayleigh solution (growth entirely dominated by inertia effects) and the Scriven solution (growth entirely controlled by heat transfer effects) are also included in Fig. 4. Comparison of the results of the present analysis or the Theofanous analysis with these limiting solutions indicates

---

*Physically, C cannot be greater than unity. However, setting C = ∞ is a convenient mathematical way of neglecting mass transfer resistance.

that for water both inertial and thermal effects are significant in controlling growth rate throughout most of the growth process

To try to uncover the reason for the discrepency between the present work and the Theofanous predictions for growth rate in low pressure water, some of the simplifying assumptions made in the present analysis of heat transfer to the growing bubble were checked quantitatively for the case investigated. The first assumption to be checked was whether or not the terms within the brackets on the right hand side of Eq. (C-14) in Appendix III could, indeed, be neglected at the point of maximum growth rate which, for $C = \infty$, occurs at $R_v/R_o \cong 6$. Calculations based on the present analysis give:

$$(h_v - h_L)\ \rho_v\ \dot{R}_v = 6 \times 10^{-2}\ \frac{\text{Btu}}{\text{in}^2\text{-sec}}$$

$$\frac{R_v}{3}\ (h_v - h_L)\ \frac{d\rho_v}{dt} = -\ 6.6 \times 10^{-4}\ \frac{\text{Btu}}{\text{in}^2\text{-sec}}$$

$$\frac{R_v}{3}\ \rho_v\ \frac{dh_v}{dt} = -\ 9.1 \times 10^{-6}\ \frac{\text{Btu}}{\text{in}^2\text{-sec}}$$

$$\frac{R_v}{3}\ \frac{1}{J}\ \frac{dP_v}{dt} = -\ 3.7 \times 10^{-5}\ \frac{\text{Btu}}{\text{in}^2\text{-sec}}$$

Hence we see that neglect of the last three terms above compared with the first term is, indeed, justifiable.

Another simplifying assumption made in the present heat transfer analysis of a growing bubble was that the quantity $(R_L - R_v)/R_v$ is much less than unity. This assumption was used in deriving Eq. (19). From the present calculations for bubble growth in water, it was determined that $(R_L - R_v)/R_v$ was always less

than .06, and generally less than .02 throughout the growth of the bubble. Hence, the assumption that this is much less than unity should not lead to gross error.

The final simplifying approximation checked was the approximation that the variable P_v could be treated as a constant in the integration of Eq. (7). In checking this, it was found that although this is a reasonably accurate approximation for the situations where bubble growth rate is dominated by a single mechanism, either hydrodynamic forces, heat transfer or mass transfer, it is not very accurate for the case where heat transfer and hydrodynamic forces are both controlling the bubble growth process. In short, therefore, it is this approximation that is responsible for the discrepencies noted in Fig. 4. However, since the discrepencies noted are only on the order of 16 percent, it seems reasonable to conclude that the present approximate solution for bubble growth rate still constitutes a useful tool for bubble growth rate calculations, particularly in view of the relative simplicity it offers compared to other more exact solutions.

The present analysis of bubble growth rate can be used quite conveniently to obtain data for use with a constitutive equation for nonequilibrium vaproization of liquid metals in the bubble flow regime. This constitutive equation is considered later in this report. Looking at the bubble growth rate curves in Fig. 3, one sees that in the vicinity of the point of maximum growth rate for highly superheated sodium, growth rate remains fairly constant over a wide range of bubble radius, i.e. from $R_v/R_o = 10$ to say $R_v/R_o = 10{,}000$.* Noting that for this case, $R_o \cong 4 \times 10^{-5}$ in., we see that bubble growth rate can be considered to remain fairly constant for $0.0004 \leq R_v \leq 0.4$. Since a bubble radius of 0.4 inches represents a size which is on the order of the radius of typical once through liquid metal boiler tubes, it seems reasonable to say that once bubbles reached this size, the flow regime would change from bubble flow to some other transition regime between bubble flow and annular flow. Essentially, then, it

---

*The same is true for water but over a much more limited range of R_v/R_o.

seems quite adequate to consider bubble growth rate $\dot{R}_v$ to be constant throughout most of the meaningful part of the growth cycle and that the maximum value of $\dot{R}_v$ could be chosen as this characteristic growth rate. In line with this approach, curves are presented in Figs. 5, 6 and 7, showing the maximum value of bubble growth rate versus degree of superheat for water, potassium and cesium. Curves are presented in each figure for three values of vaporization coefficient C. These curves of characteristic growth may be useful in analyzing nonequilibrium vapor generation following inception of nucleation in superheated liquid metals.

The variation of maximum bubble growth rate with system pressure at constant superheat θ shows some interesting characteristics depending on the value chosen for C the vaporization coefficient. For large C ($C > 1$) in potassium, bubble growth rate is controlled entirely by fluid inertia effects, and the growth rate increases monotonically with system pressure due to the fact that the driving force for bubble growth, represented by the term $\kappa = (P_{L\infty}^{*} - P_L^{*})/(T_\infty - T_L)$, increases with system pressure. On the other hand, for very low values of C ($C < 10^{-2}$) bubble growth rate is controlled by mass transfer considerations, and tends to decrease with system pressure due to the fact that the vapor density, ρ_v, increases with pressure. For values of C between 1 and 10^{-2}, bubble growth rate demonstrates a maximum at some particular value of system pressure. This behavior is illustrated in Fig. 8.

From Fig. 6 or 7, one can see that for even modest degrees of superheating in liquid metals, bubble growth rates (assuming $C = 1$) are very rapid, so rapid in fact that one would question whether a bubble flow regime would ever be obtained in boiling metal flows. For example, consider a liquid potassium boiling flow with an inlet velocity of two feet per second ($\simeq$ 60 cm/sec). If the superheat at inception of nucleation is as little as 4 F or higher, which it is certainly likely to be, then the bubble growth rate will be equal to or greater than the inlet flow velocity and a vapor bubble, once initiated, would tend to grow to fill the duct before moving any significant distance down the duct. This situation does not tend to occur in boiling water flow, not because bubble growth rates in superheated water are not comparably high, but simply because bulk superheats of even this small order of magnitude tend not to develop in boiling

water flows.

Little information is available for determining values of the vaporization coefficient C for liquid metals. A discussion of experimental measurements of C for various fluids is given in Ref. 9. There it is noted that liquid metal studies reported by Griffith indicate that values of C for Hg, K and Na are 1 only at very low pressures and decrease with pressure to become as low as 5×10^{-2} at one atmosphere. However, considerable disagreement still exists concerning the interpretation of measurements of C.

In the case where bubble growth rate is greater than flow velocity, the possibility exists that flow would pass directly from an all liquid situation to an annular type flow regime. Associated with this type of situation is the question of the stability of the location of the beginning of such an annular flow regime. If a considerable degree of superheat were required to initiate nucleation, then the possibility exists that the point of beginning of the annular flow regime may move upstream into the superheated liquid preceding the point of inception of nucleation. This postulated changing of position of the beginning of an annular type flow regime without development of new nucleation sites on the wall of the heated duct we shall refer to as propagation of a central vapor void. An analysis of this potential mechanism is presented in the next section.

PROPAGATION OF CENTRAL VAPOR VOID INTO SUPERHEATED LIQUID

In this section is developed an approximate analysis of the dynamics of a central void in a boiling flow in which thermodynamic equilibrium is not necessarily maintained. The analysis is based on a simple "shock front" constitutive model for vapor generation into the central void. A particular dynamic situation is considered wherein the void develops from inception of boiling at the exit of a heated duct. This analysis contains, as a special case, the situation of a central void stably located at some point along the heated duct.

The constitutive equation for vapor generation for a central void under conditions of thermodynamic nonequilibrium is explicitly formulated in a later section.

The void propagation analysis presented in this section provides an example of how this constitutive relation is used.

Description of Problem

Consider the situation of a heated duct containing a flowing alkali metal where q, the heat input to the duct per unit length, is gradually increased to the point where incipient nucleation of boiling will occur at the exit of the duct. With alkali metals, it usually requires a substantial degree of superheat (as much as 100°F to 300°F) to produce incipient boiling. Hence, when boiling first does occur, very large vapor voids will be created almost instantaneously due to the very rapid growth of vapor bubbles in highly superheated liquid metals (see previous section on bubble growth rate). In the situation being considered, the liquid will be superheated for some distance upstream of the duct exit. Hence, there is a strong likli-hood that once incipient nucleation does occur, the vapor void generated will propagate upstream into superheated liquid by the mechanism of void growth rather then by the mechanism of having nucleation progress upstream along the wall of the duct.

Experimental evidence does suggest that once incipient nucleation does occur [Refs. 12 and 13] boiling propagates rapidly upstream to roughly the point where the liquid is at saturated temperature. Under some circumstances, however, boiling may not be

stably maintained at this location, but rather the boiling may be quenched, and the vapor void washed downstream, the liquid in the duct then becoming superheated again until incipient nucleation occurs at the duct exit and the process repeats itself. This cyclical instability is unique to forced convection boiling of liquid metals and represents, obviously, an undesirable operating condition for the boiler.

In the following pages of this report are developed the equations and relationships governing the propagation of a vapor void upstream or downstream in a heated duct from the instant in time when incipient nucleation first occurs at the exit of the duct. In the analysis, a number of simplifying assumptions are made to bring out the essential physical mechanisms. However, the basic analysis could readily be developed with a higher degree of accuracy or generality.

Analysis

Consider Fig. 9 which shows a vapor void in a heated duct moving with velocity v into a liquid flow which is moving downstream with instantaneous entrance velocity V_L'. We denote the instantaneous position of the nose of the void as $z = \ell$. We further denote the locations just upstream and just downstream of the nose of the void by $z = \ell^-$ and $z = \ell^+$, respectively. Associated with the very rapid change in flow cross section area in going from $z = \ell^-$ to $z = \ell^+$ there is a sharp change in pressure, which we shall denote simply as ΔP. The pressure change extending from $z = 0$ to $z = \ell^+$ we denote as $\overline{\Delta P}$ given by equation (37) below:

$$\overline{\Delta P} = - \frac{f \rho_L V_L'^2 \ell}{g_c D} - \frac{\rho_L \dot{V}_L' \ell}{g_c} + \Delta P \qquad (37)$$

The next expression we write is for the superheat, Θ, defined as the difference between the temperature in the liquid just ahead of the nose of the moving void, i.e., at $z = \ell^-$ and the saturation temperature corresponding to the pressure just downstream of the head of the bubble, i.e., at $z = \ell^+$. This Θ is the driving

force for vaporization into the head of the moving void. Using the approximate relation that

$$T_{sat} \cong (T_{sat})_{entrance} + \left(\frac{dT}{dp}\right)_{sat} \overline{\Delta P} \tag{38}$$

an expression may be written for θ as follows:

$$\theta = \frac{q\,\ell}{\rho_L \overline{V}_L A (C_P)_L} + \theta_{in} - \left(\frac{dT}{dp}\right)_{sat} \overline{\Delta P} \tag{39}$$

where q = the heat input per unit length of duct

A = cross sectional area of the duct

$(C_P)_L$ = specific heat of liquid

θ_{in} = temperature of liquid at entrance to duct minus saturation temperature at inlet (θ_{in} may be negative)

$\left(\frac{dT}{dp}\right)_{sat}$ = change in saturation temperature with pressure

$(dT/dp)_{sat}$ may be evaluated approximately from the Clausius-Clapeyron equation at the inlet condition.

$$\left(\frac{dT}{dp}\right)_{sat} = \frac{T_{in}}{(h_{fg})_{in}\, \rho'_v\, J} \tag{40}$$

where T_{in} = inlet temperature of liquid

$(h_{fg})_{in}$ = heat of vaporization of liquid evaluated at inlet pressure

ρ'_v = saturation density of vapor evaluated at inlet pressure

J = mechanical equivalent of heat.

The next quantity for which an expression is to be obtained is the vapor mass flow quality $X'(z)$ referred to a control volume moving upstream with the void at velocity

v. This control volume is shown in Fig. 10. Pure liquid flow enters this control volume at a mass flow rate given by $\rho_L(V_L' + v)A$. From the end of the control volume which at the instant shown is located at some arbitrary position $z > \ell$, there issues a mass flow rate of vapor given by $\rho_v(V_v + v)\,\alpha A$ where α is the fraction of the cross section area of the duct that is occupied by the vapor phase at the position z. X'(z), the vapor mass flow quality at z, is defined as

$$X' \equiv \frac{\rho_v(V_v + v)\,\alpha}{\rho_L(V_L' + v)} \equiv \begin{array}{c}\text{mass flow vapor through moving}\\ \text{control surface divided by}\\ \text{total mass flow through moving}\\ \text{control surface}\end{array} \tag{41}$$

Note that this definition pertains to the vapor flow rate through a control surface moving at velocity v rather than the vapor flow rate past a stationary point on the wall of the duct, the latter being the more common method of defining two phase flow quality. The prime superscript will be retained on X' to indicate the fact that X' is defined with reference to a moving control surface.

At the head of the moving vapor void there will be, in general, a very rapid generation of vapor due to sudden release of superheat from the liquid coming in contact with the vapor interface. Associated with this sudden generation of vapor there will be a sudden increase in vapor void fraction α and an accompanying sharp pressure change ΔP, mentioned earlier. This pressure change is due to the rapid acceleration of the liquid in flowing around the head of the vapor void. In the present analysis, it is convenient to treat these rapid changes at the head of the void as discontinuities much in the same way as the quantities pressure, density, temperature and velocity are considered to change discontinuously across a moving normal shock. That is, at $z = \ell^-$ in Fig. 9, X' and α are zero and pressure is denoted by $P_{z=\ell^-}$. At $z = \ell^+$, an infinitesimally short distance down-stream past the nose of the bubble, X' and α are considered to have changed discontinuously to values denoted as X_ℓ' and α_ℓ while pressure has changed discontinuously by the amount denoted by ΔP.

Returning now to the problem of obtaining an expression for X', this can be accomplished approximately by assuming that the flow into and out of the moving

control volume in Fig. 10 can be treated as a steady flow process and by noting that for such a steady flow process, conservation of energy yields the result that

$$q(z - \ell) = \left[\rho_v(V_v + v)\ \alpha\ A\ h_v + \rho_L(V_L + v)(1 - \alpha)\ A\ h_L\right] - \rho_L(V_L' + v)\ h_L\Big|_{z=\ell^-} \tag{42}$$

where the subscript $z=\ell^-$ denotes quantities evaluated just before the head of the moving void.

In writing Eq. (42), kinetic and potential energy of the flow are neglected*. In assuming that the flow through the moving control volume can be treated approximately by steady flow relations, it is assumed that the rate of change of internal energy inside the moving control volume is negligible compared with the rate of change of enthalpy of the flow passing through the control volume.

Now, assuming that at $z > \ell$ we have thermodynamic equilibrium between the liquid and vapor phases, then h_v in Eq. (42) can be written as

$$h_v = h_L + h_{fg} \tag{43}$$

where h_{fg} is the latent heat of vaporization evaluated at $z > \ell$.

Substituting Eq. (43) into Eq. (42) we obtain

$$q(z - \ell) = \rho_v(V_v + v)\ \alpha\ A\ h_{fg} + \left\{\left[\rho_v(V_v + v)\ \alpha + \rho_L(V_L + v)(1 - \alpha)\right] A\ h_L\right\}_{z>\ell} - \left[\rho_L(V_L' + v)\ A\ h_L\right]_{z=\ell^-} \tag{44}$$

For the liquid phase, differences in enthalpy can be expressed approximately by

$$h_L\Big|_{z>\ell} - h_L\Big|_{z=\ell^-} = (C_P)_L\ (T_{z>\ell} - T_{z=\ell^-}) \tag{45}$$

*A derivation of this relationship may be found on pages 240-241 of Ref. 14.

With the assumption of thermodynamic equilibrium at $z > \ell$, $T_{z>\ell}$ will be the saturation temperature at $z > \ell$ and $T_{z=\ell^-} - T_{z>\ell}$ can then be expressed as

$$T_{z=\ell^-} - T_{z>\ell} = \theta - \left(\frac{dT}{dp}\right)_{sat} \Delta P'(z) \tag{46}$$

where θ is given by Eq. (39) and where $\Delta P'(z)$ denotes the pressure change occurring from $z = \ell^+$, just after the head of the moving void, up to the arbitrary position $z > \ell$. An analytic expression for $\Delta P'(z)$ will be derived later.

For steady flow through the control volume moving with the void, the rate of change of mass within the control volume is assumed to be negligible and conservation of mass gives

$$\rho_v(V_v + v)\,\alpha + \rho_L(V_L + v)(1 - \alpha) \cong \rho_L(V_L' + v) \tag{47}$$

Substituting Eqs. (45), (46) and (47) into Eq. (44) yields

$$\begin{aligned} q\,(z - \ell) &= \rho_v(V_v + v)\,\alpha\, A\, h_{fg} \\ &\quad - \rho_L(V_L' + v)\, A (C_p)_L \left[\theta - \left(\frac{dT}{dp}\right)_{sat} \Delta P'(z)\right] \end{aligned} \tag{48}$$

Dividing through by $\rho_L(V_L' + v)\, A\, h_{fg}$, and employing the definition of X' given by Eq. (41) we obtain, finally

$$X'(z) = \frac{q(z-\ell)}{\rho_L(V_L' + v)\, A\, h_{fg}} + \frac{(C_p)_L}{h_{fg}} \left[\theta - \left(\frac{dT}{dp}\right)_{sat} \Delta P'(z)\right] \tag{49}$$

which applies for $z > \ell$.

The flow quality X'_{ℓ}, just after the head of the void (i.e. at $z=\ell^{+}$) is given by

$$X'_{\ell} = \frac{(C_p)_L \theta}{h_{fg}} \tag{50}$$

Next we turn attention to the problem of obtaining an expression for the velocity v of the moving slug. To do so, we must consider in detail the physics of the flow in the vicinity of the nose of the bubble. Consider Fig. 11. Along the center liquid streamline which approaches the nose of the bubble, the pressure would first increase as the fluid decelerates in approaching the stagnation point at the center of the nose of the void. The stagnation pressure achieved would be

$$P_o = P + \rho_L \frac{(V'_L + v)^2}{2g_c} \tag{51}$$

where P is the static system pressure in the liquid just ahead of the bubble.

From the stagnation point, the liquid would then accelerate very rapidly in passing around the bubble with an accompanying sharp decrease in pressure, the final pressure obtained by the liquid in accelerating around the bubble being given by $P + \Delta P$ where, as noted earlier, ΔP denotes the sharp pressure change occurring across the nose of the moving void. (The physical significance of ΔP now becomes clearer although an expression for ΔP yet remains to be derived).

Inside the vapor void, just across the interface from the stagnation point, there is a vapor pressure P_v which, neglecting surface tension, must equal the stagnation pressure.

$$P_v = P_o = P + \rho_L \frac{(V'_L + v)^2}{2g_c} \tag{52}$$

If the approximation is made that thermodynamic equilibrium is maintained across the bubble interface, then P_v must equal the vapor pressure corresponding to the temperature $T_{z=\ell^-}$ at the nose of the bubble. This vapor pressure would be given by

$$P_v = P + \frac{1}{\left(\frac{dT}{dp}\right)_{sat}} \left[\theta + \left(\frac{dT}{dp}\right)_{sat} \Delta P\right] \tag{53}$$

Equating Eqs. (52) and (53) and solving for v we obtain

$$v = -V_L' + \sqrt{\left[\frac{2g_c}{\rho_L}\left\{\frac{\theta}{\left(\frac{dT}{dp}\right)_{sat}} + \Delta P\right\}\right]} \tag{54}$$

where $\left(\frac{dT}{dp}\right)_{sat}$ is obtained from Eq. (40) and θ is obtained from Eq. (39)*.

One can note that Eq. (54) provides a criterion for the conditions under which a vapor void will propagate upstream into superheated liquid. For such propagation v must be positive, which is true only if

$$\sqrt{\frac{2g_c}{\rho_L}\left[\frac{\theta}{\left(\frac{dT}{dp}\right)_{sat}} + \Delta P\right]} > V_L' \tag{55}$$

If this condition is not satisfied, the vapor void will be washed downstream by the entering liquid flow. To evaluate Eq. (55), however, requires an expression for ΔP. This expression will be obtained later, and the criterion for void propagation upstream will subsequently be reformulated by substitution of the expression for ΔP.

---

* Note that when Eqs. (37), (39) and (40) are substituted into Eq. (54), the pressure change ΔP is eliminated.

A momentum balance across the head of the void requires that

$$\Delta P = P_{z=\ell^+} - P_{z=\ell^-}$$

$$= -\frac{1}{g_c}\left[\alpha_\ell \rho_v (V_v+v)^2 + (1-\alpha_\ell)\,\rho_L\,(V_L+v)^2 - \rho_L (V_L'+v)^2\right] \tag{56}$$

Also, consideration of Bernoulli's relationship in the liquid film yields

$$\Delta P = -\frac{\rho_L}{2g_c}\left[(V_L+v)^2 - (V_L'+v)^2\right] \tag{57}$$

A complementary relation of Eq. (41) is

$$1 - X' = (1-\alpha)\left(\frac{V_L+v}{V_L'+v}\right) \tag{58}$$

Eliminating ΔP, V_L, and V_v amongst Eqs. (41), (56), (57), and (58), one obtains

$$\left(\frac{\rho_\ell}{\rho_v}\right)\frac{(X_\ell')^2}{\alpha_\ell} + \frac{1}{2}\left[1 - \left(\frac{\alpha_\ell}{1-\alpha_\ell}\right)^2\right](1-X_\ell')^2 - \frac{1}{2} = 0$$

Or

$$X_\ell' = \alpha_\ell \left\{ \frac{(1-2\alpha_\ell) + \sqrt{(1-2\alpha_\ell)^2 + \alpha_\ell\left[2\,\frac{\rho_L}{\rho_v}(1-\alpha_\ell)^2 + \alpha_\ell(1-2\alpha_\ell)\right]}}{2\left(\frac{\rho_L}{\rho_v}\right)(1-\alpha_\ell)^2 + \alpha_\ell(1-2\alpha_\ell)} \right\} \tag{59}$$

Substituting Eq. (58) into Eq. (57):

$$\Delta P = \frac{\rho_L}{2g_c} (V_L'+v)^2 \left[1-\left(\frac{1-X_\ell'}{1-\alpha_\ell}\right)^2\right] \tag{60}$$

Levy [Ref. 33], has obtained analogous results for a steady state two-phase flow.

Eqs. (60) and (54) are two independent equations in the unknowns ΔP and v. Substituting for ΔP in Eq. (54) by means of Eq. (60) we obtain, after rearranging

$$v = - V_L' + \frac{(1-\alpha_\ell)}{(1-X_\ell')} \sqrt{\frac{2g_c}{\rho_L} \frac{\theta}{\left(\frac{dT}{dp}\right)_{sat}}} \tag{61}$$

The criterion for propagation of a void upstream in a flowing channel becomes, then

$$\frac{(1-\alpha_\ell)}{(1-X_\ell')} \sqrt{\frac{2g_c}{\rho_L} \frac{\theta}{\left(\frac{dT}{dp}\right)_{sat}}} > V_L' \tag{62}$$

We can note at this point that a necessary condition for an annular void to be steadily maintained in a heated duct without benefit of nucleation is that the inequality Eq. (62) above be an equality. Under this condition, the present analysis reduces to the steady state solution for the flow around such an annular void.

Next we consider the evaluation of $\Delta P'(z)$, the pressure change along the void from $z=\ell^+$ back to $z>\ell$. To evaluate $\Delta P'(z)$ we continue to employ the concept that the

flow through a control volume moving with the head of the void is quasi-steady. This is, we assume that the time rate of change of quantities within this moving control volume can be neglected compared with the net rate of change of quantities passing through the control volume. Taking a control volume extending from $z=\ell^+$ to $z > \ell$ as shown in Fig. 11, we can note that the pressure change over the length of this control volume will be due to the wall shear stress resulting from the flowing liquid plus the change in momentum of the flow passing through the moving control volume. The pressure change due to wall shear stress can be evaluated approximately by

$$-\int_{z=\ell^+}^{z} \frac{f\ \rho_L\ V_L^2}{g_c D}\ dz \tag{63}$$

where the friction factor f would be evaluated as the usual duct friction factor based on the Reynolds number defined by $\rho_L\ V_L\ D/\mu$. The velocity V_L is given by

$$V_L + v = (V_L' + v)\ \frac{(1-X')}{(1-\alpha)} \tag{64}$$

The pressure change from $z=\ell^+$ to $z>\ell$ due to the change in momentum through the control volume, evaluated with respect to a frame of reference moving at velocity v, is given by

$$-\rho_L\ \frac{(V_L' + v)^2}{g_c}\left[\frac{(1-X')^2}{(1-\alpha)} - \frac{(1-X'_\ell)^2}{(1-\alpha_\ell)} + \frac{\rho_L}{\rho_v}\left(\frac{X'^2}{\alpha} - \frac{X'^2_\ell}{\alpha_\ell}\right)\right] \tag{65}$$

Combining expressions (63), (64) and (65) we obtain

$$-\Delta P'(z) = \int_{z=\ell^+}^{L} \frac{f\rho_L}{g_c D}\left[(V_L' + v)\ \frac{(1-X')}{(1-\alpha)} - v\right]^2 dz$$

$$+ \rho_L \frac{(V_L' + v)^2}{g_c}\left[\frac{(1-X')^2}{(1-\alpha)} - \frac{(1-X_\ell')^2}{(1-\alpha_\ell)} + \frac{\rho_L}{\rho_v}\left(\frac{X'^2}{\alpha} - \frac{X_\ell'^2}{\alpha_\ell}\right)\right] \qquad (66)$$

In the above equations, (X', α) are needed for all $\ell < z < L$. With a quasi-steady flow field, which is nearly time independent, Equation (62) may be used directly for all z. This would be a simple extension of Levy's "momentum exchange model" [Ref. 33]. For the more general problem, the "momentum exchange model" can be further extended by reverting to the spaced-fixed flow weighted quality defined as

$$X = \frac{\alpha\rho_v V_v}{\alpha\rho_v V_v + (1-\alpha)\rho_L V_L} \qquad (67)$$

then Eq. (59) should be replaced by

$$\left(\frac{\rho_L}{\rho_v}\right)\frac{X^2}{\alpha} + \frac{1}{2}\left\{\frac{(1-2\alpha)}{(1-\alpha)^2}\ (1-X)^2 - 1\right\} = \text{const.} \qquad (68)$$

The constant in Eq. (68) can be evaluated by using (V_v, V_L, α) at $z=\ell$ in Eq. (67) to find the corresponding value of X.

CONSTITUTIVE EQUATIONS FOR VAPOR GENERATION IN NON-EQUILIBRIUM FLOWS

In this section there will be developed expressions for calculating the net rate of vapor mass formation per unit volume, Γ_v, under conditions of thermodynamic non-equilibrium. Essentially, Γ_v can be defined by the continuity equations for the vapor phase

$$\frac{\partial(\alpha\rho_v)}{\partial t} + \frac{\partial}{\partial z}(\alpha\rho_v V_v) = \Gamma_v \tag{69}$$

In Ref. 21, a somewhat similar expression was defined as

$$\frac{\partial}{\partial t}\left[(1-\alpha)\rho_L\right] + \frac{\partial}{\partial z}\left[(1-\alpha)\rho_L \bar{V}\right] = \Gamma_L \tag{70}$$

where

$$\bar{V} = \frac{\alpha\rho_v V_v + (1-\alpha)\rho_L V_L}{\alpha\rho_v + (1-\alpha)\rho_L} \tag{71}$$

The continuity condition for the mixture is

$$\frac{\partial}{\partial t}\left[\alpha\rho_v + (1-\alpha)\rho_L\right] + \frac{\partial}{\partial z}\left[\alpha\rho_v V_v + (1-\alpha)\rho_L V_L\right] = 0 \tag{72}$$

Combining Eqs. (69), (70), and (72), one finds

$$\Gamma_v + \Gamma_f = \frac{\partial}{\partial z}\left[(1-\alpha)\rho_L(\bar{V}-V_L)\right]$$

$$= \frac{\partial}{\partial z}\left[\frac{\alpha(1-\alpha)\rho_v\rho_L}{\alpha\rho_v + (1-\alpha)\rho_L}(V_v-V_L)\right] \tag{73}$$

By considering heat balance, Γ_v can be calculated as (Ref. 1)

$$\Gamma_v = \frac{1}{h_{fg}} \left\{ \frac{q}{A} + \frac{1}{J} \frac{\partial P}{\partial t} - (1-\alpha)\rho_L \left(\frac{\partial h_L}{\partial t} + V_L \frac{\partial h_L}{\partial z} \right) - \alpha \rho_v \left(\frac{\partial h_v}{\partial t} + V_v \frac{\partial h_v}{\partial z} \right) \right\} \tag{74}$$

With thermodynamic equilibrium, h_L and h_v are known functions of pressure; therefore, Eq. (74) can be reduced to

$$(\Gamma_v)_{th.eq.} = \frac{1}{h_{fg}} \left\{ \frac{q}{A} + \left[\frac{1}{J} \frac{\partial}{\partial t} - (1-\alpha)\rho_L \left(\frac{dh_L}{dp} \right)_{sat} \left(\frac{\partial}{\partial t} + V_L \frac{\partial}{\partial z} \right) \right. \right.$$

$$\left. \left. - \alpha \rho_v \left(\frac{dh_v}{dp} \right)_{sat} \left(\frac{\partial}{\partial t} + V_v \frac{\partial}{\partial z} \right) \right] P \right\} \tag{75}$$

where $(dh_L/dp)_{sat}$ and $(dh_v/dp)_{sat}$ are respectively enthalpy-pressure derivatives of saturated liquid and vapor.

If, however, thermodynamic equilibrium does not prevail, then h_L and h_v cannot be determined as known functions of pressure but rather they, along with Γ_v, must be determined by detailed analysis of the heat and mass transfer mechanisms in the flow. Since such mechanisms depend significantly on the nature of the two phase flow regime that is occurring, different expression for Γ_v will be obtained for different flow regimes. Each expression for Γ_v, in terms of the appropriate parameters, can be considered as the constitutive equation of evaporation appropriate to a particular flow regime of a non-equilibrium evaporation process.

In deriving expressions for Γ_v, three flow regimes will be considered. These are: (a) bubble flow regime, (b) annular flow regime and (c) dispersed flow

regime. Transition flow regimes occurring between bubble flow and annular flow such as froth flow, coalecscing flow, [Ref. 16] etc. will not be considered here because it is presumed that in such flows, there would be sufficient interfacial surface area between liquid and vapor phase for thermodynamic equilibrium to be maintained. Essentially, vapor generation rate in such transition regions would not be separately considered but would be handled analytically by assuming that the expression for Γ_v developed for bubble flow regime could be extended to join with the expression for Γ_v developed for the annular flow regime.

BUBBLE FLOW REGIME

In flows in which a high degree of superheating can occur before inception of nucleation occurs, it is possible, even likely, that a bubble flow regime may not occur but instead, a single nucleate bubble may grow almost instantaneously to fill the duct cross section area before it is swept any appreciable distance down stream. If this occurs, then the flow in the heated tube will pass either directly from superheated all-liquid flow to annular flow or will develop a transient void propagation situation such as was analyzed in the previous section

One can develop a rough criterion for whether a bubble flow regime will develop or not by considering the relative magnitude of bubble growth rate to flow rate. One can readily see that if $\dot{R}_v$, the rate at which the radius of a vapor bubble grows in superheated liquid, exceeds the all liquid flow velocity in the heated duct, then a bubble, once nucleated, will tend to grow to a size which fills the duct before it has been swept away from its nucleation site. For example, if we consider liquid potassium flowing in a duct at an inlet velocity of, say, 20 inches per second, then we can say that if bubble growth rate is greater than

this value, bubble flow will not occur. Turning to Fig. 6, which gives curves of maximum bubble growth vs. superheat for liquid potassium, we see that for mass transfer coefficient C = 1.0, bubble growth rate will exceed 20 inches per second (50.8 cm/sec) for values of superheat greater than only 3.5°F. Since this degree of superheat is very likely to be obtained, we can see that the bubble flow regime is quite unlikely to occur in liquid metal flows.

Although it seems unlikely that the bubble flow regime will be obtained in boiling liquid metal flows, it does remain likely that such a flow regime will be obtained in boiling water flow and, of course, it is always possible that it will occur in liquid metal flow under some conditions*. Therefore it remains worthwhile to consider the expression for Γ_v that would apply in this flow regime. Assuming ρ_v to be constant, the expression for Γ_v would be simply

$$\Gamma_v = \int_0^\infty \frac{n(R_v,z,t)}{A} \rho_v 4\pi R_v^2 \dot{R}_v \, dR_v \tag{76}$$

where $n(R_v,z,t)\, dR_v\, dz$ is the number of vapor bubbles lying in the size interval R_v to $R_v + dR_v$ and in the length interval z to z + dz. $\dot{R}_v$, the bubble growth rate, can be determined from Eq. (33) as a function of R_v and bulk temperature**. Therefore the problem of determining Γ_v in the bubble flow regime resolves itself into a problem of determining the bubble density $n(R_v,z,t)$. This problem is considered below briefly for the general case where nucleation of bubbles occurs over a finite heated length due to arbitrary source strength S(z,t) and also in detail for the simpler but quite practical case where vapor bubbles originate from a single nucleation source. The latter situation would be approximately obtained when, for example, so called "hot fingers" are used to control or stabilize nucleation [Ref. 17].

---

* For example, if the vaporization coefficient of mass transfer, C, is on the order of .01

** Eq. (33) is really valid only for infinite bulk temperature fields which are constant in space and time. However, it may be used to provide approximate values for R_v for cases where bulk temperature varies with space and time.

Somewhat in analogy with the problem of diffusion of neutrons in nuclear reactors [Ref. 18] the one dimensional bubble density function $n(R_v,z,t)$ can be observed to obey a diffusion equation of the form

$$\frac{\partial n}{\partial t} + \frac{\partial}{\partial z}(nV_v) + \frac{\partial}{\partial R_v}(n\dot{R}_v) = 0 \tag{77}$$

where $V_v(z,t)$ is the velocity of the vapor bubbles in the z direction. Eq. (77) is subject to the "boundary" condition that

$$n(R_o,z,t)\,\dot{R}_v(R_o,z,t) = S(z,t) \tag{78}$$

where R_o is the nucleation radius of vapor bubbles, and $S(z,t)$ is the nucleation source strength in bubbles per second per unit length. Conceptually one can conceive of solving this equation by numerical integration. For example, given an initial source distribution $S(z,0)$, an initial bubble density $n(R_v,z,0)$ an initial velocity distribution $V_v(z,0)$, and an initial temperature distribution $T(z,0)$, one could determine $\dot{R}_v(R_v,z,0)$ from Eq. (37) and then determine $\partial n/\partial t\,(R_v,z,0)$ from Eq.(77). $n(R_v,z,t)$ at the next time step $t = \Delta t$ could then be directly determined from

$$n(R_v,z,t) = n(R_v,z,0) + \frac{\partial n}{\partial t}(R_v,z,0)\,\Delta t \tag{79}$$

$V_v(z,t)$, $S(z,t)$ and $T(z,t)$ would have to be separately determined from an appropriate equation of motion, an energy equation and a constitutive relation for the nucleation source strength S. These latter relationships themselves would be quite complex, but presuming that these relationships could be determined, Eq. (77) would serve as the governing equation for determining the bubble distribution $n(R_v,z,t)$ which, in turn, could be used to calculate Γ_v from Eq. (76).

To illustrate how the above equations may be used, let us consider the special case where vapor bubbles are nucleated at a single discrete source. The analytical formulation of this problem is given below.

Consider a superheated liquid flowing in a duct in which inception of nucleation occurs at the point $z = z'$ where bubbles of initial radius R_o are generated at a single discrete cavity at a rate of S_o bubbles per second. As these bubbles are swept downstream, they grow due to superheat of the liquid surrounding them. As a consequence of the growth of these bubbles, the mean flow velocity $V_m(z,t)$ increases with distance z and the liquid temperature $T(z,t)$ would tend to decrease back toward an equilibrium value.

In analyzing this flow situation, we can consider a total bubble density $N(z,t)$ bubbles per inch without regard to bubble size since, at any point z, all the bubbles would be of the same size having come from the same source and experienced the same time history. $N(z,t)$ can be seen to be related to $\ell(z,t)$ the spacing between consecutive bubbles, in the following way

$$N(z,t) = \frac{1}{\ell(z,t)} \tag{80}$$

e.g. if at any point z, consecutive bubbles were 1/10 inch apart, then the bubble density N would be 10 bubbles per inch.

We can now proceed to formulate this non-equilibrium two-phase flow problem following approximately the approach outlined by Zuber and Dougherty in Ref. 1. First we write the continuity equation for the vapor (i.e. Eq. (69)) assuming the vapor density to be constant*.

$$\rho_v \frac{\partial \alpha}{\partial t} + \rho_v \frac{\partial(\alpha V_v)}{\partial z} = \Gamma_v \tag{81}$$

---

*For simplicity, we shall consider an incompressible analysis here. Our justification for this is that the rate of change of vapor mass content in boiling flows associated with changes in vapor density are usually negligible compared with the rates of creation of vapor mass due to boiling.

The continuity equation for the mixture

$$\frac{\partial}{\partial t}\left[\alpha\rho_v + (1-\alpha)\ \rho_L\right] + \frac{\partial}{\partial z}\left[\alpha\rho_v V_v + (1-\alpha)\ \rho_L\ V_L\right] = 0 \tag{82}$$

The momentum equation for the mixture

$$\frac{1}{g_c}\left\{\frac{\partial}{\partial t}\left[\alpha\rho_v V_v + (1-\alpha)\ \rho_L V_L\right] + \frac{\partial}{\partial z}\left[\alpha\rho_v V_v^2 + (1-\alpha)\ \rho_L V_L^2\right]\right\} + \frac{\partial P}{\partial z}$$

$$+ \frac{g_z}{g_c}\left[\alpha\rho_v + (1-\alpha)\ \rho_L\right] + \frac{\partial \tau}{\partial z} = 0 \tag{83}$$

The energy equation for the mixture

$$\alpha\rho_v\left[\frac{\partial h_v}{\partial t} + V_v\ \frac{\partial h_v}{\partial z}\right] + (1-\alpha)\ \rho_L\left[\frac{\partial h_L}{\partial t} + V_L\ \frac{\partial h_L}{\partial z}\right]$$

$$+ \Gamma_v\ h_{fg} = \frac{q}{A} + \frac{1}{J}\ \frac{\partial P}{\partial t} \tag{84}$$

Eqs. (81) through (84) may be viewed as four field equations relating the 7 unknown variables* ρ_v, V_v, V_L, α, P, $\partial\tau/\partial z$ and Γ where $\partial\tau/\partial z$ represents the frictional pressure drop for the two-phase flow in the duct. In order to solve for these variables, we need to develop further relationships for the variables α, Γ_v, $\partial\tau/\partial z$ and also develop a relationship between V_v and V_L. These relationships we can refer to as constitutive relationships. In particular, we are interested in developing the constitutive relationship for Γ_v for the flow

---

* Note that, for simplicity, the heat flux q is being considered as a known variable. In general, it would not be known but would be determined by heat transfer considerations requiring a further constitutive equation.

situation we are considering.

First, following Reference 1 we can express $\partial\tau/\partial z$ in terms of the Lockhart-Martinelli correlation

$$\frac{\partial \tau}{\partial z} = f\,(X_{tt}) \tag{85}$$

where

$$X_{tt} = \left[\frac{\rho_L V_L (1-\alpha)}{\rho_v V_v \alpha}\right]^{0.9} \left(\frac{\rho_v}{\rho_L}\right)^{0.5} \left(\frac{\mu_L}{\mu_v}\right)^{0.1} \tag{86}$$

with μ_L and μ_v being viscosities of the liquid and vapor phases respectively.

V_m, the mean velocity of the mixture, is defined as total volume flow divided by duct cross-sectional area. V_m is given by

$$V_m = \alpha V_v + (1-\alpha)\, V_L \tag{87}$$

we can define a vapor drift velocity s as the difference between V_v and V_m i.e.,

$$s = V_v - V_m \tag{88}$$

The vapor slip s would have to be experimentally determined for bubble flow. Since we are not primarily interested here in determining s, let us presume that we have an appropriate constitutive equation from which we can evaluate s, which we shall write symbolically as

$$s = s\,(V_v,\ V_L,\ \alpha,\ \mu_v \text{ etc.}) \tag{89}$$

The void fraction α at any point is given simply by

$$\alpha = \frac{N}{A}\,\frac{4\pi R_v^{\,3}}{3} \tag{90}$$

which introduces into our system of equations the two new variables $N(z,t)$ and $R_v(z,t)$.

The constitutive equation for Γ_v is, for our discrete source flow*

$$\Gamma_v = \frac{4\pi N}{A} \rho_v R_v^2 \dot{R}_v \tag{91}$$

which is merely a specialization of Eq. (76) for the case where bubbles of only one size exist at any given location z. Eq. (91) introduces the new variable $R_v(T_L, P, R_v)$ and, implicitly, the new variable T_L which is the liquid temperature. R_v would be obtained from Eq.(33) i.e. from the analysis performed of bubble growth rate in superheated liquid. T_L would be obtained from the energy equation as shown below.

The energy equation (84) may be rewritten explicitly in terms of the liquid temperature T_L and local pressure P if we assume that the vapor phase behaves like a perfect gas and that the liquid and vapor phase are of the same temperature (not necessarily equilibrium temperature). For a perfect gas, the enthalpy h_v is a function only of the temperature, so we may rewrite Eq. (84) as

$$\alpha\rho_v \left[\left(\frac{dh_v}{dT_L}\right) \frac{\partial T_L}{\partial t} + V_v \left(\frac{dh_v}{dT_L}\right) \frac{\partial T_L}{\partial z} \right] + (1-\alpha)\, \rho_L (C_P)_L \left[\frac{\partial T_L}{\partial t} + V_L \frac{\partial T_L}{\partial z} \right]$$

$$+ \Gamma_v h_{fg} = \frac{q}{A} + \frac{1}{J} \frac{\partial P}{\partial t} \tag{92}$$

where dh_v/dT_L represents a known thermodynamic function.

We can develop further relationships for our new variables $N(z,t)$, $R_v(z,t)$ and R_v. Following a bubble, the total time rate of change of bubble spacing $\ell(z,t)$ is

---

* Eq. (91) is valid only for ρ_v = constant.

$$\left.\frac{d\ell}{dt}\right|_{\text{following a bubble}} = \frac{\partial \ell}{\partial t} + V_v \frac{\partial \ell}{\partial z} \tag{93}$$

We can also note that the increase in the spacing ℓ between consecutive bubbles comes about because of the fact that bubble velocity increases with z. Hence, we can write

$$\left.\frac{d\ell}{dt}\right|_{\text{following a bubble}} = \ell \frac{\partial V_v}{\partial z} \tag{94}$$

Equating (93) and (94) we obtain

$$\frac{\partial \ell}{\partial t} + V_v \frac{\partial \ell}{\partial z} = \ell \frac{\partial V_v}{\partial z} \tag{95}$$

Substituting $\ell = 1/N$ into Eq. (95) from Eq. 80 and differentiating we obtain

$$-\frac{1}{N^2}\frac{\partial N}{\partial t} - \frac{V_v}{N^2}\frac{\partial N}{\partial z} = \frac{1}{N}\frac{\partial V_v}{\partial z} \tag{96}$$

or

$$\frac{1}{N}\frac{\partial N}{\partial t} + \frac{V_v}{N}\frac{\partial N}{\partial z} = -\frac{\partial V_v}{\partial z} \tag{97}$$

Note that this result could have been written directly from the general equation for bubble diffusion (Eq. (77)) by integrating the equation with respect to R_v and applying the relations

$$\int_0^\infty n \, dR_v = N \tag{98}$$

$$n \dot{R}_v \Big|_0^\infty = 0 \tag{99}$$

A boundary condition for Eq. (97) is that

$$N = \frac{S_o}{V_v} \quad \text{at} \quad z = z' \tag{100}$$

where, as noted earlier, S_o is the number of bubbles nucleated per second at the single discrete source located at $z = z'$.

A further relationship which we can write down is that the total time rate of change of bubble radius R_v following a bubble is

$$\left.\frac{\partial R_v}{\partial t}\right|_{\substack{\text{following}\\ \text{a bubble}}} \equiv \dot{R}_v = \frac{\partial R_v}{\partial t} + V_v \frac{\partial R_v}{\partial z} \tag{101}$$

This provides a differential relationship for the space and time variation of $R_v(z,t)$ in terms of bubble growth rate $\dot{R}_v$. Eq. (97) can be obtained by substituting Eqs. (97) and (91) into the incompressible continuity equation for the vapor phase (Eq. (81)) and hence does not represent a new independent equation.

We now have established a sufficient number of independent equations to determine the discrete source flow problem under non-equilibrium flow conditions. We have a total of 11 unknown variables, V_v, V_L, P, T, α, N, R_v, $\dot{R}_v$, Γ_v, $\partial\tau/\partial z$, and s. These are related by four equations which could be referred to as field equations (Eqs. (81), (82), (83) and (92); three equations which express either geometric or kinematic relationships between the variables (Eqs. (88), (90) and (97); and four equations which can be referred to as constitutive equations (Eqs. (85), (89), (91) and (33)). Of these, the significant equations from the standpoint of non-equilibrium flows are Eqs. (89) and (33), which provide the constitutive relationships necessary to calculate Γ_v, the mass rate of vapor generation.

ANNULAR FLOW REGIME

In the annular flow regime, vapor flows in a large continuous vapor core in the center of a duct while the liquid flows predominantly in an annular film along the wall of the duct. The annular flow regime in "classical" boiling flows of ordinary fluids develops by coalescing of bubbles formed in the bubble flow regime. However, in liquid metal flows, we have seen that bubble growth rate may be sufficiently high so that an annular flow regime may develop immediately from inception of a single bubble.

The present consideration of the annular flow regime will include both the steady state situation where the "head" of the annular flow regime remains at a fixed location and also the dynamic situation, analyzed earlier, where a central void

may propagate along a duct due to superheating of the liquid upstream of the annular void.

In an annular flow regime, downstream of the "head" of the regime, the interfacial surface area between liquid and vapor phases should be sufficient to maintain thermodynamic equilibrium between these phases. Experimental measurements of wall temperature obtained with liquid metal boiling flows [Ref. 13 and 19], which are the most prone to superheating, indicates that thermodynamic equilibrium is fairly closely obtained in the annular flow regime. Some slight superheating of the liquid layer along the duct wall would be expected to occur due to the necessity of maintaining a temperature gradient in this layer to conduct heat to the vaporizing interface, but this should be negligible. Greater superheating of the liquid layer could conceptually occur if the vaporization coefficient C at the vapor-liquid interface were sufficiently low. (See Eq. (5)). However, there is no evidence to suggest that this occurs.

For the reasons cited above, it will be assumed that for annular flow thermodynamic equilibrium does prevail <u>downstream</u> of the head of the annular void so that, in this region, Γ_v can be calculated from the energy equation (Eq. 75)) i.e., a separate constitutive equation for Γ_v is not required. This is not so however, in the region at the head of the annular void i.e. at $z = \ell$. Here, at the start of the annular flow regime, there will be a very rapid release of superheat from the liquid flowing around the head of the void. This will be so whether the annular flow regime is or is not preceded by a bubble flow regime.

Because this release of superheat at the head of the annular flow regime would be very rapid, it seems reasonable to treat it as an instantaneous release, as was done in the analysis of a propagating void. Mathematically we can express this instant release in terms of a delta function $\delta(\ell)$

$$\left.\begin{aligned} \int_{z<\ell} f(z)\,\delta(\ell)\,dz &= \int_{z>\ell} f(z)\,\delta(\ell)\,dz = 0 \\ \int_{z<\ell}^{z>\ell} f(z)\,\delta(\ell)\,dz &= f(\ell) \end{aligned}\right\} \tag{102}$$

Γ_v at $z = \ell$ becomes

$$\Gamma_v = \left[\alpha\rho_v(V_v+v)\right]_{z=\ell}\,\delta(\ell) \tag{103}$$

To find $(V_v + v)$, it is necessary to solve a simultaneous set of equations previously given as Eqs. (50), (56), (61), (41):

$$X'_\ell = \frac{(C_P)_L\,\theta}{h_{fg}} \tag{104}$$

$$X'_\ell = \alpha_\ell \left\{ \frac{(1-2\alpha_\ell) + \sqrt{(1-2\alpha_\ell)^2 + \alpha_\ell\left[2\frac{\rho_L}{\rho_v}(1-\alpha_\ell)^2 + \alpha_\ell(1-2\alpha_\ell)\right]}}{2\left(\frac{\rho_L}{\rho_v}\right)(1-\alpha_\ell)^2 + \alpha_\ell(1-2\alpha_\ell)} \right\} \tag{105}$$

$$(V'_L + v) = \left(\frac{1-\alpha_\ell}{1-X'_\ell}\right)\frac{2g_c\,\theta}{\rho_L(dT/dp)_{sat}} \tag{106}$$

$$\alpha_\ell\rho_v(V_v + v) = X'_\ell\,\rho_L\,(V'_L + v) \tag{107}$$

where,

θ = superheat at the head of the void based on the pressure on its downstream side.

V_L' = liquid velocity ahead of the void.

Across the head of the void, there is a pressure drop, which is needed to determine θ. This was derived earlier as Eq. (60):

$$\Delta P = \frac{\rho_L (V_L' + v)^2}{2g_c} \left[\left(\frac{1-X_\ell'}{1-\alpha_\ell} \right)^2 - 1 \right] \tag{108}$$

The expressions given here neglected vapor bubbles immediately ahead of the void (or annular flow region). As pointed out earlier, this would be valid for boiling of liquid metals with superheat [Refs. 12 and 13]. If one should desire to allow for bubbles ahead of the void then Γ_v at $z = \ell$ becomes

$$\Gamma_v = \left\{ \left[\alpha \rho_v (V_v + v) \right]_{z=\ell^+} - \left[\alpha \rho_v (V_v + v) \right]_{z=\ell^-} \right\} \delta(\ell) \tag{109}$$

To determine $(V_v + v)_{z=\ell^+}$ and $(V_v + v)_{z=\ell^-}$, an analysis on the propagation of void into a bubble flow region must be carried out.

DISPERSED FLOW REGIME

In forced convection flows which are being heated to total evaporation, a condition will be reached where the mass flow rate of vapor will be sufficiently high so that the mass flow rate of liquid will be carried predominantly in the form of droplets suspended in the vapor stream rather than flowing as a continuous liquid layer along the duct wall. This high vapor quality flow regime is referred to as the dispersed flow regime or fog flow regime. Because of the fact that there is not a continuous layer of liquid along the wall in the dispersed flow regime, the heat transfer characteristics for this type of flow are quite different from those of annular flow. In the latter flow regime, all heat is transferred from the duct wall to the liquid layer which, being essentially in

thermodynamic equilibrium with the vapor core, tends to evaporate either by means of surface evaporation at the vapor-liquid interface or by nucleation of new vapor bubbles in the liquid layer at the duct surface. In the dispersed flow regime, however, since the duct wall is not continually covered by liquid, some heat is transferred directly to the vapor phase, and thence to the liquid droplets in the vapor phase. Even for those areas of the duct wall "covered" by liquid patches due to diffusion of droplets to the duct wall, the mechanism of heat transfer tends usually to be that of film boiling, in which heat is transferred to a thin vapor between the liquid and the duct wall and thence to the liquid patch.

Since, in the dispersed flow film boiling regime, heat is transferred first to the vapor phase, considerable vapor superheat is likely to result because this superheat is the primary driving force for evaporation in the film boiling process [Ref. 20]. Hence, thermodynamic equilibrium cannot be presumed to exist in this region and a constitutive equation is required for determination of Γ_v.

One can consider a number of physical mechanisms leading to evaporation of the liquid droplets in a dispersed flow regime. One mechanism is the "flashing" of the droplets due to the pressure drop along the direction of flow. This particular mechanism has been analyzed by D. Dougherty [Ref. 21] and a constitutive equation derived for this process of evaporation. Dougherty's derivations are included as Appendix II for the convenience of the reader.

A second mechanism for evaporation is that of heat transfer to the vapor and thence to the liquid droplets in the flow. For this mechanism, heat transfer to the vapor could be estimated by some accepted correlation for all vapor convective heat transfer. Heat transfer to the droplets could then be estimated on the basis of a number of recent experimental studies of heat transfer to droplets suspended in superheated vapor [cf. Refs. 22, 28].

A third mechanism for evaporation of liquid in the dispersed flow regime is the impingement of droplets directly on the duct wall due to turbulent diffusion. At low heat fluxes, these liquid droplets may directly contact the wall, so that the heat transfer mechanism is one of solid to liquid. It is much more likely,

However, that the heat flux level in "once through" evaporators would be sufficiently high so that a "film boiling" vapor layer would develop between impinging droplets and the duct wall; a "Leidenfrost" type of heat transfer mechanism then exists for these droplets.

One possible approach to analyzing the isolated problem of the vaporization rate of droplets impinging on the duct wall would be to assume that all droplets transferred to the wall by turbulent diffusion are evaporated. The problem then becomes one of calculating the droplet diffusion rate. Attempts to analyze this problem have been made in connection with trying to predict burnout in forced convection boiling [Refs. 23 and 24]. The principal difficulty in the development of such analyses has been that of determining realistic diffusion coefficients for droplets.

Aside from the mechanism of "flashing," the best available comprehensive attacks on this problem appear to be the works of Laverty and Rohsenhow [Ref. 20] and Forslund and Rohsenhow [Ref. 25]. In both investigations significant superheating was observed in the dispersed flow regime of forced convection flow of boiling nitrogen. The first of these works offers an analysis of dispersed flow boiling based on consideration of heat transfer from superheated vapor to liquid droplets. The latter work extends this analysis by including the effects of droplet breakup, "Leidenfrost" heat transfer from the wall to the droplets, and modifies the drag coefficient for accelerating droplets. A general description of a method for calculating Γ_v for dispersed flow, based on the work of Laverty and Rohsenhow and Forslund and Rohsenhow, is given below.

Forslund and Rohsenhow assumed that entrained droplets, being sufficiently dispersed, probably would not encounter one another. They postulated that the identity of each droplet remains distinct until it impinges on the wall, whereupon it receives heat directly from the wall and becomes completely evaporated. If the slip velocity exceeds that which is allowed by the critical Weber number, then Forslund and Rohsenhow assumed that each droplet would divide in two. Weber number is defined as

$$We = \rho_v (V_v - V_L)^2 \, \delta/\sigma \tag{110}$$

where δ is the droplet diameter.

The critical Weber number has been determined experimentally, [Refs. 26 and 29], to range between 6.7 to 9.6. Presumably, the range reflects some Reynolds number influence. A recommended value for critical Weber number suggested in [Ref. 25] is

$$(We)_{critical} = 7.5 \tag{111}$$

Putting aside the problem of droplet breakup for now, one can write

$$\frac{\partial N_L}{\partial t} + \frac{\partial}{\partial z}(N_L V_L) + \left(\frac{\delta N_L}{\delta t}\right)_w = 0 \tag{112}$$

where N_L is the number of droplets per unit volume, and $(\delta N_L/\delta t)_w$ is the rate of wall impingement, which can be estimated according to experimentally determined "Leidenfrost" heat transfer data. According to [Refs. 25,27], for horizontal ducts, $(\delta N_L/\delta t)_w$ was found to be

$$\left(\frac{\delta N_L}{\delta t}\right)_w = \frac{1.2 N_L^{2/3}}{D\delta(1-\Delta T_L^*)} \left[\frac{g_n \rho_v}{\mu_v(\pi\delta^3/6)^{1/3}}\right]^{1/4} \left[\left(\frac{K_v}{\rho_L C_P}\right)\left(\frac{\Delta T_w^*}{1+\frac{7}{20}\Delta T_w^*}\right)\right]^{3/4} \tag{113}$$

where g_n is the effective acceleration perpendicular to the axial direction and may include the centrifugal acceleration if spiraled inserts are used. The vapor properties (μ_v, K_v, C_P) are to be evaluated at the average of the wall temperature, T_w, and the local saturation temperature, T_{sat}. D is the diameter of the duct. ΔT_w^* and ΔT_L^* are the dimensionless wall and liquid superheats

$$\Delta T_w^* = C_P(T_w - T_{sat})h_{fg} \tag{114}$$

$$\Delta T_L^* = (C_P)_L(T_L - T_{sat})h_{fg} \tag{115}$$

T_L is the temperature of the superheated liquid droplets and $(C_P)_L$ is the constant pressure specific heat of the liquid.

The vapor generation rate is numerically equal to the liquid evaporation rate. Therefore, one can write

$$\Gamma_v = - \left\{ \frac{\partial}{\partial t} \left[N_L \left(\frac{\pi \delta^3}{6} \right) \rho_L \right] + \frac{\partial}{\partial z} \left[N_L \left(\frac{\pi \delta^3}{6} \right) \rho_L V_L \right] \right\} \tag{116}$$

Making use of Eq. (112), one obtains

$$\Gamma_v = \left(\frac{\pi \delta^3}{6} \right) \rho_L \left(\frac{\delta N_L}{\delta t} \right)_w - \frac{\pi}{6} N_L \rho_L \left(\frac{\partial}{\partial t} + V_L \frac{\partial}{\partial z} \right) \delta^3 \tag{117}$$

The droplet diameter, δ, changes as its surface evaporates under the combined heating from the superheated vapor environment as well as its internal superheat (flashing). Therefore, from the energy balance, one can write

$$\frac{\pi}{6} \rho_L h_{fg} \left(\frac{\partial}{\partial t} + V_L \frac{\partial}{\partial z} \right) \delta^3 = - \pi \delta^2 \left(q''_v + q''_{f\ell} \right)$$

or

$$\frac{\pi}{6} N_L \rho_L \left(\frac{\partial}{\partial t} + V_L \frac{\partial}{\partial z} \right) \delta^3 = - \frac{\pi N_L \delta^2}{h_{fg}} \left(q''_v + q''_{f\ell} \right) \tag{118}$$

Therefore,

$$\Gamma_v = \left(\frac{\pi \delta^3}{6} \right) \rho_L \left(\frac{\delta N_L}{\delta t} \right)_w + \frac{\pi \delta^2 N_L}{h_{fg}} \left(q''_v + q''_{f\ell} \right) \tag{119}$$

where, q''_v is the heat flux from the superheated vapor and is given by

$$\frac{\pi N_L \delta^2}{h_{fg}} q''_v = \pi \left\{ 2 + 0.55 \left[\frac{(V_v - V_L)\delta}{\nu_v} \right]^{1/2} Pr^{1/3} \right\} \frac{\delta N_L K_v}{C_P} \Delta T_v^* \tag{120}$$

according to Ref. 28. ΔT_v^* is the dimensionless vapor superheat

$$\Delta T_v^* = \frac{C_p(T_v - T_{sat})}{h_{fg}} \tag{121}$$

Here, various vapor properties (K_v, C_p, ν_v, Pr) should be evaluated at the film temperature or $(T_v + T_{sat})/2$. Pr is the Prandtl number of the vapor. The heat flux due to droplet internal superheat was derived in Ref. 21 to be

$$\frac{\pi N_L \delta^2}{h_{fg}} q''_{f\ell} = \frac{3\pi\delta N_L K_L}{(C_p)_L} \left\{ \frac{(\Delta T_L^*)^2 - \left[\left(\frac{\delta_i}{\delta}\right)^3 - 1\right]^2 (1-\Delta T_L^*)^2}{\left(\frac{\delta_i}{\delta}\right)^3 - 1 \quad (1-\Delta T_L^*)} \right\} \tag{122}$$

where K_L is the thermal conductivity of the liquid, and δ_i is the initial droplet diameter. Examining Eqs. (113), (119), (120) and (122), one may make some interesting qualitative observations. According to the critical Weber number condition (110), the droplet diameter would be proportional to the surface tension. Thus, for a given value of $N_L\delta^3$, the "Leidenfrost" term would be relatively more important for a liquid with a larger surface tension. Also, the "flashing" term would be more important if the thermal conductivity is large. For these reasons, these two terms should become relatively more important in liquid metal boiling than in water boiling.

The droplets tend to follow the vapor flow closely. Therefore $(V_v - V_L)$, which appears in Eq. (120) expressing the convective heat transfer between vapor and the droplets, may be neglected in the first approximation. However, if the vapor is rapidly accelerating, then a finite slip would develop, which in turn would accelerate the droplets. The relation between droplet acceleration and velocity slip is

$$a_L = \left(\frac{\partial}{\partial t} + V_L \frac{\partial}{\partial z}\right) V_L = \frac{3}{4} \frac{C_D \rho_v (V_v - V_L)^2}{\rho_L \delta} + g_z \tag{123}$$

g_z is the component of gravitational acceleration along the duct. C_D is the drag coefficient and has been measured by Ingebo [Ref. 26] as well as by Forslund and Rohsenow [Ref. 25]. Fig. 12, which is reproduced from Ref. 25, shows the drag coefficients for liquid droplets (C_{D1}) as measured by Ingebo as well as for the solid sphere (C_{D2}). Ingebo's data was generally taken with $a_L > 5500$ ft/sec^2. Forslund and Rohsenow found in their experiments that for larger droplets, typically $a_L < 500$ ft/sec^2, C_{D2}) was more accurate. Therefore, they recommended the following interpolation formula:

$$C_D = C_{D2} + F\,(C_{D1} - C_{D2}) \tag{124}$$

where

$$F = \begin{cases} 0 & \text{if } a_L \leq 500 \text{ ft/sec}^2 \\ (a_L - 500)/5000 & \text{if } 500 < a_L < 5500 \\ 1.0 & \text{if } a_L \geq 5500 \end{cases} \tag{125}$$

Having determined $(V_v - V_L)$, the Weber number can be calculated from Eq. (110) to test if breakup would take place. In fact, Eqs. (110), (111), and (123) can be combined to yield the breakup criterion:

$$\left| a_L - g_z \right| \frac{\rho_L}{C_D} \frac{\delta^2}{\sigma} \geq 5.625 \tag{126}$$

If breakup should take place, and if one original droplet should split into two;

$$\left.\begin{aligned} (N_L)_{\text{after}} &= 2(N_L)_{\text{before}} \\ (\delta)_{\text{after}} &= 2^{-1/3}\,(\delta)_{\text{before}} \end{aligned}\right\} \tag{127}$$

In order to use Eqs. (120) and (121), T_v is needed. If the heat input to the duct is known, then a heat balance yields

$$\frac{4}{\pi D^2} = C_P\left[\frac{\partial}{\partial t}(\alpha\rho_v T_v) + \frac{\partial}{\partial z}(\alpha\rho_v V_v T_v)\right] + \left(\frac{\delta N_L}{\delta t}\right)_w \left(\frac{\pi\delta^3}{6}\right)\rho_L\, h_{fg}(1-\Delta T_L^*) \tag{128}$$

The void fraction α can be calculated from

$$\alpha = 1 - N_L\left(\frac{\pi\delta^3}{6}\right) \tag{129}$$

One would expect that $\alpha \approx 1$ would be an adequate approximation in most situations. If the wall temperature, T_w, instead of the heat input is known, then the vapor temperature can be calculated according to the single phase heat transfer formula:

$$C_P\left[\frac{\partial}{\partial t}(\alpha\rho_v T_v) + \frac{\partial}{\partial z}(\alpha\rho_v V_v T_v)\right]$$

$$= 0.076\left(\frac{\rho_v V_v D}{\mu_v}\right)^{0.8} Pr^{0.4}\,\frac{K_v}{D^2}(T_w - T_v) \tag{130}$$

The vapor-phase mass velocity can be calculated from the formula

$$\alpha\rho_v V_v + (1-\alpha)\,\rho_L V_L = G$$

or

$$\rho_v V_v = \frac{G - N_L\left(\frac{\pi\delta^3}{6}\right)\rho_L V_L}{1 - N_L\left(\frac{\pi\delta^3}{6}\right)} \tag{131}$$

To carry out computations according to the above analysis, it is necessary to first establish the conditions at which the dispersed flow regime begins. There appear to be three plausible mechanisms for the liquid phase to cease to form a continuous film on the duct wall. First of these is entirely of hydrodynamic nature. Then, the mechanism is primarily a surface wave instability, and the relevant parameters are vapor phase dynamic head, liquid viscosity and surface tension. A well known empirical flow regimes map reflecting such views is due to Baker [Ref. 30]. The "Baker Chart" is reproduced as Fig. 13. Similar ideas are contained in Refs. 31 and 32. A second mechanism which is also hydrodynamic in nature, concerns the diffusion rate of the droplets from the core to the wall. Transverse acceleration field, gravitational or centrifugal, would be a principal physical parameter in this case. Refs. 23, 34, 35, and 36 expounded this idea. This last concept can be approximately expressed as

$$\frac{4}{\pi D^2} q = \left(\frac{\delta N_L}{\delta t}\right)_w \left(\frac{\pi \delta^3}{6}\right) \rho_L h_{fg} \quad \text{at transition} \tag{132}$$

A third view addresses attention to the surface evaporation rate and thus would bring out heating rate as a principal variable [Refs. 37, 38, 39 and 40]. In any case, in so far as the disappearance of the liquid layer would substantially alter the heat transfer mode, criteria for "Critical Heat Flux" probably have some significance in the transition of annular flow to dispersed flow in forced convection boiling. At the present, there is no experimental data on the transition conditions for liquid metal boiling. Presuming that the transition condition could be determined, then the initial droplet diameter may be estimated from the critical Weber number. That is

$$\delta_i = \left[\frac{7.5\sigma}{\rho_v (V_v - V_L)^2}\right]_{\text{transition}} \tag{133}$$

Together with the knowledge of flow quality, or void fraction, the initial value of N_L can be determined from Eqs. (129) and (133), then computation of boiling dispersed flow can commence.

SUMMARY OF CONSTITUTIVE RELATIONSHIPS FOR VAPOR GENERATION IN ONCE-THROUGH BOILER

In preceding sections of this report there have been put forth constitutive relationships for calculating Γ_v, the net vapor generation per unit volume, in various boiling flow regimes. Below is discussed how these relationships may be combined or linked together to permit one to predict vapor generation at each position along a once-through boiler in which the flow is not, in general, in thermodynamic equilibrium. In discussing this problem two different situations will be considered: (a) the situation in which the point of inception of boiling in the duct wall and a bubble flow regime exists for some length downstream of this inception point, (b) the situation in which boiling first takes place in a duct as a result of superheated flow coming directly in contact with the interface or "head" of an annular vapor void.

The question of which of these situations is likely to prevail can be answered by means of the following analytical considerations.

If boiling first takes place in a duct by the mechanism of having nucleation take place at a site along the duct wall, then it seems physically reasonable to expect that such nucleation should satisfy the criteria for incipient nucleation set forth in Ref. 39. That is, for nucleation to take place at the duct of a wall requires a degree of superheating which is at least roughly predictable by the equations presented in Ref. 39. With this degree of superheat determined, one can next make the following calculations to determine whether or not a bubble flow regime will develop downstream from the boiling nucleation sites. One first calculates the maximum growth rate $\dot{R}_v$ of a single vapor bubble corresponding to the degree of bulk superheat associated with inception of nucleation. In making this calculation one has to make some decision concerning the appropriate value to use for C, the coefficient of vaporization*. Having determined $(\dot{R}_v)_{max}$, one can then apply the rough criterion that for bubble flow to develop $(\dot{R}_v)_{max}$ must

---

*There is little experimental information available at present to guide one in this choice. Hopefully, more information will become available in the future. At present it is recommended that one take C = 1.

be less than the inlet velocity of liquid into the boiler tube. Should this criterion be met, then one would proceed to analyze the flow in the duct in the following manner.

For a first attempt to treat force convection boiling flow, the single discrete source model may be analyzed. Most of the important physical features would be displayed in the results of such an analysis. The experience gained in the mathematical treatment of this simpler problem would be a logical starting point for the development of a comprehensive analysis which would synthesize a statistical distribution of nucleation sites on the duct wall.

As liquid superheat is released in the bubble flow regime due to growth of discrete bubbles, a point will be reached where the bubble flow regime will cease and a transition to a higher vapor flow rate type of flow regime will occur. As noted earlier, insofar as calculation of Γ_v is concerned, it is proposed that it be considered that bubble flow be followed directly by annular flow, and that transition flow regimes such as slug flow or coelescing flow be neglected. Our constitutive model for annular flow is that at the "head" or start of this flow regime, all superheat present in the approaching liquid flow is released immediately, and that downstream of this point, for the remainder of the annular flow regime, thermodynamic equilibrium be maintained. The point at which the bubble flow regime would be considered to end would be determined as a function of vapor flow quality according to the best empirical data available for mapping flow regimes. [c f Ref. 16].

In summary then, our overall model for thermodynamic non-equilibrium vapor generation in flow situations where annular flow would be proceeded by bubble flow is one of incipient nucleation occurring at a degree of superheat predicted by the criteria of Ref. 39, followed by gradual and continuous release of superheat due to individual bubble growth rate. This is then followed by instantaneous release of all remaining superheat as the start of the annular flow regime is reached, and the maintaining of thermodynamic equilibrium throughout the remainder of the annular flow regime.

Should bubble growth rate at the point of inception of nucleation be sufficiently large such that a bubble flow regime would not be obtained, then the situation would be quite adequate by "flashing" of superheated liquid into a flow regime having a continuous central vapor void. The constitutive model for this flow situation would be one of immediate and discontinuous release of liquid superheat at the head of this annular flow regime. The problem to be solved relevant to this flow regime concerns the stability of the location of the "head" of the annular flow regime. The question of whether or not the head of the central vapor void can remain fixed in space can be answered by applying the criterion for vapor void propagation developed earlier in this report. Should this criterion predict that the vapor void head velocity v be zero, then the head of the void will remain stably "attached" to the point of inception of nucleation. Should this criterion predict that v be negative, than the void would tend to be washed downstream and one would again be forced to consider the existence of a bubble flow regime preceding an annular flow regime. Should this criterion predict that the void tend to propagate upstream, then one would be led into an analysis of the propagation of a central void, such as the one developed earlier in this report, in order to determine whether the head of the central void can take up a stable position or would tend to oscillate indefinitely, leading to an instability of the type frequently observed in liquid metal boiling flows when considerable superheat is required for inception of nucleation.

For both the situation where annular flow is preceeded by a bubble flow regime and the situation where it is not, the condition will finally be reached in a once-through boiler where the liquid content of the flow is sufficiently small such that a continuous liquid film is not maintained over the periphery of the duct, and the flow will pass from the annular flow regime to the dispersed flow regime.

Experimental information on the transition from the annular regime to the dispersed flow regime is limited to ordinary fluids and the effect of heat flux has been postulated to be related to the "critical heat flux" burn-out correlation. Consistent with the latter thinking, a heat balance between the vaporizing heat of the impinging droplets and the input heat flux provides a condition which

should be an upper limit estimate in the extent of the annular flow regime, since additional hydrodynamic effect would be present to breakup the liquid film on the duct wall. The transition from annular to despersed flow regime can be delayed by employing swirl-inducing tube geometries for once-through boiler.

Once the dispersed flow regime is reached, further evaporation of the liquid droplets would again take place with superheating simultaneously present in the vapor phase, in the droplets themselves, as well as at the duct wall. So far as a total field description of the hydraulic system, the dispersed flow regime is relatively more completely defined at the level of phenomenological first principles. The actual computation, however, is contingent on the availability of adequate initial conditions, which would be, at least in part, dependent on the upstream history of other flow regimes.

REFERENCES

1. Zuber, N. and Dougherty, D.E., "Liquid Metals Challenge to the Traditional Methods of Two-Phase Flow Investigation", Submitted for Presentation at the EURATOM Symposium of Two-Phase Flow Dynamics, Tech. Univ. of Eindhoven, Eindhoven Holland, September 4-9 (1967).

2. Lord Rayleigh, "On the Pressure Developed in a Liquid During the Collapse of a Spherical Cavity", Phil. Mag. S. 6, Vol. 34, No. 200, pp 94-98, August (1917).

3. Plesset, M.S. and Zwick, S.A., "The Growth of Vapor Bubbles in Superheated Liquids, Journal of Applied Physics, Vol. 25, pp 493-500 (1954).

4. Forster, H.K. and Zuber, N., "Growth of a Vapor Bubble in a Superheated Liquid", Journal of Applied Physics, Vol. 25, No. 4, pp 474-478, April (1954).

5. Birkhoff, G., Margulies, R.S. and Horning, W.A., "Spherical Bubble Growth", Physics of Fluids, Vol. 1, No. 3, pp 201-204, May-June (1958).

6. Griffith, P., "Bubble Growth Rates in Boiling", Trans. ASME, Vol. 80, pp 721-727, (1958).

7. Scriven, L.E., "On the Dynamics of Phase Growth", Chemical Engineering Science, Vol. 10, Nos. 1/2, pp 1-12, (1959).

8. Bankoff, S.G., "Asymptotic Growth of a Bubble in a Liquid with Uniform Initial Superheat", Applied Science Res., Section A, Vol. 12, pp 267-281, (1963-1964)

9. Theofanous, T., Biasi, L., Isbin, H.S., and Fauske, H., "A Theoretical Study of Bubble Growth in Constant and Time-Dependent Pressure Fields", Accepted for Publication in Chemical Engineering Science.

10. Bornhorst, W. J. and Hatsopoulos, G.N., "Bubble-Growth Calculation Without Neglect of Interfacial Discontinuities", Journal of Applied Mechanics, pp 847-853, (1967)

11. Waldman, L.A. and Houghton, G., "Spherical Phase Growth in Superheated Liquids", Chemical Engineering Science, Vol. 20 pp 625-636, (1965).

12. Lewis, James P., Groesbeck, Donald E. and Christenson, Harold H., "Tests of Sodium Boiling in a Single Tube-in-Shell Heat Exchanger Over the Range 1720° to 1980°F (1211 to 1355 K), NASA Technical Note, NASA TN D-5323, July (1969).

13. Bond, J.A. and Converse, G.L., "Vaporization of High-Temperature Potassium in Forced Convection at Saturation Temperatures of 1800° to 2100°F", NASA Contractor Report, NASA CR-843, July (1967).

REFERENCES (Continued)

14. Hunsaker, J.C. and Rightmire, B.G., "Engineering Applications of Fluid Mechanics", 2nd Edition, McGraw Hill Book Co., New York, N.Y.

15. Von Glahn, Uwe H., and Polcyn, Richard P., "On the Effect of Heat Addition in the Empirical Correlation of Void Fractions for Steam-Water Flow", NASA Technical Note, NASA TN D-1440, November (1962).

16. Vohr, John H., "Flow Patterns of Two-Phase Flow - A Survey of Literature", Prepared for U.S. Atomic Energy Commission, Report TID-11514, Contract No. AT(30-3)-187, Task IX, December (1960).

17. Hoffman, E.E., "Boiling Potassium Stability Studies", Metals and Ceramics Division Annual Progress Report for Period Ending May 31, 1963, ORNL-3470, pp 114-118, November (1963).

18. Glasstone, S. and Edlund, M., "The Elements of Nuclear Reactor Theory", Von Nostrand Co., Inc. (1957).

19. Peterson, J.R., "High Performance "Once-Through" Boiling of Potassium in Single Tubes at Vapor Temperatures from 1500°F to 1750°F", Topical Report Prepared for NASA under Contract NAS 3-2528 (1966).

20. Laverty, W.F., and Rohsenow, W.M., "Film Boiling of Saturated Nitrogen Flowing in a Vertical Tube", Trans. of ASME, Journal of Heat Transfer, pp 90-98, February (1967).

21. Zuber, N., Dougherty, D.E., "Fluid Dynamics of Dispersed Two-Phase Vapor-Liquid Flow in Lubricant Films", Part I & II, MTI Technical Report MTI-68TR30, (1968).

22. Lee, Kwan, and Ryley, D.J., "The Evaporation of Water Droplets in Superheated Steam", Trans. ASME, Journal of Heat Transfer, pp 445-451, November (1968).

23. Goldmann, K., Firstenberg, H., and Lombardi, C., "Burnout in Turbulent Flow - A Droplet Diffusion Model", Trans. ASME, Journal of Heat Transfer, pp 158-162, May (1961).

24. Topper, L., "A Diffusion Theory Analysis of Boiling Burnout in the Fog Flow Regime", Trans. ASME, Journal of Heat Transfer, pp 284-285, August (1963).

25. Forslund, R.P., Rohsenow, W.M., "Dispersed Flow Film Boiling", Trans. ASME, Journal of Heat Transfer, pp 399-406, November (1968).

26. Ingebo, R.D., "Drag Coefficients for Droplets and Solid Spheres in Clouds Accelerating in Airstreams", NACA TN 3762, September (1956).

REFERENCES (Continued)

27. Baumeister, K.J., Hamill, T.D., and Schoessow, G.J., "A Generalized Correlation of Vaporization Times of Drops in Film Boiling on a Flat Plate", US-AIChE No. 120, 3rd International Heat Transfer Conference and Exhibit, August 7-12 (1966).

28. Tsubouchi and Sato, "Heat Transfer Between Single Particles and Fluids in Relative Forced Convection", Chemical Engineering Progress Symposium Series, Vol. 55, 1960.

29. Isshiki, N., "Theoretical and Experimental Study on Atomization of Liquid Drop in High Speed Gas Stream", Report No. 35, Transportation Technical Research Institute, Tokyo, Japan.

30. Baker, O., "Simultaneous Flow of Oil and Gas", Oil Gas Journal, 53, 12, 185-190 (1954).

31. Quandt, E., "Analysis of Gas-Liquid Flow Patterns", Heat Transfer-Boston, Chemical Engineering Progress Symposium Series, No. 57, Vol. 61, 128-135, (1965).

32. Kozlov, B. K., "Forms of Flow of Gas-Liquid Mixtures and their Stability Limits in Vertical Tubes", Zh. Tekh. Fiz., 24, 2285-2288 (1954), Translated by Assoc. Tech. Services, Translation 136R.

33. Levy, S., "Steam Slip-Theoretical Prediction From Momentum Model", Journal of Heat Transfer, ASME Trans., Series C, Vol. 82, 113-124 (1960).

34. Tippets, F. E., "Analysis of the Critical Heat-Flux Condition in High Pressure Boiling Water Flows", Journal of Heat Transfer, ASME Trans., Series C, Vol. 86, 23-38, February (1964).

35. Isbin, H. S., Vanderwater, R., Fauske, H., and Singh, S., "A Model for Correlating Two-Phase, Steam-Water, Burnout Heat Transfer Fluxes", Journal of Heat Transfer, ASME Trans., Series C, Vol. 83, 149-157, May (1961).

36. Collier, J. G., Wikhammer, G. A., Moeck, E. O., and MacDonald, I.P.L., "The Effect of Certain Geometrical Factors on Dryout for High Quality Steam/Water Mixtures Flowing in a Vertical Internally Heated Annulus at 1,000 lb/sq.in. Abs.", Series, No. 57, Vol. 61, 192-204, (1965), Heat Transfer-Boston, Chemical Engineering Progress Symposium

37. Hewitt, G. F., Kearsey, M. A., Lacey, P.M.C., Pulling, D. J., "Burnout and Nucleation in Climbing Film Flow", AERE-R-4374 (1963).

38. Lacey, P.M.C., Hewitt, G. F., Collier, J. G., "Climbing Film Flow", AERE-R-3962 (1962).

39. Levy, S., "Critical Heat Flux in Forced Convection Flow", Lecture Series on Boiling and Two-Phase Flow for Heat Transfer Engineers, Univ. of California at Berkeley and Los Angeles, May 27-28, 1965.

40. Biasi, L., Clerici, G. C, Salu, R., and Tozzi, A., "A Non-Equilibrium Description of Two Phase Annular Flow", International Journal of Heat and Mass Transfer, 12, 3, 319-331 (1969).

41. Vohr, J. H. and Chiang, T., "A Review of Criteria for Predicting Incipient Nucleation in Liquid Metals and Ordinary Fluids", Technical Report MTI-69TR45, Prepared for NASA Headquarters, Washington, D.C., under Contract NASw-1705, Mechanical Technology Incorporated, Latham, N. Y. 12110, Nov. (1969).

FIGURES

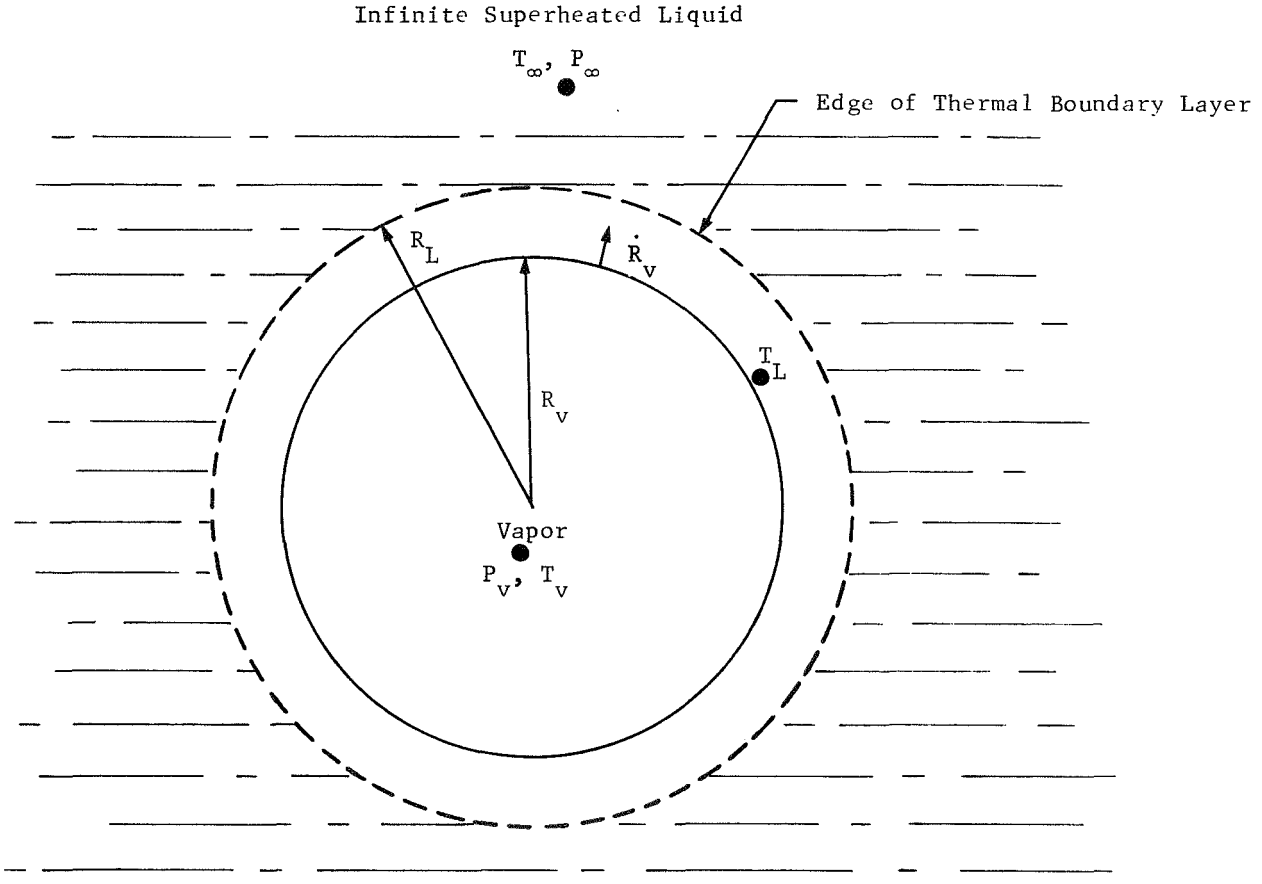

Fig. 1 Schematic of Vapor Bubble Growing in Infinite Superheated Liquid

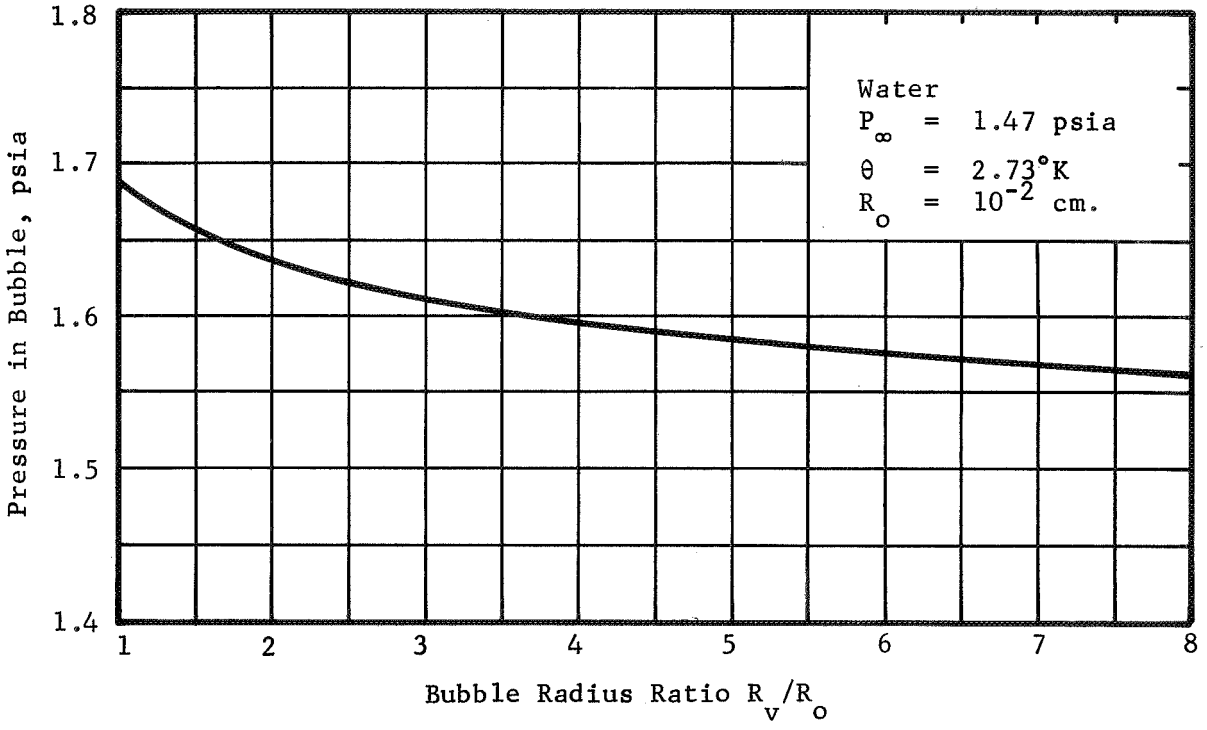

Fig. 2 Bubble Pressure Vs. Bubble Radius Ratio

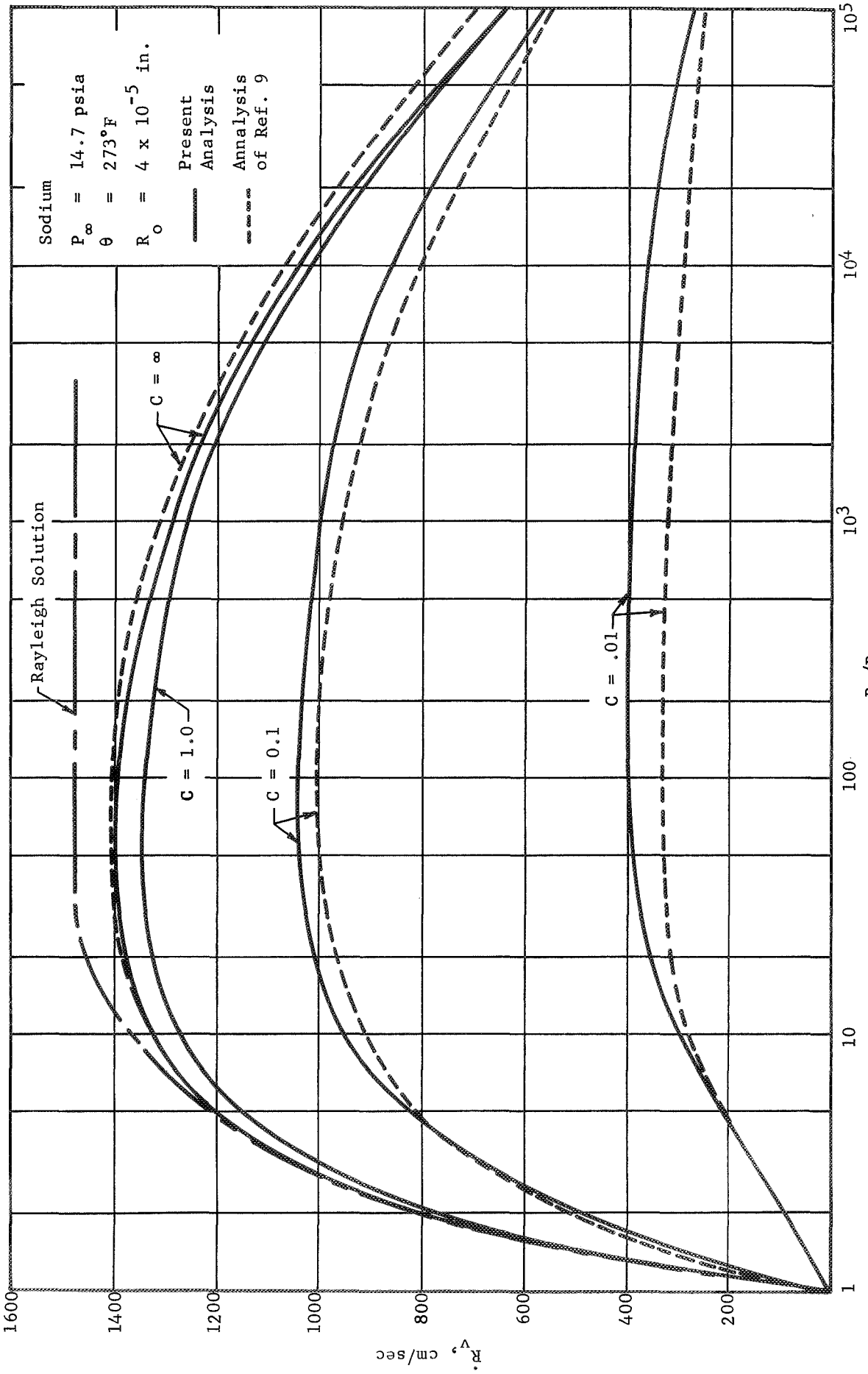

Fig. 3 Bubble Growth Rate for Superheated Sodium

MU1-10075

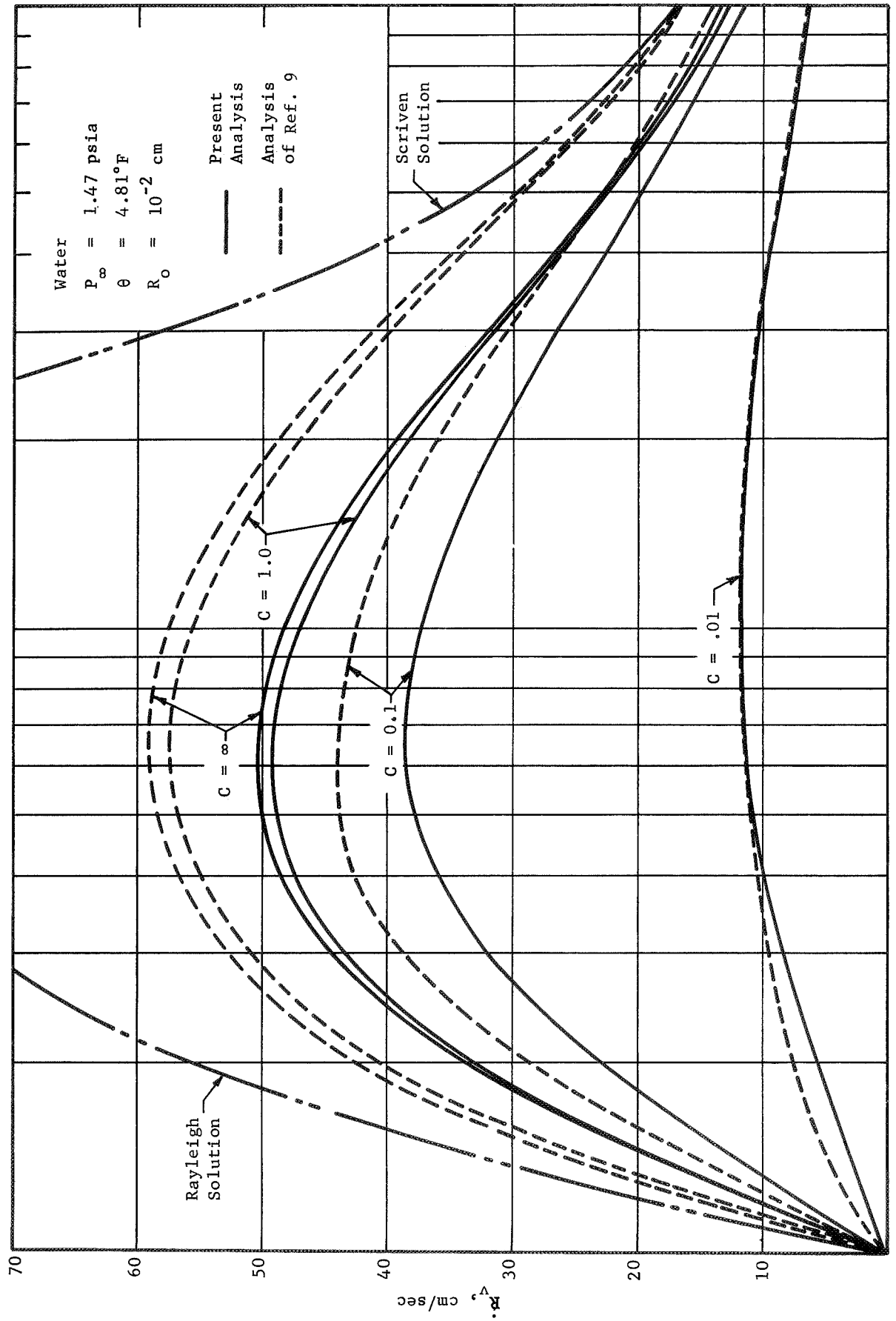

Fig. 4 Bubble Growth Rate for Superheated Water

MTI-10074

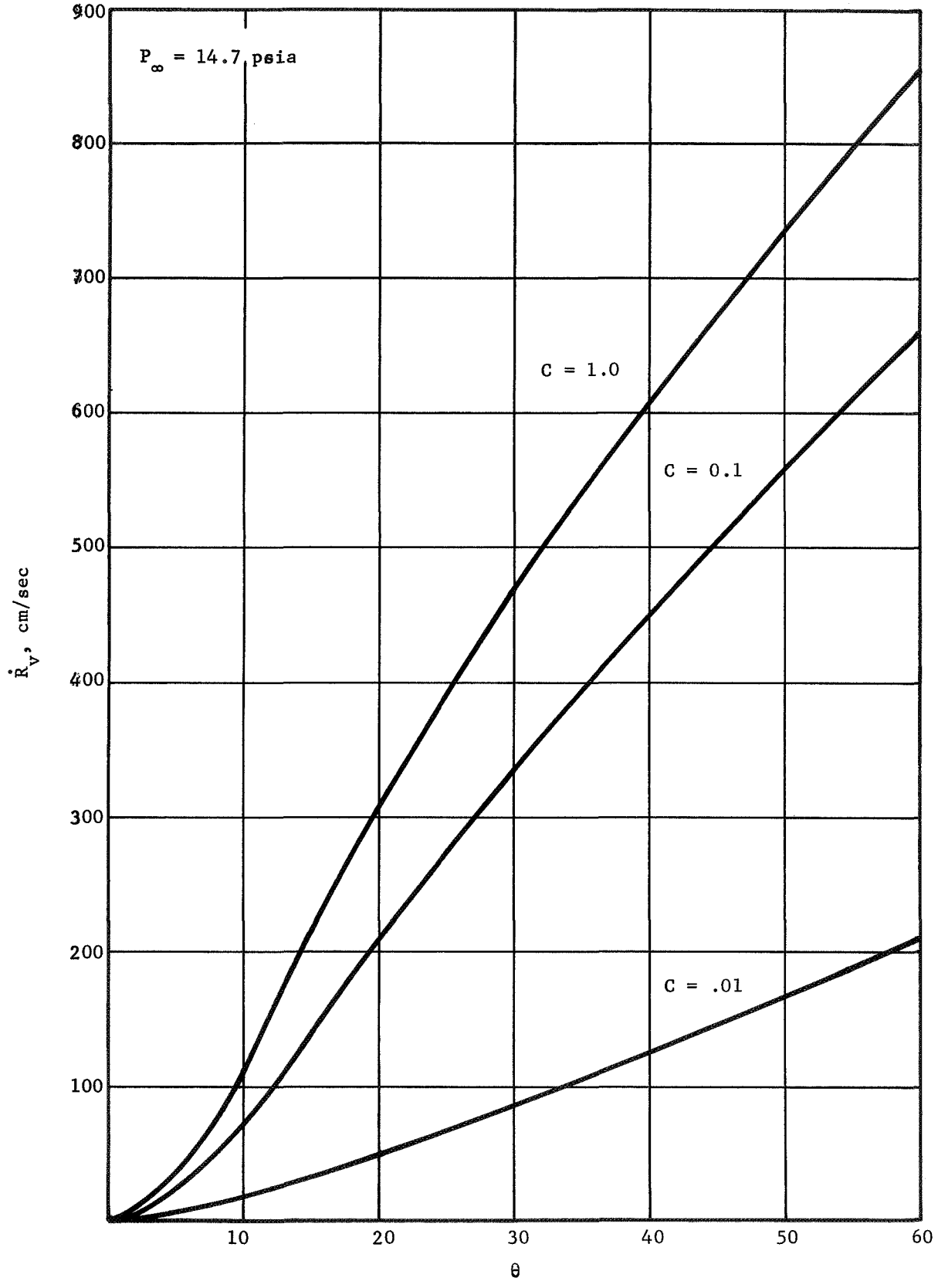

Fig. 5 Maximum Bubble Growth Rate vs Superheat in Water

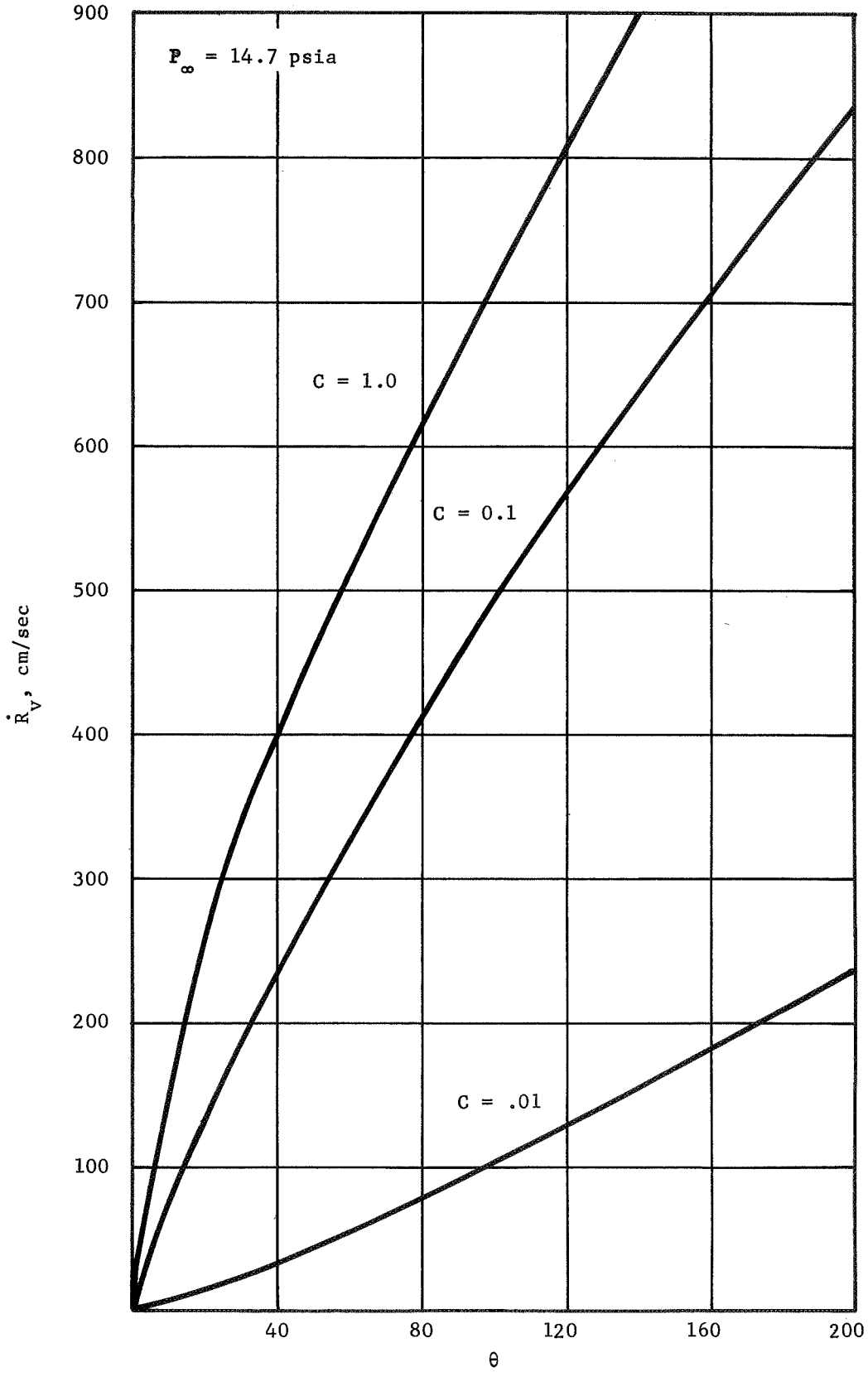

Fig. 6 Maximum Bubble Growth Rate vs Superheat in Potassium

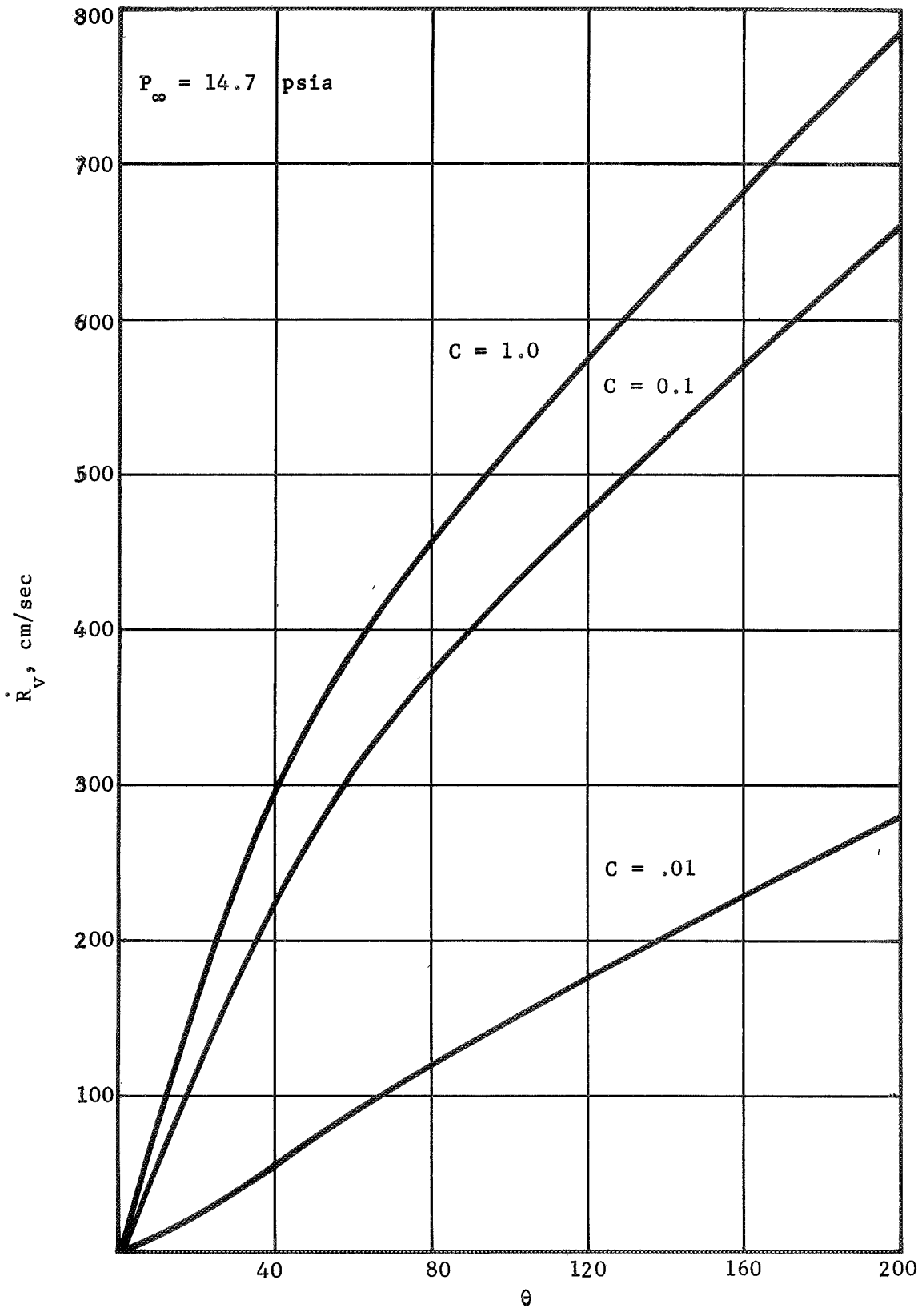

Fig. 7 Maximum Bubble Growth Rate vs Superheat in Cesium

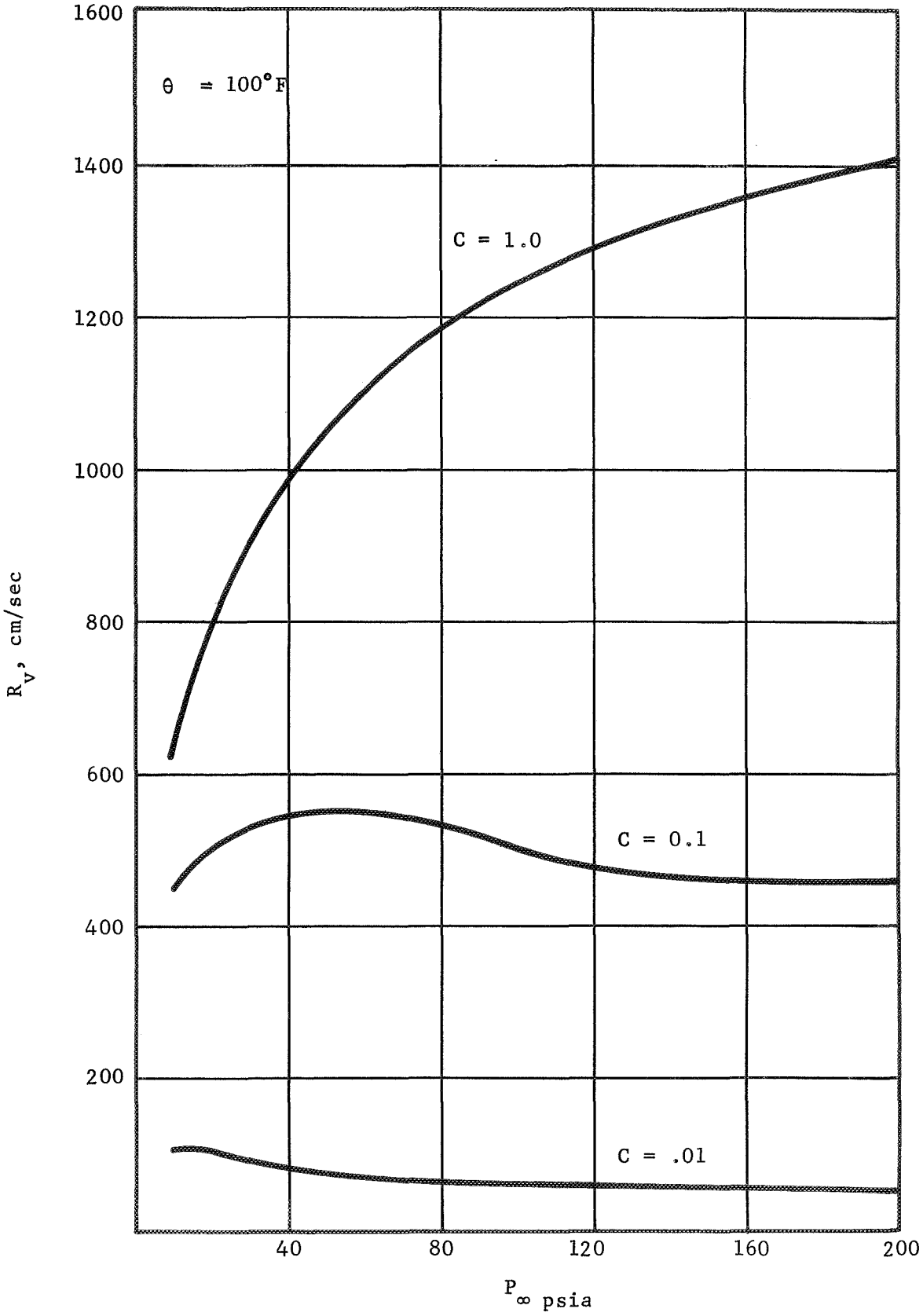

Fig. 8 Maximum Bubble Growth Rate vs. System Pressure in Potassium

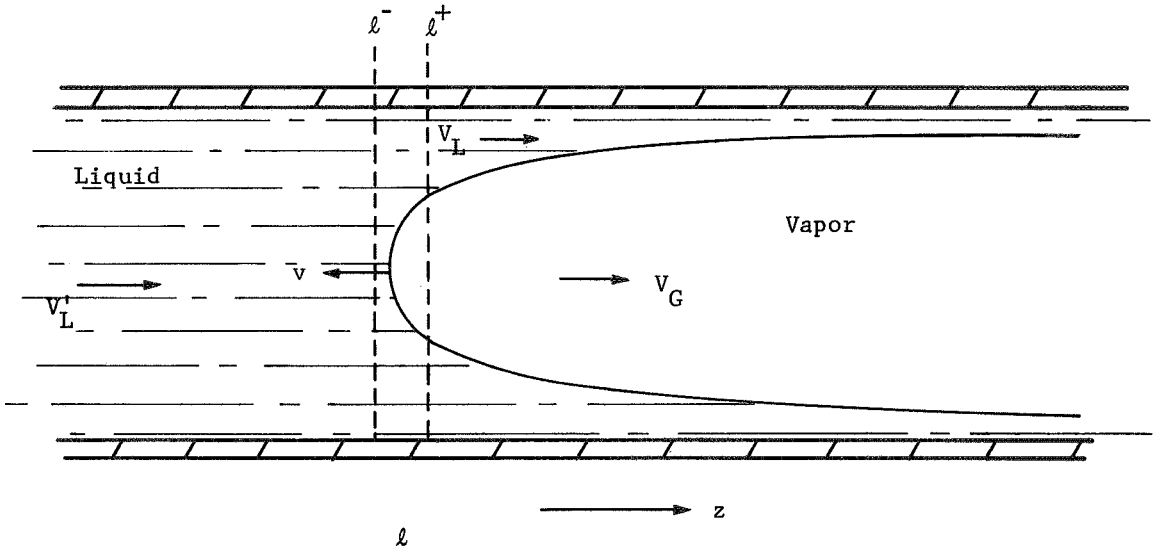

Fig. 9 Schematic of Propogating Void in Duct

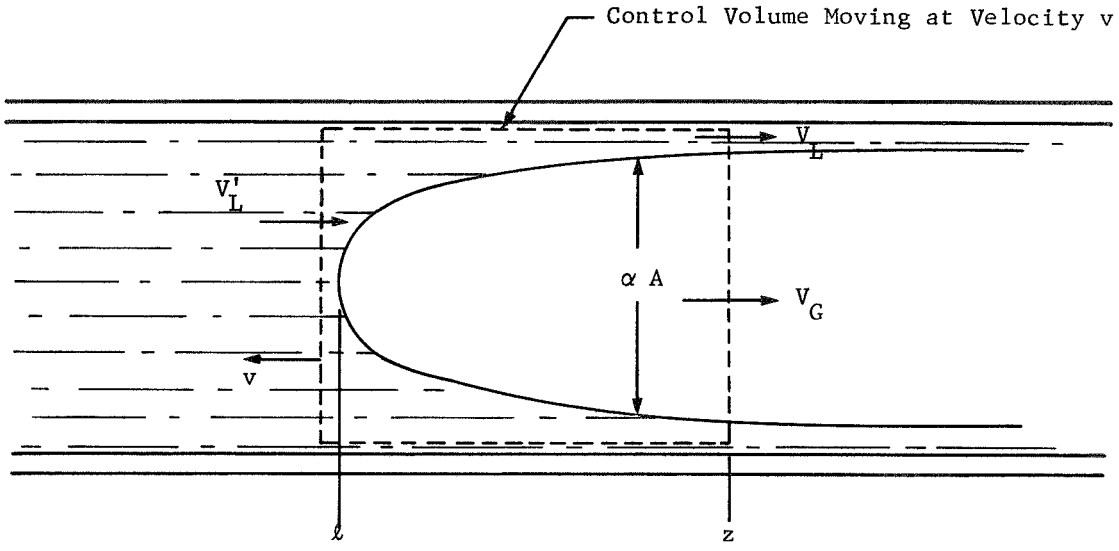

Fig. 10 Control Volume

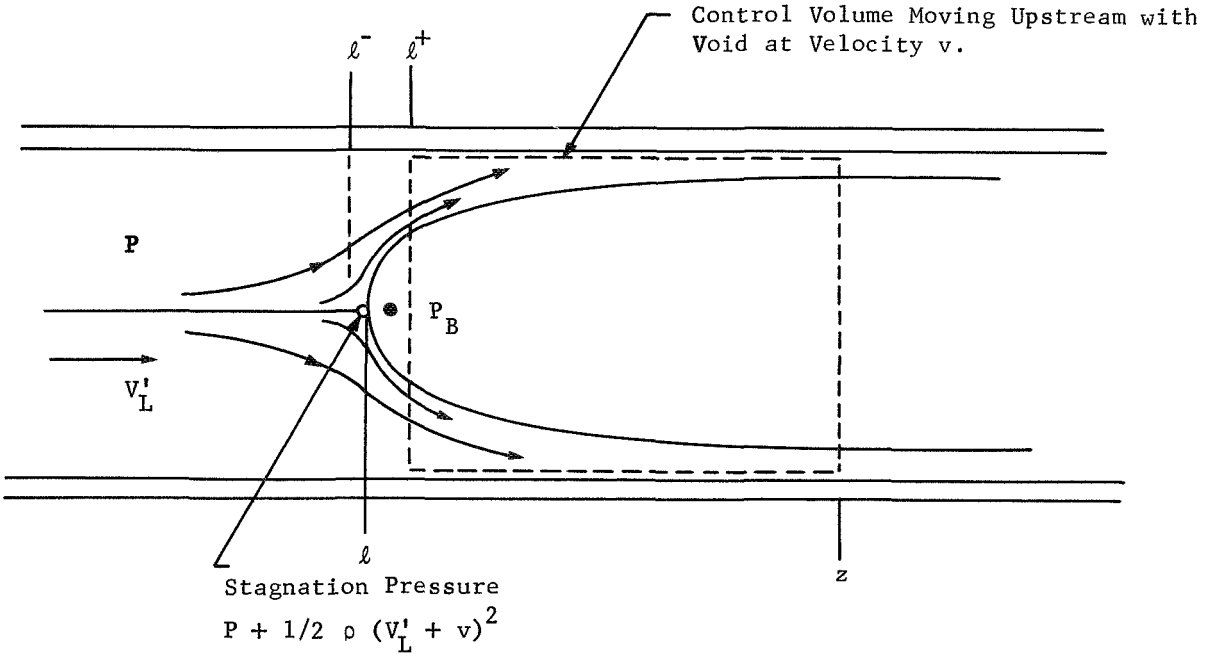

Fig. 11 Stagnation Pressure at Nose of Propogating Void

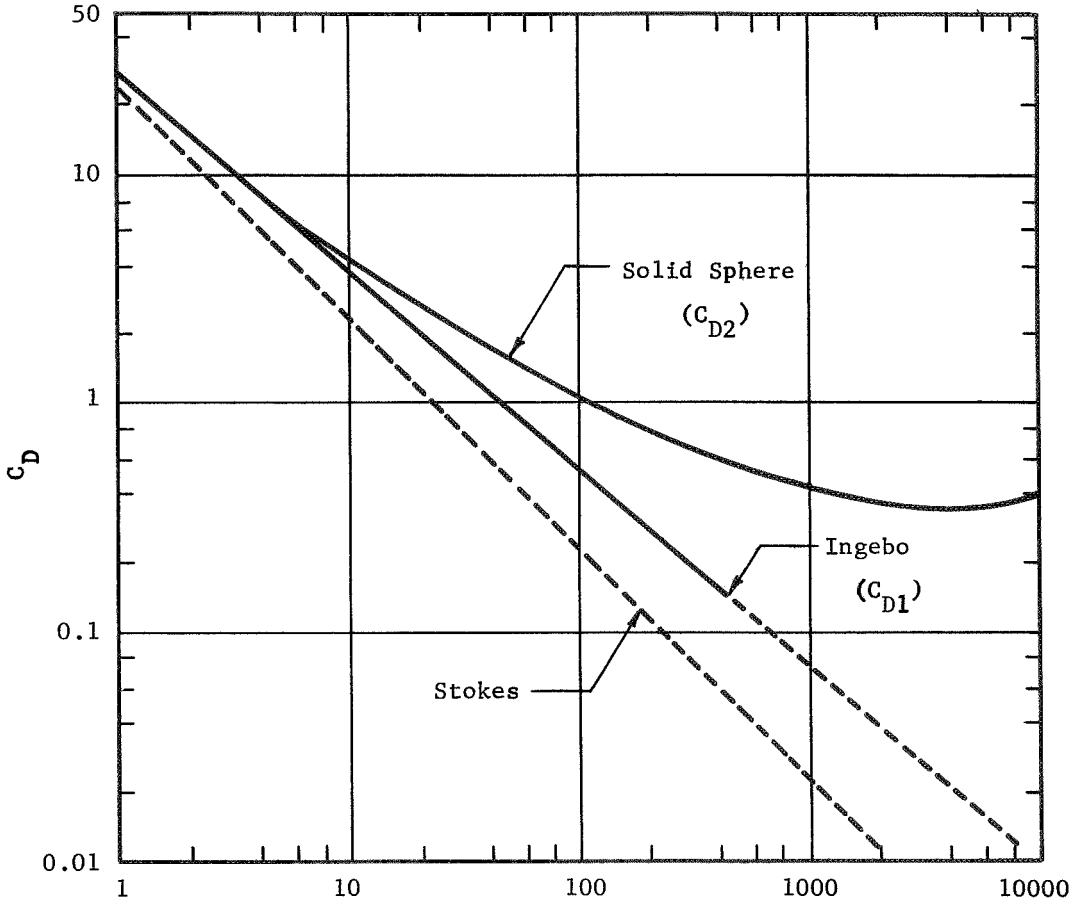

Fig. 12 Drag Coefficients

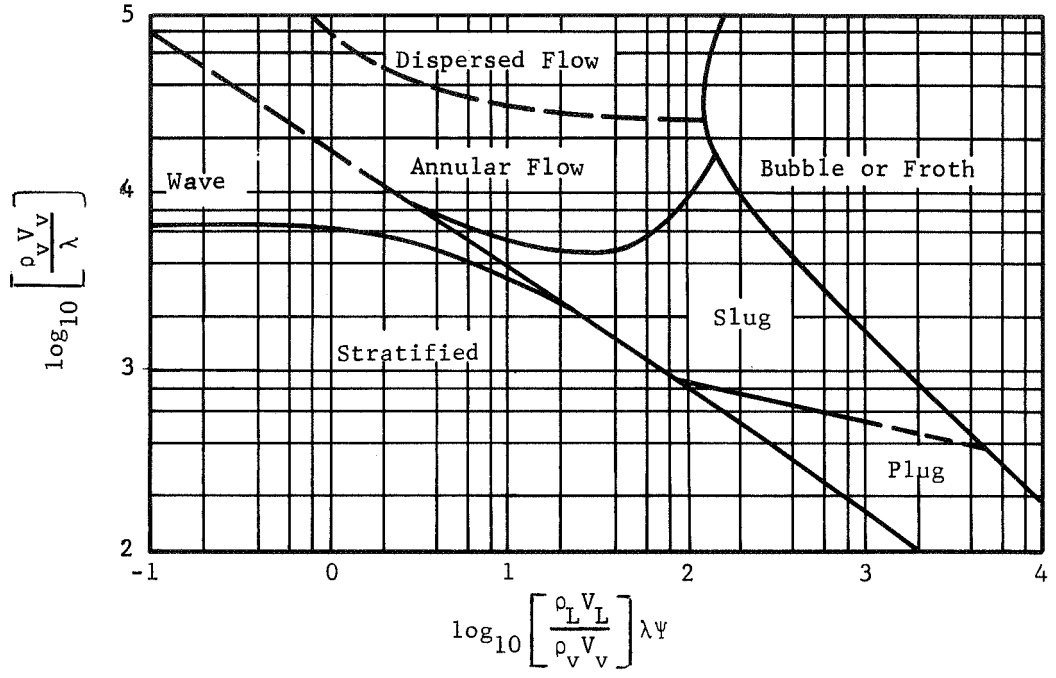

$$\lambda = \left[\left(\frac{\rho_v}{0.075}\right)\left(\frac{\rho_L}{62.3}\right)\right]^{1/2}$$

$$\Psi = \left(\frac{73}{\sigma}\right)\left[\mu_L\left(\frac{62.3}{\rho_L}\right)^2\right]^{1/3}$$

units: ρ_v, ρ_L lbs/ft^3

σ dynes/cm

μ_L centipoise

Fig. 13 Flow-Pattern Regions
(Baker Chart [30])

NOMENCLATURE

a_L	=	Droplet acceleration
A	=	Cross sectional area of the duct
C	=	Vaporization coefficient
C_D	=	Drag coefficient for liquid droplets
(C_{D1})	=	Steady-state drag coefficient for liquid droplets
(C_{D2})	=	Steady-state drag coefficient for solid sphere
$(C_P)_L$	=	Constant pressure specific heat of liquid
dz	=	The number of vapor bubbles lying in the size interval R_v to $R_v + dR_v$
D	=	Diameter of the duct
f	=	Friction factor
g_c	=	Gravitational constant
g_n	=	Effective acceleration perpendicular to the axial direction
g_z	=	The component of gravitational acceleration along the duct
h_{fg}	=	Latent heat of vaporization
$(h_{fg})_{in}$	=	Heat of vaporization of liquid evaluated at inlet pressure
$(dh_v/dp)_{sat}$	=	Enthalpy - pressure derivatives of saturated vapor
$(dh_L/dp)_{sat}$	=	Enthalpy - pressure derivatives of saturated liquid
h_v	=	Specific enthalpy of saturated vapor
h_L	=	Specific enthalpy of saturated liquid
J	=	Mechanical equivalent of heat converting thermal to mechanical units
K_v	=	Thermal conductivity of the vapor
K.E.	=	Kinetic energy
K_L	=	Thermal conductivity of the liquid
ℓ	=	Spacing between consecutive bubbles; also axial location of the nose of the void

ℓ^+ = Location just downstream of the nose of the void

ℓ^- = Axial location just upstream of the nose of the void

$\dot{m}$ = Net evaporation rate of fluid

n = Bubble density in the size interval between R_v and $R_v + dR_v$

N = Bubble density per unit length

N_L = Number of droplets per unit volume

P = Static system pressure in the liquid just ahead of the bubble, also denoted as $P_{z=\ell^-}$

ΔP = Pressure change across the nose of the moving void

$\Delta P^*(z)$ = Pressure change occurring from ℓ^+ to $z > \ell$

Pr = Prandtl number of the vapor

P_v = Vapor pressure inside the bubble

P_L = Pressure of the liquid at the bubble surface

P_L^* = Saturation vapor pressure corresponding to T_L

$P_{L\infty}^*$ = Saturation vapor pressure corresponding to T_∞

P_∞ = Liquid pressure

q = Heat input per unit length of duct

q''_{fl} = Liquid side conduction heat flux at droplet surface

q''_v = Heat flux into the liquid drpplet from the superheated vapor

$\frac{dQ}{dt}$ = Rate of heat transfer into the bubble

r = Radius

R = Gas constant

R_o = Nucleation radius of vapor bubbles

R_v = Vapor bubble radius

$\dot{R}_v$ = Bubble radius growth rate

R_L = Radius at edge of the thermal boundary layer in the liquid

s = Vapor slip

S = Nucleation source strength

S_o = Number of bubbles nucleated per second at the single discrete source located at $z = z'$

t = Time

Δt = Time interval used in numerical integration

T = Temperature

$\left(\frac{dT}{dp}\right)_{sat}$ = Saturation temperature - pressure derivative

ΔT_w^* = Dimensionless wall superheat

ΔT_L^* = Dimensionless liquid superheat

T_{in} = Inlet temperature of liquid

T_v = Temperature of the vapor within the bubble

T_L = Temperature in the liquid at the bubble surface

T_{sat} = Saturation temperature corresponding to P_∞

T_w = Wall temperature

$T_{z=\ell^-}$ = Liquid temperature at the nose of the bubble

T_∞ = Temperature of the liquid

u_L = Specific internal energy of the liquid

$\frac{dU_v}{dt}$ = Time rate of change of the total internal energy inside the bubble

v = Propagation velocity of void

V = Volume of the bubble

$\bar{V}$ = Mass weighted mean velocity

V_m = Mean velocity of the mixture

V_L' = Velocity of liquid at duct entrance

$V_v(z,t)$ = Velocity of the vapor bubbles in the z direction

We = Weber number

X = Flow weighted quality

X_ℓ' = Flow quality just after the head of the void

X_{tt} = Dimensionless parameter in Lockhart-Martinelli correlation, see Eq. (86)

$X'(z)$ = Vapor mass flow quality

z = Axial distance

$\partial\tau/\partial z$ = Frictional pressure gradient for the two-phase flow in the duct

α = The fraction of the cross section area of the duct that is occupied by the vapor phase at the position z

Γ_f = Net rate of liquid mass formation per unit volume based on mean convection

Γ_v = Net rate of vapor mass formation per unit volume

δ = Droplet diameter

δ_i = Initial droplet diameter

$\delta(\ell)$ = Dirac delta function at ℓ

$\left(\frac{\delta N_L}{\delta t}\right)_w$ = Wall inpingement rate of liquid droplets

θ = Superheat

θ_{in} = Superheat of liquid at entrance to duct (may be negative)

κ = Average saturation pressure - temperature derivative between T_{sat} and T_∞

μ_L = Viscosity of the liquid phase

μ_v = Viscosity of the vapor phase

ρ_L = Liqdid density

ρ_v = Vapor density

ρ_v' = Saturation density of vapor evaluated at inlet pressure

σ = Surface tension

τ = Wall friction shear stress

φ = Dimensionless parameter defined by Eq. (32)

APPENDIX I

SOLUTION SCHEME FOR EQUATION (38) AND LISTING OF ASSOCIATED COMPUTER PROGRAM

Let us symbolically denote Eq. (34) as

$$\Psi(P_v) = 0 \tag{A-1}$$

where $\Psi(P_v)$ represents the entire left hand side of Eq. (34). Let us denote the existing n^{th} guess at the solution of Eq. (A-1) as P_{vn} and the n + 1 guess as P_{vn+1}. Since we want to select P_{vn+1} such that

$$\Psi(P_{vn+1}) = 0 \tag{A-2}$$

we can use the relationship

$$\Psi(P_{vn+1}) = \Psi(P_{vn}) + \frac{d\Psi(P_{vn})}{dP_v} (P_{vn+1} - P_{vn}) = 0 \tag{A-3}$$

in order to determine our n + 1 guess for P_v. Solving (A-3) for P_{vn+1} we obtain

$$P_{vn+1} = P_{vn} \frac{\Psi(P_{vn})}{\frac{d\Psi(P_{vn})}{dP_v}} \tag{A-4}$$

This is, in essence, the Newton-Raphson method for iterating to find the roots of an equation. It converges very rapidly provided the initial guess for P_v is reasonably close to the root being sought.

To apply the method expressed symbolically by Eq. (A-4) to Eq. (34), we need to obtain the derivative of the left hand side of Eq. (34) with respect to P_v i.e. $d\Psi/dP_v$. This derivative is

$$\frac{d\Psi(P_v)}{dP_v} = CRT_{sat}\left[- \frac{P_{L\infty}}{P_v^2} + \frac{1/2\ P_{L\infty}^{*}\ \varphi'}{P_v^2\sqrt{\left(\frac{P_{L\infty}^{*}}{P_v} - 1\right)\varphi' + \left(\frac{\varphi'}{2}\right)^2}}\right]$$

$$- \frac{2\pi RT_\infty/3\rho_L}{\sqrt{\frac{4\pi RT_\infty}{3\rho_L}\left\{(P_v - P_\infty)\left(1 - \frac{R_o^3}{R_v^3}\right) - \frac{3\sigma}{R_v}\left(1 - \frac{R_o^2}{R_v^2}\right)\right\}}} \qquad \text{(A-5)}$$

Since the solution we seek for P_v must give a positive value to the radical in Eq. (11) and also must be less than $P_{L\infty}^{*}$, we can state that our solution must lie in the range

$$P_\infty + \frac{3\sigma}{R_v}\ \frac{\left(1 - \frac{R_o^2}{R_v^2}\right)}{\left(1 - \frac{R_o^3}{R_v^3}\right)} < P_v < P_{L\infty}^{*} \qquad \text{(A-6)}$$

a reasonable first guess at a solution for P_v, which we'll denote as P_{v1}, would be halfway between the limits on P_v set by (A-6) i.e.

$$P_{v1} = 1/2\left[(P_{L\infty}^{*} + P_\infty) + \frac{3\sigma}{R_v}\ \frac{\left(1 - \frac{R_o^2}{R_v^2}\right)}{\left(1 - \frac{R_o^3}{R_v^3}\right)}\right] \qquad \text{(A-7)}$$

Our next guess for P_v i.e. P_{v2} would then be given by Eq. (A-4) i.e.

$$P_{v2} = P_{v1} - \frac{\Psi(P_{v1})}{\frac{d\Psi(P_{v1})}{dP_v}} \tag{A-8}$$

and so forth.

In using Eq. (A-4) to iterate for the solution for P_v, one must constantly check to make sure that the n + 1 guess for P_v predicted by Eq. (A-4) satisfies the inequalities indicated by (A-6). If Eq. (A-4) predicts a value for P_{vn+1} which is, say greater than $P_{L\infty}^*$, then one must not accept this value for P_{vn+1}, but should, instead, evaluate P_{vn+1} from the relation

$$P_{vn+1} = \frac{P_{vn} + P_{L\infty}^*}{2} \tag{A-9}$$

One then returns to Eq. (A-4) to evaluate P_{vn+2}.

Similarly, if Eq. (A-4) predicts a value for P_{vn+1} which is less than the lower limit on P_v, one must then evaluate P_{vn+1} from the relationship

$$P_{vn+1} = 1/2 \left[P_{vn} + P_\infty + \frac{3\sigma}{R_v} \frac{\left(1 - \frac{R_o^2}{R_v^3}\right)}{\left(1 - \frac{R_o^3}{R_v^3}\right)} \right] \tag{A-10}$$

In principle, the iteration scheme outlined above for solving Eq. (34) can be done by hand, convergence to a very high degree of accuracy (four significant figures) being obtained usually in three to four iterations. However, the algebra involved in evaluating $\Psi(P_v)$ and $d\Psi(P_v)/dP_v$ is tedious, and since the iteration scheme is very easy to program for a computer, this was done. For the convenience of the reader, this program is listed on following pages in this Appendix together with a description of the input to the program. The program is written in FORTRAN IV for a Control Data Corporation 6600 computer.

COMPUTER PROGRAM FOR DETERMINING BUBBLE GROWTH

A computer program has been written for solving the equations described in the text using a Newton Raphson Convergence technique.

An input description, listing and example of input, output follows:

Input Description

Card 1	Format (55H)
Title	Alphameric description of case to be investigated
Card 2	**Format (1015)**
NINT	Iteration limit - usually set equal to 20. When exceeded, indicates a possible error in input.
NCV	Diagnostic control - when set equal to 1, program prints number of iteration step and pressures currently being used by the Newton Raphson technique. Used for debugging purposes. Usually set equal to 0.
LAST	Set equal to 0 for another case to follow. Set equal to 1, indicates the last case will be read.
NOOFC	Total number of coefficients of vaporizations to be read.
MAXRV	Set equal to 0 for normal use. Set equal to 1 if interest is only in the maximum value of $\dot{R}_v$. As soon as program determines a decrease in $\dot{R}$ it will procede to the next set of conditions. If more accuracy is desired, resubmittal is required with finer increments around the maximum $\dot{R}_v$ attained.
Card 3	**Format (8E10.3)**
PA	Ambient pressure of liquid (P_∞), units - lb/in^2
TA	Ambient temperature of liquid (T_∞), units - ^oR
TASTAR	Saturation temperature of liquid corresponding to P_∞ (T_∞*), units - ^oR
Card 4	**Format (8E10.3)**
BKL	Thermal conduction of liquid corresponding to T_∞ (K_L), units - BTU/(sec.in ^oR)

CP	Specific heat of liquid corresponding to T_∞ (C_p), units - BTU/(lb ^oR)
RHOL	Density of liquid corresponding to T_∞ (ρ_L), units - lb/in^3
SIGMA	Surface tension corresponding to T_∞ (σ), units - lb/in
PLSTAR	Saturation pressure of liquid corresponding to T_∞ (P_L^*), units - lb/in^2

Card 5 Format (8E10.3)

RHOV	Density of vapor corresponding to T_∞ (ρ_v), units lb/in^3
R	Gas constant of vapor, units - in/^oR
ADDC(1)	First value of coefficient of vaporization
ESP	Convergence limit (usually .001)

Card 6(a → MORER = 1) Format (3E10.3,I5)

(RR = Radius Ratio = R_v/R_o

RRI	Initial value of R_v/R_o
RRF	Final value of R_v/R_o
RINC	Increment
MORER	Set equal to 0 indicates another set to follow. Set equal to 1 indicates the last set is being read. This parameter allows the program to build an array of R_v/R_o in unequal intervals by using sets of equal intervals.

Ex.	RRI	RRF	RINC	MORER
	2.	10.	1.	0
	20.	100.	10.	0
	200.	1000.	100.	1

Card 7 Format (8E10.3)

ADDC(I) I≥2 NOOFC	Additional values of the coefficient of vaporization. This card may be omitted if NOOFC equal to 1.

```
      PROGRAM GROWTH (INPUT,OUTPUT,TAPE5=INPUT,TAPE6=OUTPUT)
C BUBBLE GROWTH WITH HEAT TRANSFER  - JULY 1,1969
      DIMENSION RAD(30),ADDC(10)
      FA1(P)= FAC2*((PLSTAR/P-1.)+PHI/2.-SQRT((PLSTAR/P-1.)*PHI+(PHI/2)*
     1*2))
      FA2(P) =  FAC1* SQRT((2./(3.*RHOL)*((P-PA)*RR3-(3.*SIGMA/RV*RR2)))
     1*GC)
      FA1P(P)=FAC2*(.5*PHI*PLSTAR/P**2/SQRT((PLSTAR/P-1.)*PHI+PHI**2/4.)
     1 -PLSTAR/P**2)
      FA2P(P)=.5*FAC1*RR3*SQRT((2./(3.*RHOL)/((P-PA)*RR3-(3.*SIGMA/RV*R
     1R2)))*GC)
      NR=5
      NW=6
   12 READ(NR,100)
      WRITE(NW,100)
      READ(NR,103) MINI,MCV,LAST,NOOFC,MAXRV
      PI = 3.14159
C  GC = IN/SEC**2
      GC = 386.088
C
C  PHYSICAL PROPERTIES OF LIQUID
C  BKL=THERMAL CONDUCTIVITY - BTU/R-IN-SEC
C  CP=SPECIFIC HEAT- BTU/LB-R
C  PA= PRESSURE - LB/IN**2
C  RHOL= DENSITY - LB/IN**3
C  DELH= LATENT HEAT VAPORIZATION- BTU/LB
C  SIGMA= SURFACE TENSION - LB/IN
C  TA = TEMP - R
C  PLSTAR = SATURATION PRESSURE AT TA  - LB/IN**2
C  TASTAR=TEMPERATURE AT PA- R
C
      READ(NR,101) PA,TA,TASTAR
      READ(NR,101) BKL,CP,RHOL,DELH,SIGMA,PLSTAR
C
C  PHYSICAL PROPERTIES OF VAPOR
C  RHOV=DENSITY AT SATURATION CONDITIONS AND TA - LB/IN**3
C  R = GAS CONSTANT -  IN/R
C  C = COEFFICIENT OF VAPORIZATION
      RO=2.*SIGMA/(PLSTAR-PA)
C  RO= INITIAL BUBBLE RADIUS - IN
C
      READ(NR,101) RHOV,R, ADDC(1),ESP
C
      WRITE(NW,112) PA,TA,TASTAR
      WRITE(NW,113) BKL,CP,RHOL,DELH,SIGMA,PLSTAR
      WRITE(NW,108) RHOV,R,RO
      XKK=(PLSTAR-PA)/(TA-TASTAR)
      NORAD=1
C
C  RR IS  RV/RO   MORER =1,LAST SET , =0,ANOTHER SET TO FOLLOW
C
   10 READ(NR,102) RRI,RRF,RINC,MORER
      RAD(NORAD)=RRI
  200 NORAD=NORAD+1
      IF(RAD(NORAD-1).GE.RRF) GO TO 99
      IF(NORAD.GT.30) STOP1
      RAD(NORAD)=RAD(NORAD-1)+RINC
```

```
      GO TO 200
   99 IF(MOREK.EQ.0) GO TO 10
      NORAD=NORAD-1
      IF(NOOFC.GT.1) READ(NR,101)(ADDC(I),I=2,NOOFC)
      DO 30 J=1,NOOFC
      MAX=0
      C=ADDC(J)
      WRITE(NW,114)C
      OLDRV=R0
      OLDTIM=0.
      N=0
      FAC2=C*R*TASTAR
      OLDDOT=0.
      DO 40 K=1,NORAD
      RR=RAD(K)
      D2=       SQRT(TA    *8.*PI*R**3/GC)*BKL*CP*RHOL*TASTAR
      FAC1 = SQRT(2.*PI* R * TA / GC)
   20 RR3=1.-1./RR**3
      RR2=1.-1./RR**2
      RV = RR * R0
      P2 =  3. * SIGMA/RV * RR2
      PV=((PA+P2/RR3)+PLSTAR)/2.
      D1  = C* DELH**2 *  XKK**2 * RV *RR3
      PHI =   D1/D2
      IF(NCV.EQ.0) GO TO 25
      WRITE(NW,110) PHI
      GO TO 26
   25 IF(N.EQ.1) GO TO 26
      WRITE(NW,109)
   26 DO 70 I=1,NINT
      P1 =(PV-PA) * RR3
      P3 =  (PLSTAR -PV  )
      P4 = P3 * PHI + (PHI/2.)**2
      IF(PV.LT.PA) GO TO 40
      A1=FA1(PV)
      PSI=A1-FA2(PV)
      PSIP= FA1P(PV)-FA2P(PV)
      PV2 = -PSI/PSIP + PV
      IF(NCV.EQ.0) GO TO 27
      WRITE(NW,106) I,PV,PV2
   27 IF(PV2.GT.PLSTAR) PV2=(PV+PLSTAR)/2.
      IF(PV2.LT.(PA+P2/RR3)) PV2=(PV+PA+P2/RR3)/2.
      PSI2 =  FA1(PV2) - FA2(PV2)
      CHECK = ABS(PSI2/FA1(PV2))
      IF(CHECK.LT.ESP) GO TO 80
      PV = PV2
   70 CONTINUE
      WRITE(NW,104) NINT,PV,RV
      GO TO 40
   80 PV = PV2
      RVDOT =  FA1(PV)/FAC1
      DELR  =  SQRT(2.*BKL/(CP* RHOL* RV* RVDOT)*RR3)
      DELT  = DELH* PV  *SQRT( RV*RVDOT/(2.*BKL*CP* RHOL)*RR3)/R/TASTAR
      DOTAVE=(RVDOT+OLDDOT)/2.
      TIME = (RV-OLDRV)/DOTAVE+OLDTIM
      IF(MAXRV.EQ.1.AND.RVDOT.LT.OLDDOT) MAX = 1
      OLDRV=RV
      OLDTIM = TIME
```

```
      OLDDOT = RVDOT
      IF(NCV.EQ.1) WRITE(NW,109)
      RV=RV*2.54
      RVDOT=RVDOT*2.54
      WRITE(NW,105) RR,RV,PV,RVDOT,DELR,DELT,TIME
      N=1
      IF(MAX.EQ.1) GO TO 30
   40 CONTINUE
   30 CONTINUE
      WRITE(NW,111) ESP
      IF(LAST.EQ.0) GO TO 12
      CALL EXIT
  100 FORMAT(55H                \                                        )
  101 FORMAT(8E10.3)
  102 FORMAT(3E10.3,I5)
  103 FORMAT(10I5)
  104 FORMAT(21H MAXIMUM ITERATION OFI4,23H CURRENT VALUE OF PV IS, E10.
     13,  10H AT RV OF ,E10.3 /)
  105 FORMAT(7(1X,E11.4))
  106 FORMAT(I15,2E14.7)
  108 FORMAT(/30X,19H***     VAPOR     ***/30X,19HPHYSICAL PROPERTIES/26X,
     1 30HDENSITY       GAS         INITIAL  /24X,35HAT AMB-TEMP  CONSTANT
     2  BUBBLE RAD. / 25X,30H(LB/IN**3)    (IN/R)        (IN) /22X,3E12.4)
  109 FORMAT(3X,6HRADIUS,7X,5HVAPOR,6X,5HVAPOR,7X,7HRATE OF,6X,6HCHANGE,
     16X,6HCHANGE,6X,4HTIME/3X,5HRATIO,8X,6HRADIUS,5X,20HPRESSURE   RV C
     2HANGE,5X,7HIN RAD.,4X,8HIN TEMP./17X,4H(CM),5X,20H(LB/IN**2)  (CM/
     3SEC),17X,7H(DEG-R),6X,5H(SEC)   /)
  110 FORMAT(1H1,18X,1HI,6X,2HPV,11X,3HPV2,6X,5HPHI = ,E14.7)
  111 FORMAT(/15X,16HABOVE DATA USED ,E8.1,27H AS A CONVERGENCE CRITERIO
     1N              )
  112 FORMAT(/27X,26H*** AMBIENT CONDITIONS ***/35X,23HTEMPERATURE  SATU
     1RATION /25X,8HPRESSURE,6X,2HOF,7X,11HTEMPERATURE/37X,23HLIQUID
     2 AT AMB.PRESS /25X,10H(LB/IN**2), 2(13H  (DEG-R)    )/22X,3E12.4 )
  113 FORMAT(/30X,19H***     LIQUID    ***/30X,19HPHYSICAL PROPERTIES//5X,
     1 75H   THERMAL     SPECIFIC      DENSITY   LATENT HEAT   SURFACE
     2SATURATION                        /5X,
     3 75H CONDUCTIVITY   HEAT                    VAPORIZATION  TENSION
     4 PRESSURE                         /5X,
     5 75H(BTU/R-IN-SEC)(BTU/LB-R)  (LB/IN**3)   (BTU/LB)     (LB/IN)
     6(LB/IN**2)                        / 4X,6E12.4)
  114 FORMAT(1H1,14X,30HCOEFFICIENT OF VAPORIZATION = , E8.1)
      END
```

```
1  WATER   RV/RO VS RVD01
   20     0     1     4
 1.47        579.5       574.69
 8.600E-06    1.          .03572     1026.        .426E-03 1.687      4.505E-02
 2.837E-06    1025.       1.         .001
 2.           10.         1.
 20.          100.        10.           1
 .1           .01         10.
```

WATER RV/RO VS RVDOT

*** AMBIENT CONDITIONS ***

PRESSURE (LB/IN**2)	TEMPERATURE OF LIQUID (DEG-R)	SATURATION TEMPERATURE AT AMB.PRESS (DEG-R)
1.4700E+00	5.7950E+02	5.7469E+02

*** LIQUID ***
PHYSICAL PROPERTIES

THERMAL CONDUCTIVITY (BTU/R-IN-SEC)	SPECIFIC HEAT (BTU/LB-R)	DENSITY (LB/IN**3)	LATENT HEAT VAPORIZATION (BTU/LB)	SURFACE TENSION (LB/IN)	SATURATION PRESSURE (LB/IN**2)
8.6000E-06	1.0000E+00	3.5720E-02	1.0260E+03	4.2600E-04	1.6870E+00

*** VAPOR ***
PHYSICAL PROPERTIES

DENSITY AT AMB-TEMP (LB/IN**3)	GAS CONSTANT (IN/R)	INITIAL BUBBLE RAD. (IN)
2.8370E-06	1.0250E+03	3.9263E-03

COEFFICIENT OF VAPORIZATION = 1.0E+00

RADIUS RATIO	VAPOR RADIUS (CM)	VAPOR PRESSURE (LB/IN**2)	RATE OF RV CHANGE (CM/SEC)	CHANGE IN RAD.	CHANGE IN TEMP. (DEG-R)	TIME (SEC)
2.0000E+00	1.9945E-02	1.6351E+00	3.2271E+01	6.4986E-02	1.0735E+00	6.1806E-04
3.0000E+00	2.9918E-02	1.6116E+00	4.3068E+01	4.8184E-02	1.5705E+00	8.8281E-04
4.0000E+00	3.9891E-02	1.5962E+00	4.7231E+01	4.0288E-02	1.9018E+00	1.1037E-03
5.0000E+00	4.9864E-02	1.5847E+00	4.8832E+01	3.5576E-02	2.1547E+00	1.3113E-03
6.0000E+00	5.9836E-02	1.5754E+00	4.9251E+01	3.2393E-02	2.3605E+00	1.5147E-03
7.0000E+00	6.9809E-02	1.5676E+00	4.9061E+01	3.0073E-02	2.5343E+00	1.7175E-03
8.0000E+00	7.9782E-02	1.5609E+00	4.8538E+01	2.8296E-02	2.6846E+00	1.9219E-03
9.0000E+00	8.9754E-02	1.5550E+00	4.7827E+01	2.6883E-02	2.8167E+00	2.1289E-03
1.0000E+01	9.9727E-02	1.5498E+00	4.7008E+01	2.5729E-02	2.9343E+00	2.3392E-03
2.0000E+01	1.9945E-01	1.5177E+00	3.8258E+01	2.0176E-02	3.6676E+00	4.6784E-03
3.0000E+01	2.9918E-01	1.5021E+00	3.1434E+01	1.8175E-02	4.0299E+00	7.5404E-03
4.0000E+01	3.9891E-01	1.4931E+00	2.6409E+01	1.7172E-02	4.2398E+00	1.0989E-02
5.0000E+01	4.9864E-01	1.4875E+00	2.2638E+01	1.6589E-02	4.3724E+00	1.5055E-02
6.0000E+01	5.9836E-01	1.4838E+00	1.9742E+01	1.6217E-02	4.4616E+00	1.9761E-02
7.0000E+01	6.9809E-01	1.4812E+00	1.7460E+01	1.5965E-02	4.5240E+00	2.5123E-02
8.0000E+01	7.9782E-01	1.4793E+00	1.5627E+01	1.5785E-02	4.5697E+00	3.1151E-02
9.0000E+01	8.9754E-01	1.4779E+00	1.4130E+01	1.5651E-02	4.6044E+00	3.7854E-02
1.0000E+02	9.9727E-01	1.4768E+00	1.2883E+01	1.5550E-02	4.6310E+00	4.5238E-02

COEFFICIENT OF VAPORIZATION = 1.0E-01

RADIUS RATIO	VAPOR RADIUS (CM)	VAPOR PRESSURE (LB/IN**2)	RATE OF RV CHANGE (CM/SEC)	CHANGE IN RAD.	CHANGE IN TEMP. (DEG-R)	TIME (SEC)
2.0000E+00	1.9945E-02	1.6223E+00	2.2810E+01	7.7296E-02	8.9548E-01	8.7440E-04
3.0000E+00	2.9918E-02	1.5931E+00	3.2030E+01	5.5873E-02	1.3388E+00	1.2381E-03
4.0000E+00	3.9891E-02	1.5758E+00	3.5988E+01	4.6154E-02	1.6388E+00	1.5313E-03
5.0000E+00	4.9864E-02	1.5639E+00	3.7740E+01	4.0467E-02	1.8693E+00	1.8019E-03
6.0000E+00	5.9836E-02	1.5549E+00	3.8427E+01	3.6672E-02	2.0579E+00	2.0637E-03
7.0000E+00	6.9809E-02	1.5477E+00	3.8548E+01	3.3927E-02	2.2180E+00	2.3228E-03
8.0000E+00	7.9782E-02	1.5418E+00	3.8349E+01	3.1834E-02	2.3571E+00	2.5822E-03
9.0000E+00	8.9754E-02	1.5368E+00	3.7961E+01	3.0175E-02	2.4800E+00	2.8436E-03
1.0000E+01	9.9727E-02	1.5324E+00	3.7463E+01	2.8822E-02	2.5900E+00	3.1080E-03
2.0000E+01	1.9945E-01	1.5073E+00	3.1311E+01	2.2302E-02	3.2952E+00	6.0082E-03
3.0000E+01	2.9918E-01	1.4957E+00	2.6271E+01	1.9881E-02	3.6684E+00	9.4721E-03
4.0000E+01	3.9891E-01	1.4890E+00	2.2483E+01	1.8611E-02	3.9011E+00	1.3563E-02
5.0000E+01	4.9864E-01	1.4847E+00	1.9588E+01	1.7834E-02	4.0595E+00	1.8304E-02
6.0000E+01	5.9836E-01	1.4819E+00	1.7317E+01	1.7315E-02	4.1731E+00	2.3709E-02
7.0000E+01	6.9809E-01	1.4798E+00	1.5499E+01	1.6945E-02	4.2584E+00	2.9787E-02
8.0000E+01	7.9782E-01	1.4783E+00	1.4014E+01	1.6669E-02	4.3244E+00	3.6545E-02
9.0000E+01	8.9754E-01	1.4771E+00	1.2781E+01	1.6456E-02	4.3770E+00	4.3989E-02
1.0000E+02	9.9727E-01	1.4762E+00	1.1743E+01	1.6287E-02	4.4196E+00	5.2121E-02

COEFFICIENT OF VAPORIZATION = 1.0E-02

RADIUS RATIO	VAPOR RADIUS (CM)	VAPOR PRESSURE (LB/IN**2)	RATE OF RV CHANGE (CM/SEC)	CHANGE IN RAD.	CHANGE IN TEMP. (DEG-R)	TIME (SEC)
2.0000E+00	1.9945E-02	1.6102E+00	5.4107E+00	1.5871E-01	4.3289E-01	3.6863E-03
3.0000E+00	2.9918E-02	1.5717E+00	8.2404E+00	1.1016E-01	6.6995E-01	5.1474E-03
4.0000E+00	3.9891E-02	1.5496E+00	9.7738E+00	8.8563E-02	8.3985E-01	6.2546E-03
5.0000E+00	4.9864E-02	1.5355E+00	1.0658E+01	7.6150E-02	9.7535E-01	7.2308E-03
6.0000E+00	5.9836E-02	1.5257E+00	1.1187E+01	6.7967E-02	1.0895E+00	8.1438E-03
7.0000E+00	6.9809E-02	1.5185E+00	1.1507E+01	6.2098E-02	1.1889E+00	9.0227E-03
8.0000E+00	7.9782E-02	1.5131E+00	1.1696E+01	5.7643E-02	1.2775E+00	9.8823E-03
9.0000E+00	8.9754E-02	1.5088E+00	1.1800E+01	5.4122E-02	1.3575E+00	1.0731E-02
1.0000E+01	9.9727E-02	1.5053E+00	1.1846E+01	5.1253E-02	1.4307E+00	1.1575E-02
2.0000E+01	1.9945E-01	1.4890E+00	1.1246E+01	3.7213E-02	1.9508E+00	2.0212E-02
3.0000E+01	2.9918E-01	1.4831E+00	1.0349E+01	3.1675E-02	2.2831E+00	2.9448E-02
4.0000E+01	3.9891E-01	1.4801E+00	9.5502E+00	2.8556E-02	2.5274E+00	3.9471E-02
5.0000E+01	4.9864E-01	1.4782E+00	8.8668E+00	2.6507E-02	2.7192E+00	5.0301E-02
6.0000E+01	5.9836E-01	1.4769E+00	8.2799E+00	2.5041E-02	2.8759E+00	6.1933E-02
7.0000E+01	6.9809E-01	1.4759E+00	7.7712E+00	2.3930E-02	3.0075E+00	7.4360E-02
8.0000E+01	7.9782E-01	1.4752E+00	7.3258E+00	2.3055E-02	3.1201E+00	8.7571E-02
9.0000E+01	8.9754E-01	1.4746E+00	6.9320E+00	2.2345E-02	3.2180E+00	1.0156E-01
1.0000E+02	9.9727E-01	1.4742E+00	6.5812E+00	2.1756E-02	3.3041E+00	1.1632E-01

COEFFICIENT OF VAPORIZATION = 1.0E+01

RADIUS RATIO	VAPOR RADIUS (CM)	VAPOR PRESSURE (LB/IN**2)	RATE OF RV CHANGE (CM/SEC)	CHANGE IN RAD.	CHANGE IN TEMP. (DEG-R)	TIME (SEC)
2.0000E+00	1.9945E-02	1.6372E+00	3.3560E+01	6.3726E-02	1.0961E+00	5.9433E-04
3.0000E+00	2.9918E-02	1.6144E+00	4.4522E+01	4.7391E-02	1.5995E+00	8.4977E-04
4.0000E+00	3.9891E-02	1.5992E+00	4.8659E+01	3.9692E-02	1.9340E+00	1.0638E-03
5.0000E+00	4.9864E-02	1.5877E+00	5.0227E+01	3.5078E-02	2.1894E+00	1.2655E-03
6.0000E+00	5.9836E-02	1.5783E+00	5.0604E+01	3.1957E-02	2.3972E+00	1.4633E-03
7.0000E+00	6.9809E-02	1.5704E+00	5.0371E+01	2.9680E-02	2.5726E+00	1.6609E-03
8.0000E+00	7.9782E-02	1.5636E+00	4.9805E+01	2.7934E-02	2.7241E+00	1.8600E-03
9.0000E+00	8.9754E-02	1.5576E+00	4.9052E+01	2.6545E-02	2.8573E+00	2.0617E-03
1.0000E+01	9.9727E-02	1.5523E+00	4.8193E+01	2.5411E-02	2.9757E+00	2.2668E-03
2.0000E+01	1.9945E-01	1.5191E+00	3.9114E+01	1.9954E-02	3.7119E+00	4.5513E-03
3.0000E+01	2.9918E-01	1.5030E+00	3.2066E+01	1.7995E-02	4.0725E+00	7.3535E-03
4.0000E+01	3.9891E-01	1.4937E+00	2.6884E+01	1.7020E-02	4.2793E+00	1.0737E-02
5.0000E+01	4.9864E-01	1.4879E+00	2.3003E+01	1.6457E-02	4.4085E+00	1.4735E-02
6.0000E+01	5.9836E-01	1.4840E+00	2.0027E+01	1.6101E-02	4.4944E+00	1.9370E-02
7.0000E+01	6.9809E-01	1.4814E+00	1.7688E+01	1.5862E-02	4.5540E+00	2.4659E-02
8.0000E+01	7.9782E-01	1.4794E+00	1.5813E+01	1.5692E-02	4.5972E+00	3.0613E-02
9.0000E+01	8.9754E-01	1.4780E+00	1.4283E+01	1.5567E-02	4.6296E+00	3.7240E-02
1.0000E+02	9.9727E-01	1.4769E+00	1.3012E+01	1.5473E-02	4.6543E+00	4.4547E-02

ABOVE DATA USED 1.0E-03 AS A CONVERGENCE CRITERION

APPENDIX II

Reference 21 is reproduced in its entirety in the following pages for the convenience of the reader.

MTI-68TR30

FLUID DYNAMICS OF DISPERSED TWO-PHASE VAPOR-LIQUID FLOW IN LUBRICANT FILMS

Part I: The Field Equations for Two Phase Reynolds Film Flow with a Change of Phase

by

N. Zuber

Part II: The Constitutive Equation of Evaporation and/or Condensation for Non-Equilibrium Dispersed Droplet Flow

by

D. E. Dougherty

Mechanical Technology Incorporated - 968 Albany-Shaker Road - Latham, N.Y. 12110

TABLE OF CONTENTS

TABLE OF CONTENTS (continued)

A. INTRODUCTION

Interest in vapor film lubrication has been spurred on by new technological requirements, e.g., steam cooled nuclear power plants, and by the overall potential advantages of using steam instead of conventional oil lubrication in rotating Rankine cycle machinery. Some of the advantages to be gained by steam lubrication are reiterated from the references given in Parts I and II of this report. They include:

1. Elimination of a separate lube oil system with associated pumps, sumps, coolers, filters, controls and piping.

2. Elimination of bearing oil seals with potential gains in reliability, simplicity and reduced axial length of the machine. Exhaust steam from the bearings can be vented directly into the machine casing.

3. Operation of the bearings at or close to the turbine temperature thus sharply reducing temperature gradients within the machine.

4. Reduction of contamination and fire hazards.

5. Potential reduction in machinery size, weight and cost.

This investigation was supported by the Atomic Energy Commission for the purpose of developing analytical methods to predict the static and dynamic behaviour of vapor lubrication films with particular emphasis given to steam lubricated bearings. Earlier steam lubrication studies showed that the presence of condensate in a vapor lubrication film is critical to bearing performance. Thus a theory and model for two-phase film lubrication was needed. To these purposes a general theory for two-phase Reynolds' film flow has been developed. This analysis describes the static and dynamic behaviour of a dispersed two-phase film flow including the effects of a change of phase.

In part I the general two-phase film flow equation is obtained. This equation is

exactly the same as the general non-condensible gas lubrication equation with the exception of a vapor sink or a vapor source term which accounts for the effect of a phase change. It is shown that the flow of a saturated vapor lubrication film depends on two dimensionless numbers: the standard Strouhal number S, and the phase change number N. When the ratio N/S is small, the characteristics of a saturated vapor film should resemble those of a non-condensible gas film. Conversely, for large values of this ratio a significant difference is to be expected.

In Part II a non-equilibrium two-phase lubrication film model is developed. From this model the constitutive equation of condensation and/or evaporation is obtained and combined within the framework of the general two-phase Reynolds' equation obtained in Part I. The constitutive equation must be specified to obtain a complete set of equations for the film pressure profiles and flow rates.

As a first step toward solving the general two-phase lubrication equations, the steady state, one-dimensional evaporative film was analyzed. This simple bearing film geometry can also be used to synthesize externally pressurized steam journal bearing configurations. The results of the analysis show the major thermo-hydrodynamic parameters of wet vapor bearings and the influence these parameters, such as the inlet moisture fraction, the liquid-droplet Weber number, the evaporation relaxation constant have on the film pressure and flow rate.

B. Part I: The Field Equations for Two Phase Reynolds Film Flow with a Change of Phase

1. INTRODUCTION

1.1 Significance of the Problem and Applications

The importance of condensation and evaporation processes in traditional drying, distillation and Rankine Cycle power systems is well known. However, more recently, it has been shown, Refs. [1, 2, 3], that these phenomena are critical to process fluid lubrication concepts using saturated vapors.

The systems where such advanced lubrication concepts are being considered include stationary power plants, shipboard machinery, remote operating underwater, surface and space power plants, etc. Some specific application for saturated vapor lubrication are pressurized and self-acting steam bearings for stationary and mobile power plant machinery, also seals for saturated vapor and/or liquid in feed pumps and turbo machinery. The working fluids of interest are water, organic compounds and liquid metals.

The precedent for saturated vapor lubrication has been established by the rather well developed gas (non-condensible) lubrication technology, Refs. [4 - 9]. The growth of this technology and its impetus centered upon the development of a realistic and reliable lubrication theory for predicting bearing and seals performance. This theory and applications evolved from the well known Reynolds' lubrication equation extended to include the effects of compressibility, Ref. 4 In general, the agreement between theoretical prediction based on this equation, and experimental data for gas (non-condensible) lubricant has been satisfactory.

However, experiments of Refs. [1, 10], with saturated vapor lubricants, have shown that the presence of a relatively small amount of condensate in a lubrication film can cause significant changes in the lubrication film pressure profile and dynamics. These changes could <u>not</u> have been predicted by analyses based on Reynolds equation for gas (non-condensible) lubricants.

What is required therefore is an extended lubrication theory for two-phase, vapor-liquid mixtures which accounts for the effects of a change of phase. Such a theory

and formulation should be applicable to both static and dynamic analyses.

1.2 Purpose and Significance of the Report

This report has two purposes:

First, to present a general formulation which describes the dynamic behavior of two-phase, vapor-liquid flow of lubrication films, and second, to derive an equation equivalent to Reynolds equation, which takes however, into account the effects of evaporation and/or condensation.

Intuitively it could be expected that the formation of a condensate acts as a vapor sink whereas the evaporation acts as a vapor source in the lubricant film flow. This indeed is the case as shown by the equation derived in this report: the processes of condensation and/or evaporation are accounted for by a net sink and/or source term in a two-phase, Reynolds lubrication film flow.

The results derived in this report clearly demonstrate that the effects of the vapor sink and/or of the vapor source term can become of primary importance in determining the static and dynamic characteristics of saturated vapor bearings.

The general formulation and analysis presented herein is of particular interest because it can be readily applied to the important conditions of thermodynamic non-equilibrium between the vapor and the liquid phase.

2. FORMULATION

2.1 The Physical System

The physical system to be analyzed consists of a vapor either slightly superheated or at saturation with entrained droplets flowing between two solid surfaces. Depending on operating conditions, these droplets can undergo evaporation and/or condensation. For example, with the vapor wet at the inlet, droplets may start evaporating as the pressure drops along the channel. Similarly, droplet nucleation and attendant vapor condensation can take place in flows having time and/or spatially variable clearances.

Clearly, if the temperature of the solid surface is below saturation, the vapor will condense on the wall forming a liquid film. This aspect of the problem, i.e. separated two-phase flow, is however not considered in this report. It is assumed here that the temperatures of boundary surfaces are above or at saturation temperature. Since the evaporating or condensing droplets are dispersed in the vapor phase, we are considering here a problem of dispersed, two-phase flow in thermodynamic non-equilibrium.

2.2 Assumptions and the Governing Set of Equations

In order to formulate the problem we shall make the following assumptions:

1) The vapor phase behaves essentially as a perfect gas.

2) The density of the liquid is constant.

3) The effects of droplets is to change the density of the mixture.

4) The effect of droplet concentration on the viscosity of the mixture is neglected.

5) The effect of the relative velocity between the two-phases is neglected, i.e., the flow of the mixture is assumed to be homogeneous.

6) The energy equation can be decoupled from the momentum and the continuity equations.

These assumptions and their validity are considered and discussed in more detail in the appendices to this report. Suffice to say here that the first and the last assumption are customary in gas bearing analyses and have been examined already in the literature (see for example, Ref. [7]).

In view of these assumptions and following Refs. [11, 12], the problem is formulated in terms of three field equations and three constitutive equations. The three field equations are:

The continuity equation for the mixture:

$$\frac{\partial \rho}{\partial t} + \text{div}\,(\rho \vec{v}) = 0 \tag{1}$$

where ρ and $\vec{v}$ are the density and the velocity of the mixture.

The equation of motion of the mixture:

$$\rho \frac{D\vec{v}}{Dt} = -\,\text{grad}\, P + \mu \nabla^2 \vec{v} + (\beta + \mu)\,\text{grad}\,(\text{div}\,\vec{v}) \tag{2}$$

where in view of the fourth assumption, μ is the viscosity of the vapor and λ is the bulk viscosity. We note that because of the fifth assumption the drift stress tensor, Ref. [12], which accounts for the effect of the relative velocity between the vapor and liquid phase, does not appear in Eq. (2). The magnitude of this term is evaluated in Appendix B for the flow regime analyzed in this paper.

The third field equation is the continuity equation for the liquid, which as a consequence of the fifth assumption, can be written as*:

---

*Note that the homogeneous flow assumption implies that the velocities of the liquid, of the vapor and of the mixture, are all equal.

$$\frac{\partial \rho c}{\partial t} + \text{div}\,(\rho c \vec{v}) = \Gamma_f \tag{3}$$

where c is the mass concentration of the liquid and where the source term Γ_f, is the mass rate of liquid formation per unit volume.

The three constitutive equations which are needed to completely define the problem are:

The thermal equation of state for the mixture:

$$\frac{1}{\rho} = \frac{1-c}{\rho_g} + \frac{c}{\rho_f} \tag{4}$$

where ρ_g and ρ_f are the densities of the vapor and of the liquid.

The thermal equation of state for the vapor, which in view of the first assumption, is given by:

$$\rho_g = \frac{P}{RT_o} \tag{5}$$

We note that the thermal equation of state for the liquid does not appear since according to the second assumption, ρ_f in Eq. (4) is a constant.

The final equation is the constitutive equation of condenstaion or of evaporation:

$$\Gamma_f = \Gamma_f\,(P) \tag{6}$$

which specifies the mass rate of liquid formation or disappearance per unit

volume. It depends on the rate of droplet nucleation as well as on droplet condensation and/or evaporation. The significance of this constitutive equation in non-equilibrium two-phase flow is discussed in more detail in Ref. [11]. It is shown there that the constitutive equation of vaporization and/or of condensation plays a primary role in determining the degree of thermal non-equilibrium.

It can be seen from the foregoing that the problem is formulated in terms of six variables: ρ, $\vec{v}$, P, c, ρ_g, Γ_f which are defined by six independent equations, i.e. by Eq. (1) through Eq. (6). It is of interest to note here that whereas a gas bearing problem is formulated in terms of three equations, i.e., Eqs. (1), (2) and (5), the presence of droplets in vapor-liquid two-phase bearings requires three additional equations, i.e., Eq. (3), (4) and (6), in order to physically describe the problem as well as to define it mathematically.

2.3 Dimensionless Groups and Equations

In order to express the governing set of equations in a dimensionless form we shall use the standard approach of gas bearing analyses (see for example Ref. [7]) expanding it however to take into account the effect of phase change.

Consider a thin vapor film bounded by a plane at y = 0 which may move only in the x and z directions, and a surface y = h (x,y,z,t). Denoting by h_o and L the characteristic lengths in the normal and lateral directions, the "thin film" approximation implies that

$$\frac{h_o}{L} = \epsilon << 1 \qquad (7)$$

In gas bearing problems this ratio is of the order of $\epsilon \sim 10^{-3}$.

Following the standard approach of gas bearing analyses we shall define the following dimensionless quantities.

$$x^* = \frac{x}{L}, \quad z^* = \frac{z}{L}, \quad y^* = \frac{y}{L} \tag{8}$$

$$t^* = \omega t, \quad P^* = \frac{p h_o^2}{\mu V L} \tag{9}$$

$$u^* = \frac{u}{V}, \quad w^* = \frac{w}{V}, \quad v^* = \frac{v}{h_o \omega} \tag{10}$$

$$\rho_g^* = \frac{\rho_g}{\rho_a}, \quad \rho^* = \frac{\rho}{\rho_a} \tag{11}$$

where V is the characteristic velocity for the lateral motion; ρ_a is the ambient, i.e., reference density, and ω^{-1} is the relevant time scale of the motion; for example if the surface $y = h\ (x,y,z,t)$ is oscillating in the vertical direction ω is the frequency.

The continuity equation for the mixture, Eq. (1), can be expressed in a dimensionless form by means of the relation above, thus

$$S\left[\frac{\partial \rho^*}{\partial t^*} + \frac{\partial(\rho^* v^*)}{\partial y^*}\right] + \frac{\partial(\rho^* u^*)}{\partial x^*} + \frac{\partial(\rho^* w^*)}{\partial z^*} = 0 \tag{12}$$

where S is the Strouhal number defined by

$$S = \frac{\omega L}{V} \tag{13}$$

Similarly, the equation of motion, i.e. Eq. (2) can be cast in a dimensionless form, thus the x component becomes:

$$\mathrm{Re}_s\,\rho^*\left[\frac{\partial u^*}{\partial t^*} + v^*\frac{\partial u^*}{\partial y^*}\right] + \mathrm{Re}\,\epsilon\left[u^*\frac{\partial u^*}{\partial x^*} + w^*\frac{\partial u^*}{\partial z^*}\right] = -\frac{\partial P^*}{\partial x^*}$$

$$+ \frac{\partial^2 u^*}{\partial y^{*2}} + \epsilon^2\left\{\frac{\partial^2 u^*}{\partial x^{*2}} + \frac{\partial^2 u^*}{\partial z^{*2}} + \left(\frac{\lambda+\mu}{\mu}\right)\left[\frac{\partial}{\partial x^*}\left(\frac{\partial u^*}{\partial x^*} + \frac{\partial w^*}{\partial z^*}\right) + S\frac{\partial^2 v^*}{\partial x^*\partial y^*}\right]\right\} \tag{14}$$

where, following the customary definitions (see for example Ref. [7]), the "squeeze" Reynolds number Re_s, is given by:

$$\mathrm{Re}_s = \frac{\omega\rho_a h_o^2}{\mu} \tag{15}$$

and the Reynolds number Re, by:

$$R_e = \frac{\rho_a V h_o}{\mu} \tag{16}$$

In most gas bearing applications, Refs. [4 - 8], the groups Re_s and ϵR_e are small whereas the Strouhal number is of the order of unity. For example, $\mathrm{Re}_s \sim 0.05$, $\epsilon R_e \sim 10^{-3}\,.10^2 = 10^{-1}$, and $S \sim 1$. Consequently, it follows from Eq. (14) that for the "thin film" approximation the x component of the equation of motion can be reduced to:

$$\frac{\partial P^*}{\partial x^*} = \frac{\partial^2 u^*}{\partial y^{*2}} + 0\left(\epsilon\mathrm{Re},\ \mathrm{Re}_s,\ \epsilon^2 S,\ \epsilon^2,\ \epsilon^2\,\frac{\lambda}{\mu}\right) \tag{17}$$

Using similar arguments it can be shown, Refs. [4 - 9], that the other two components, i.e., the y and z components reduce to:

$$\frac{\partial P^*}{\partial y^*} = 0 + 0\left[\epsilon^2 \text{ St}, \epsilon^2 \text{ S} \frac{\beta}{\mu}, \epsilon^2 \text{S Re}_s, \epsilon^2 \text{ Re}_s\right] \tag{18}$$

and

$$\frac{\partial P^*}{\partial z^*} = \frac{\partial^2 w^*}{\partial z^{*2}} + 0\left[\epsilon \text{ Re}, \text{Re}_s, \epsilon^2 \text{ S}, \epsilon^2, \epsilon^2 \frac{\beta}{\mu}\right] \tag{19}$$

Finally, the continuity equation for the liquid, Eq. (3), can be expressed in dimensionless form, thus

$$\text{S}\left[\frac{\partial(\rho^* c)}{\partial t^*} + \frac{\partial(\rho^* c v^*)}{\partial y^*}\right] + \left[\frac{\partial(\rho^* c u^*)}{\partial x^*} + \frac{\partial(\rho^* c w^*)}{\partial z^*}\right] = \text{N} \tag{20}$$

where S is the Strouhel number defined by Eq. (13), and N is the <u>phase change number</u>, given by

$$\text{N} = \frac{\Gamma_f}{\rho_a} \frac{\text{L}}{\text{V}} \tag{21}$$

Before proceeding further with the analysis, it is desirable to elucidate the meaning of this dimensionless group. Multiplying the numerator and the denominator of Eq. (21), by the cross sectional area A, of the film we obtain

$$\text{N} = \frac{\Gamma_f \text{LA}}{\rho_a \text{VA}} \tag{22}$$

Since LA is the scale of the film volume, the numerator of Eq. (22), denotes the mass rate of liquid formation by condensation(or disappearance by evaporation) in the vapor film, whereas the denominator represents the total mass flow rate through the film.

It can be seen from the foregoing that the dynamic characteristics of saturated vapor bearings depend on four dimensionless groups: the "squeeze" Reynolds number, Eq. (15); the Reynolds number, Eq. (16); the Strouhal number, Eq. (13); and the phase change number Eq. (21).

Whereas the first three groups appear also in gas (non-condensible) lubrication problems, the last one appears only in two-phase flow bearing problems where it was introduced through the continuity equation for the liquid. The importance of the phase change number as a scaling parameter, is discussed further in section 4 of this report. We shall proceed now with the derivation of the governing equation.

3. DERIVATION OF THE EQUATION

It was noted in Ref. [9] that the lubrication theory is the hydrodynamic analog of shell theory, since the thickness of the film is much smaller than its lateral dimensions. Consequently, the dependence upon one of the three spatial variables can be eliminated from the hydrodynamic equations. This observation is used in deriving the Reynolds equation, upon which the entire gas lubrication technology is based. In particular, the continuity equation is integrated <u>across</u> the film and the Navier-Stokes equation is used to evaluate the quantities appearing as integrands.

The same approach can be used in deriving the governing equation for two-phase lubricant films. However, as the density of the mixture depends on the concentration (see Eq. (4)), the equation which is obtained from the equation of motion and the integrated continuity equation is a function of concentration. This functional dependence can be eliminated by means of the integrated continuity equation for the liquid. The results yield the governing equation for dispersed, two-phase lubrication film flow in which the phase change number N, appears as a sink or a source term.

In order to integrate the equation it is necessary to define the boundary conditions. Following the standard approach in lubrication analyses, these will be taken as:

$$\text{at} \quad y^* = 0 : \quad u^* = U_o^*$$

$$w^* = W_o^*$$

$$v^* = 0 \tag{23}$$

whereas at $y^* = \frac{h}{h_o} = h^*$:

$$u^* = U_h^*$$
$$v^* = V_h^* \qquad (24)$$
$$w^* = W_h^*$$

and
$$V_h^* = S\,\frac{\partial h^*}{\partial t^*} + u^*\,\frac{\partial h^*}{\partial z^*} + w^*\,\frac{\partial h^*}{\partial z^*} \qquad (25)$$

The last equation is a kinematic condition which states that a fluid particle at the surface $y^* = h^*(x^*, z^*, t^*)$, moves with the same velocity of the surface.

With these boundary conditions, the integration of the continuity equation for the mixture, i.e., of Eq. (1), across the film thickness yields:

$$h^*\,S\,\frac{\partial \rho^*}{\partial t^*} + S\,\rho^* V_h^* + \int_0^{h^*} \frac{\partial(\rho^* u^*)}{\partial x^*}\,dy^* + \int_0^{h^*} \frac{\partial(\rho^* w^*)}{\partial z^*}\,dy^* = 0 \qquad (26)$$

Recalling that

$$\frac{d}{dx}\int_0^{h(x)} f(y)\,dy = \int_0^{h(x)} \frac{df}{dx}\,dy + \left\{ f\,\frac{dh}{dx} \right\}_{y=h} \qquad (27)$$

and in view of the boundary conditions, i.e., of Eqs. (24)and (25) the continuity equation for the mixture, Eq. (26), can be expressed as

$$S\,\frac{\partial}{\partial t^*}(\rho^* h^*) + \frac{\partial}{\partial x^*}\int_0^{h^*} \rho^* u^* dy^* + \frac{\partial}{\partial z^*}\int_0^{h^*} \rho^* w^* dz^* = 0 \qquad (28)$$

Following the same procedure we can integrate the continuity equation for the liquid, Eq. (20), across the film and obtain:

$$S\frac{\partial}{\partial t^*}(\rho^* h^* c) + \frac{\partial}{\partial x^*}\int_0^{h^*} \rho^* c u^* dy^* + \frac{\partial}{\partial z^*}\int_0^{h^*} \rho^* c w^* dz^* = \langle N \rangle h^* \qquad (29)$$

where N is averaged over the film thickness so that $\langle N \rangle$ equals $\frac{1}{h^*}\int_0^{h^*} N\, dy^*$

We shall examine now the integrals in these two equations.

The density of the mixture ρ^* which appears in Eq. (28) and Eq. (29) is given by the constitutive equation of state for the mixture, Eq. (4), thus

$$\frac{1}{\rho^*} = \frac{1-c}{\rho_g^*} + \frac{c}{\rho_f^*} \qquad (30)$$

For most problems of practical interest the mass concentration is much smaller than unity, whereas the density of the liquid is considerably larger than that of the vapor. Consequently, Eq. (30) can be approximated by

$$\rho^* = \frac{\rho_g^*}{1-c} \qquad (31)$$

which will be valid as long as:

$$c << \frac{\rho_f}{\rho_f + \rho_g} \qquad (32)$$

The density of the vapor ρ_g^* in Eq. (30) and Eq. (31) is specified by the thermal

equation of state, expressed here by the perfect gas law, Eq. (5). It is standard procedure in gas lubrication analyses to neglect the temperature variation across the gas film. Furthermore, in view of Eq. (18), the pressure is assumed to be constant across this film. It follows then from the equation of state that the gas density does not vary in the y* direction. Similar arguments can be advanced in the present problem. Consequently, as a first approximation, the density of the vapor ρ_g in Eq. (31), will be constant across the vapor film.

With this approximation, the substitution of Eq. (31) in Eq. (28) and Eq. (29) leads to:

$$S\frac{\partial}{\partial t^*}\left\{\frac{\rho_g^*}{1-c}\,h^*\right\}+\frac{\partial}{\partial x^*}\left\{\rho_g^*\int_0^{h^*}\frac{u^*}{1-c}\,dy^*\right\}+\frac{\partial}{\partial z^*}\left\{\rho_g^*\int_0^{h^*}\frac{w^*}{1-c}\,dy^*\right\}=0 \tag{33}$$

and

$$S\frac{\partial}{\partial t^*}\left\{\frac{\rho_g^* c}{1-c}\,h^*\right\}+\frac{\partial}{\partial x^*}\left\{\rho_g^*\int_0^{h^*}\left(\frac{c}{1-c}\right)u^*\,dy^*\right\}+\frac{\partial}{\partial z^*}\left\{\rho_g^*\int_0^{h^*}\left(\frac{c}{1-c}\right)w^*\,dy^*\right\}=\langle N\rangle h^* \tag{34}$$

By subtracting Eq. (34) from Eq. (33) we obtain:

$$S\frac{\partial}{\partial t^*}\left\{\rho_g^*\,h^*\right\}+\frac{\partial}{\partial x^*}\left\{\rho_g^*\int_0^{h^*}u^*\,dy^*\right\}+\frac{\partial}{\partial z^*}\left\{\rho_g^*\int_0^{h^*}w^*\,dy^*\right\}=-\langle N\rangle h^* \tag{35}$$

The integrands in this equation can be evaluated once the velocities u* and w* are determined from the equation of motion and the appropriate boundary conditions.

For the problem under consideration, the three components of the Navier-Stokes equation reduce to Eq. (17), (18) and (19), whereas the boundary conditions are given by Eqs.(23),(24) and(25). Then it can be easily shown, Refs. [4 - 9], that the two lateral components of the velocity are given by:

$$U^* = -\frac{1}{2}\frac{\partial P^*}{\partial x^*} h^{*2} \frac{y^*}{h^*}\left(1 - \frac{y^*}{h^*}\right) + (U_h^* - U_o^*)\frac{y^*}{h^*} + U_o^* \tag{36}$$

and

$$W^* = -\frac{1}{2}\frac{\partial P^*}{\partial z^*} h^{*2} \frac{y^*}{h^*}\left(1 - \frac{y^*}{h^*}\right) + (W_h^* - W_o^*)\frac{y^*}{h^*} + W_o^* \tag{37}$$

Substituting these two equations in Eq. (35), and upon evaluating the integrals we obtain:

$$12S\frac{\partial}{\partial t^*}\left\{\rho_g^* h^*\right\} + \frac{\partial}{\partial x^*}\left\{6h^* \rho_g^* (U_h^* + U_o^*) - h^{*3} \rho_g^* \frac{\partial P^*}{\partial x^*}\right\}$$

$$+ \frac{\partial}{\partial z^*}\left\{6h^* \rho_g^* (W_h^* + W_o^*) - h^{*3} \rho_g^* \frac{\partial P^*}{\partial z^*}\right\} = -12\langle N\rangle h^* \tag{38}$$

which for a perfect gas and isothermal process, reduces to:

$$12S\frac{\partial}{\partial t^*}\left\{P^* h^*\right\} + \frac{\partial}{\partial x^*}\left\{6h^* P^* (U_h^* + U_o^*) - h^{*3} P^* \frac{\partial P^*}{\partial x^*}\right\} +$$

$$+ \frac{\partial}{\partial z^*}\left\{6h^* P^* (W_h^* + W_o^*) - h^{*3} P^* \frac{\partial P^*}{\partial z^*}\right\} = -12\langle N\rangle h^* \tag{39}$$

Eq. (38), i.e., Eq. (39) is the governing equation for dispersed, two-phase lubrication film flow.

4. DISCUSSION

4.1 The Vapor Sink or Source Term

By examining Eq. (38), it can be seen that the governing equation for dispersed, two phase lubrication film flow differs from the standard Reynolds equation by the presence of a sink or source term on the right hand side. Since this term represents the only difference, it is desirable to analyze it in more detail.

As was already noted in Section 1, it could be expected intuitively that the formation of condensate acts as a vapor sink in the lubrication film flow, whereas the evaporation acts as a vapor source. This observation is indeed supported by, and expressed in, quantitative form in Eq. (38). The sink or source term which appears on the right hand side of Eq. (38), depends on the dimensionless film thickness and on the phase change number, which is a function of the liquid source Γ_f, see Eq.(21) and Eq.(3). The strength of this source is specified by an appropriate constitutive equation of condensation and/or evaporation, Eq. (6), which in general depends on a particular two phase flow regime, Refs. [11, 13].

The flow regimes of interest to the present problem are the dispersed droplet condensing and evaporating flows. For condensing flows, the liquid source Γ_f depends on the rates of droplet nucleation and vapor condensation on these droplets. For evaporating flows, Γ_f depends on the droplet number density, size distribution and rate of evaporation, Ref. [11]. In either case the constitutive equation of condensation and/or evaporation is a strong function of the vapor saturation pressure.

For condensing flows, the liquid source Γ_f in Eq. (3) is positive. It follows then from Eq. (21), that the phase change number N is also positive. Consequently for condensing flows, the term on the right hand side of the governing equation, Eq. (38), acts as a vapor sink, since it has a negative sign. Conversely, for evaporating flows Γ_f and therefore N are negative; the right hand side of Eq. (38) becomes then positive and acts as a vapor source. In absence of condensation or of evaporation Γ_f and therefore N are zero, reducing Eq. (38) to the standard

Reynolds equation for gas (non-condensible) film flow.

It is well known that the rates of droplet nucleation, condensation and evaporation are strong functions of the vapor pressure. Since the phase change number N, depends on these processes it can be expected that the right hand side of Eq. (39) will be a strong function of vapor pressure among others. Thus, if either or both P* and h* oscillate, the right hand side of Eq. (39) will become a pulsating source or sink. Clearly, such a pulsating source or sink will have a significant effect on the dynamic characteristics of the vapor film. Since this term does not appear in the Reynolds equation for gas (non condensible) films, it is not surprising that this latter equation was not adequate in describing and predicting the observed behavior of saturated vapor bearings. It is of interest to note in closing that even for a constant phase change number N, the right hand side of Eq. (39) can have the effect of a pulsating source or sink because of its dependence upon this film thickness h*.

4.2 Scaling Criteria

When planning experimental investigations or considering design alternatives it is desirable to have available criteria which can be used to scale a physical process of an engineering system. In this section we shall discuss the role of the phase change number N as a scaling criterion.

It was noted in Section 2 that N represents, the ratio of the net liquid formation in the vapor film to the total vapor-liquid mass flow rate through the film. It is instructive to express this number also in terms of the two characteristic time constants of the process: the transit time τ and the characteristic frequency of phase change Ω, Refs. [12, 14, 15].

We observe that the ratio L/V in Eq. (21) is a fluid particle transit, i.e. residence time τ, thus

$$\frac{L}{V} = \tau \tag{40}$$

whereas the ratio Γ_f/ρ_a is the characteristic frequency of condensation (or of evaporation) Ω, i.e.

$$\frac{\Gamma_f}{\rho_a} = \Omega \tag{41}$$

which scales the rate of phase change Refs. [12, 14, 15]. The phase change number can be expressed then also as the product of the particle residence time τ and the characteristic frequence of phase change Ω, thus

$$N = \Omega \tau \tag{42}$$

It can be expected therefore, that the equality of the phase change number N, in two different systems will ensure that the phase change has progressed equally in both. If this condition is not satisfied, the dynamic conditions of the two systems will not be similar, since the phase change in one would have progressed further than in the other.

We note that the phase change number expressed as a product of the characteristic frequency of phase change and the particle residence time, is of a form similar to the Damkohler first group, Ref. [16], which is one of the most important similarity criteria used in sealing chemical reactors as well as jet and rocket engines, Ref. [17, 18]. It is recalled here that Damkohler first group is defined as the product of the particle residence time and the chemical reaction frequency for reacting gases or for reacting liquids. In Ref. [12 - 15] we observed that in two phase flow problems with a change of phase, the characteristic frequency of evaporation Ω, has the same meaning as the reaction frequency in chemically reacting gases. It can be expected therefore that in two phase flow systems with a change of phase, the phase change number N, will play the same role as Damkohler first group in chemically reacting systems.

The governing equation, Eq. (39), indicates that the static and dynamic characteristics of dispersed two phase lubrication film flow depends on <u>two</u> dimensionless groups: the phase change number N given by Eq. (21), i.e. Eq. (42), and the Strouhal number, Eq. (13), which in view of Eq. (40), can be expressed also as

$$S = \omega T \tag{43}$$

Since the effect of a phase change appear only in the phase change number N, it can be expected that the ratio

$$\frac{N}{S} = \frac{\Omega}{\omega} \tag{44}$$

will reflect the importance of condensation or of evaporation on the dynamics of saturated vapor bearings. For very small values of this ratio, the dynamic characteristics of a vapor bearing should be similar to that of a gas (non-condensible) bearing. Whereas for large values, a significant difference should be expected.

By definition, the phase change number, Eq. (13) depends on the constitutive equation of condensation or evaporation, Eq. (6), appropriate to the particular flow regime. It was noted in Ref. [11] that at present the constitutive equation of evaporation or condensation are not known for some flow regimes and only in a rudimentary manner for others. It was stressed therefore in Ref. [11], that the determination of these constitutive equations and their experimental verification should constitute the primary objective of future investigations. This is particularly true for liquid metal systems which are characterized by a high degree of thermal non-equilibrium.

The constitutive equation of condensation and evaporation for lubrication film flow are presently under investigation. Part II of this report develops the constitutive equation for evaporative film flow. However, it can be stated already

that depending on the form of such a constitutive equation, the governing equation for dispersed two phase lubrication film flow, Eq. (39), predicts different static and dynamic characteristics of saturated vapor bearings.

5. CONCLUSIONS

1) The governing equation has been derived for dispersed, two-phase lubrication film flow. It can be used to predict both the static and the dynamic characteristics of saturated vapor bearings.

2) It was shown that the processes of condensation and/or evaporation are accounted by a dimensionless phase change number N, which appears respectively as a vapor sink or a vapor source in the governing equation. When this number is zero, the equation reduces to the standard Reynolds equation for gas (non-condensible) lubrication film flow.

3) The effect of this source or sink term on the static and dynamic characteristics of the vapor film were discussed. It was concluded that this effect can become the dominant when the sink or source pulsates.

4) It was shown that the flow of a saturated vapor lubrication film depends on two dimensionless numbers: the standard Strouhal number S, and the phase change number N. The significance of the latter number as a scaling criterion was discussed. It was shown that when the ratio N/S is small, the characteristics of a saturated vapor film should resemble those of a gas (non-condensible) film. Conversely, for large values of this ratio a significant difference is to be expected.

5) In the development of the vapor lubrication technology it can be expected that the governing equation Eq. (38), i.e. Eq. (39) described in this report will play a role similar to that which the Reynolds equation has played in the development of the gas (non-condensible) lubrication technology.

6. REFERENCES

1. Orcutt, F. K., "Experimental Investigation of Condensing Vapor Lubricated Thrust Bearing", ASLE Trans., Vol. 7, 168, 1964.

2. Ausman, J. S., Unterberg, W., "Condensing Vapor Lubrication of Self-Acting Long Journal Bearing", Journ. of Basic Engineering, Trans. ASME, Series D, No. 1, March, 1966.

3. Dougherty, D. E. and Pan, C.H.T., "Process Fluid Lubrication", Rept. ONR/AD 641369, U.S. Department of Commerce, 1967.

4. Harrison, W. J., "The Hydraulic Theory of Lubrication with Special Reference to Air vs. a Lubricant", Trans. Cambridge Phylosophical Soc., Vol. 22, 39, 1913.

5. Elrod, H. G. and Burgdorfer, A., "Refinements of the Theory of the Infinitely Long Self-Acting Gas-Lubricated Journal Bearing", First International Symposium on Gas-Lubricated Bearings", Washington, D.C., U. S. Office of Naval Research, 1959.

6. Pinkus, O., and Sternlicht, B., Theory of Hydrodynamic Lubrication, McGraw-Hill Book Company, New York, 1961.

7. Gross, W. A., Gas Film Lubrication, J. Wiley and Sons, Inc., New York, 1962.

8. Constantinescu, V. N., Lubricatia cu Gaze, Acad. Rep. P op. Romire, Bucurenti, 1963.

9. Langlois, W. E., Slow Viscous Flow, the MacMilan Company, New York, New York, 1964.

10. Orcutt, F. K., Dougherty, D. E. and Malanoski, S. B., "Steam Lubrication Studies, Part I Experimental Investigation of a Steam Lubricated Journal Bearing", MTI Rept. 67TR76, MTI, Latham, New York, 1967.

11. Zuber, N., and Dougherty, D. E., "Liquid Metal Challenge to the Traditional Methods of Two-Phase Flow Investigation", Proceedings of the EURATOM- E.T.H. Symposium on Two Phase Flow Dynamics, Eindhoven, Netherlands, 1967.

12. Zuber, N., "Flow Excursions and Oscillations in Boiling Two-Phase Flow Systems with Heat Addition", Proceedings of the EURATOM - E.T.H. Symposium on Two-Phase Flow Dynamics, Eindhoven, Netherlands, 1967.

13. Zuber, N., Staub, F. W. and Bijwaard, G., "Vapor Void Fraction in Subcooled Boiling and in Saturated Boiling Systems", Proceedings of the Third International Heat Transfer Conference, Chicago, Vol. 5, 24, 1966.

14. Zuber, N., and Staub, F. W., "The Propagation and Wave Form of the Vapor Volumetric Concentration in Boiling Forced Convection Systems Under Oscillatory Conditions", Int. J. Heat and Mass Transfer, Vol. 9, 87, 1966.

15. Zuber, N., and Staub, F. W., "An Analytical Investigation of the Transient Response of the Volumetric Concentration in a Boiling Forced-Flow System", Nuclear Science and Engineering, Vol. 30, 268, 1967.

16. Damköhler, G., "Einflusse der Stromung, Diffusion und des Wärmenberganges auf die Leistung von Reaktionsofen", Zeitch. Electrochemie, Vol. 42, 846, 1936.

17. Bosworth, R. C. L., "Chemical Similarity in Heterogeneous Catalysis", Trans. Faraday Soc., Vol. 43, 399, 1947.

18. Penner, S. S., Chemistry Problems in Jet Propulsion, Pergamom Press, New York, 1957.

19. Einstein, A., "A New Determination of Molecular Dimensions", Annalen der Physik (4), Vol. 19, 289, 1906.

20. Roscoe, R., "The Viscosity of Suspension of Rigid Spheres", Brit. of Appl. Phys. Vol. 3, 267, 1952.

21. Brinkman, H. C., "The Viscosity of Concentrated Suspensions and Solutions", J. of Chemical Physics, Vol. 20, 571, 1952.

NOMENCLATURE

Units M,L,T,θ

A = Cross sectional area of the film $[L^2]$
c = Mass concentration of the liquid $[-]$
h = Film thickness $[L]$
L = Characteristic length in the lateral direction $[L]$
N = Phase change number, Eq. (21) or Eq. (42)
p = Film pressure $[M\ L^{-1}\ T^{-2}]$
Re_s = "Squeeze" Reynolds number, Eq. (15), $[-]$
R = Gas constant $[L^2\ T^{-2}\ \theta^{-1}]$
R_e = Reynolds number, Eq. (16), $[-]$
T = Temperature $[\theta]$
t = Time $[T]$
S = Strouhal number, Eq. (13) or Eq. (43) $[-]$
u = x component of the velocity $[LT^{-1}]$
U_h, U_o = The x component of the velocity evaluated at y = h and y = 0, $[L\ T^{-1}]$
v = y component of the velocity $[L\ T^{-1}]$
V = Reference velocity in the lateral direction $[L\ T^{-1}]$
w = z component of the velocity $[L\ T^{-1}]$
W_h, W_o = The z component of the velocity evaluated at y = h and y = 0, $[L\ T^{-1}]$

Greek letters:

Γ_f = Volumetric liquid-phase source generation rate $[ML^{-3}\ T^{-1}]$
ϵ = h_o/L $[-]$
ρ = Density of the vapor-liquid mixture, $[M\ L^{-3}]$
ρ_g = Vapor density $[M\ L^{-3}]$
ρ_f = Liquid density $[M\ L^{-3}]$
ρ_a = Ambient density $[M\ L^{-3}]$
β = Bulk viscosity of the vapor $[M\ L^{-1}\ T^{-1}]$
μ = Vapor viscosity $[M\ L^{-1}\ T^{-1}]$
τ = Particle transit time, Eq. (40) $[T]$

Ω = Characteristic frequency of phase change, Eq. (41) $\left[T^{-1} \right]$

ω = Frequency of oscillation T^{-1}

Superscript: * denotes dimensionless quantities

Subscript: o denotes reference values

APPENDIX A

The Effect of Concentration on the Viscosity

There are several methods and equations which have been proposed for evaluating the effect of the concentration on the viscosity μ_m, of the mixture. Among them perhaps the best known is that of Einstein, Ref. [19], given by:

$$\mu_m = \mu(1 + 2.5\ \alpha) \tag{A-1}$$

where μ is the viscosity of the continuous phase and α is the volumetric concentration. The assumption used in deriving this equation limits its validity to $\alpha < 0.05$. For higher values of α, Roscoe, Ref. [20] and Brinkman, Ref. [21], have proposed the following relation:

$$\mu_m = \frac{\mu}{(1-\alpha)^{2.5}} \tag{A-2}$$

In the present analysis the effect of concentration on the viscosity was neglected, i.e., it was assumed that $\mu_m = \mu$. In order to demonstrate the validity of this assumption we shall express the volumetric concentration α, by means of the mass concentration c, thus

$$\alpha\ \rho_f = c\rho \tag{A-3}$$

whence in view of Eq. (31), we obtain

$$\alpha = \frac{c}{1-c}\left(\frac{\rho_g}{\rho_f}\right) \tag{A-4}$$

It is evident that in the present problem, α is very much smaller than unity, justifying its omission from Eq. (A-1).

APPENDIX B

The Effect of the Drift Stress Tensor

When the equation of motion of the two phase mixture is expressed in terms of the center of mass, the effect of the relative velocity between the two phases appears as a drift stress tensor, Ref. [12]. In the present problem this drift stress tensor was omitted from the equation of motion. In order to show that this omission was permissible, we shall evaluate the **X** component of this term which is given, Ref. [12], by

$$\tau^{D}_{xx} = (1-c)\, c\rho\, u_r^2 \tag{B-1}$$

which in view of Eq. (31), can be reduced to

$$\tau^{D}_{xx} = c\rho_g\, u_r^2 \tag{B-2}$$

The relative velocity u_r, between the vapor and liquid droplets is defined by

$$u_r = u_g - u_f \tag{B-3}$$

It can be determined from the equation of motion of a droplet located in a vapor stream with a pressure gradient. Neglecting the effects of virtual mass and of acceleration on the drag, the equation of motion for the laminar, i.e. Stokes flow regime is given by:

$$\rho_f \frac{4\Pi}{3} r^3 \frac{Du_f}{Dt} = 6\Pi \mu r\, u_r - \frac{4\Pi r^3}{3} \frac{\partial P}{\partial x} \tag{B-4}$$

where r is the radius of the droplet.

The scale of the relative velocity can be easily evaluated by considering a flow with constant liquid velocity, for which Eq. (B-4) reduces to:

$$\frac{\partial P}{\partial x} = \frac{9}{2} \frac{\mu}{r^2} u_r \tag{B-5}$$

We introduce now the dimensionless relative velocity u_r^* defined by

$$u_r^* = \frac{u_r}{\eta} \tag{B-6}$$

where η is the scale of the relative motion, to be determined from Eq. (B-5). Substituting Eq.(B-6) in Eq. (B-5) and recalling that the pressure and the X coordinate are scaled by Eq. (9) and Eq. (8), we obtain the dimensionless form of Eq. (B-5)., i.e.,

$$\frac{\partial P^*}{\partial x^*} = \frac{9}{2} \left(\frac{h_o}{r}\right)^2 \frac{\eta}{V} u_r^* \tag{B-7}$$

Since the dimensionless pressure gradient and the dimensionless relative velocity are of the same order of magnitude, the scale of the relative velocity must be given by

$$\frac{\eta}{V} = \frac{2}{9} \left(\frac{r}{h_o}\right)^2 \tag{B-8}$$

Considering even a large droplet with a diameter equal to say $h_o/2$, Eq. (B-8) indicates that the velocity ratio is still negligibly small, i.e., equal to 1/72.

Since the relative velocity is smaller (by approximately two orders of magnitude) than the lateral velocity, Eq. (B-2) indicates that in the present problem, it was permissible to neglect the effect of the drift stress tensor, i.e., of the relative velocity.

APPENDIX C

The Effect of Phase Change on the Temperature

It is shown (see for example Ref. [5, 7]) that gas (non-condensible) lubrication film flow can be considered as isothermal. Here we want to examine under what condition it is permissible to neglect the effects of phase change on the enthalpy of the film.

Defining by i_g and i_f the enthalpies of the vapor and of the liquid respectively, the enthalpy of the mixture is then given by

$$i_m = ci_f + (1-c)\, i_g \tag{C-1}$$

or

$$i_m = i_g \left[1-c \left(\frac{i_g - i_f}{i_g}\right)\right] \tag{C-2}$$

It can be seen that the enthalpy of the mixture can be approximated by that of the vapor as long as

$$c \left(\frac{i_g - i_f}{i_g}\right) << 1 \tag{C-4}$$

Consequently as long as this inequality is valid it is permissible as a first approximation, to neglect the effect of phase change on the mixture enthalpy.

C. Part II: The Constitutive Equation of Evaporation and/or Condensation for Non-Equilibrium Dispersed Film Flow

1. INTRODUCTION

1.1 Steam Lubrication Studies

Condensable-vapor, being a common process fluid, has been considered for lubricating surfaces requiring relative motion within or in close proximity to a condensable-vapor environment. In particular, steam lubricated bearings have recently been studied for applications in rotating Rankine cycle machinery, Ref. [1, 2]. These studies showed that the presence of condensate in the lubrication film was critical to the bearing performance. Tests of an externally pressurized journal bearing configuration, Refs. [3, 4] supplied with either saturated or superheated steam demonstrated that;

1. A dry steam lubrication film would perform as predicted by the compressible Reynolds' lubrication theory.

2. A small moisture fraction of condensate introduced into the lubrication film can cause a noticeable perturbation in the dry film pressure profile and flow rate.

3. The presence of condensate in the film may induce a bearing instability (steam hammer) which would not exist for a dry film under the same bearing operating conditions.

To understand and control this phenomena, a realistic model for high quality two-phase film flow is required.

1.2 Dispersed Two-Phase Film Flow Model

The basic elements of the two-phase thermo-hydrodynamic film flow model are:

1. Derivation of the two-phase field equations

2. Derivation of the constitutive equation of evaporation and/or condensation.

Part I was concerned with the first aspect of the two-phase film flow model, Part II the second aspect of the model which in particular assumes:

a. Entrained liquid droplet flow.

b. Non-equilibrium droplet evaporation and/or condensation neglecting surface energy effects, i.e. "capillary superheating" is assumed to be negligible.

c. Moisture weight fractions much less than unity.

Justification for considering a liquid-droplet flow regime is based in part on the fact that the boundaries of the lubrication film were locally superheated in the series of tests reported in Ref. [4]. Thus a separated two-phase flow of film wall condensate and bulk vapor is highly improbable. The condensate, when present was carried over from the steam supply into the bearing film or it was formed in the feed supply region, Ref. [5], and subsequently stripped off in the form of small droplets. Typical Weber numbers $\rho_g V^2 D_H/\sigma_f$, for the feed supply region of externally pressurized bearings, are much greater than the critical value (17, Ref. [6]) for film stripping. Also the stable droplet Weber number criteria, Ref. [7] shows that maximum ratio of the liquid-droplet diameter and film clearance is approximately 1/5, see section (3). Therefore in accordance with the results of Appendix B in Part I of this report, droplets of this size range will be essentially entrained in the vapor flow.

It should be noted that a superheated vapor film environment for steam lubricated externally pressurized bearings is typical, and an operating condition which can be readily designed into pressurized vapor bearings due to the vapor film pressure gradient and the attendant drop in the local saturation temperatures.

The phenomenological aspects of a steady-state non-equilibrium dispersed two-phase film flow primarily involve the evaporation of condensate which in droplet form is transported through the pressure gradient of the vapor-liquid mixture, and thereby caused to flash into vapor. This flow regime is illustrated in Fig.I.

The evaporation rate is controlled by the thermal diffusion of heat energy to the vaporizing surface of the liquid droplets. Because of the large thermal conductivity and volumetric heat capacity of the liquid droplets compared to that of the vapor phase, the majority of the latent heat for evaporation is supplied by the available thermal energy of the liquid droplets themselves. The available thermal energy of a droplet, which is initially in thermal equilibrium with its environment or superheated, increases in the presence of a decreasing environmental pressure since the liquid superheat increases with respect to the local saturation temperature of the evaporating droplet surface.

Due to the droplet evaporation the specific volume of the vapor-liquid mixture increases in the direction of the flow. This steepens the film pressure gradient which further increases the specific mixture volume. The formulation of this complex regenerative process is greatly simplified by the fact that the evaporation process is insensitive to the vapor phase bulk temperature level. This insensitivity as previously noted, and as shown in Fig. I, is a consequence of the small vapor-liquid interface heat flux ratio.

In general, dynamic film flow effects can lead to condensation of the vapor phase on the entrained liquid droplets. This occurs if the local film pressure is perturbed such that it exceeds the inital saturation pressure of the droplets at the film inlet. In the case of pressurized vapor bearings the film pressure under dynamic conditions does not exceed the bearing supply pressure. The temperature of the liquid droplet condensate introduced into the film, usually, see Section (3), equals the supply saturation temperature which is therefore never exceeded in dynamic or steady state film flow. This implies that evaporation effects dominate both the static and dynamic behavior of pressurized wet vapor bearings. It should also be noted that the non-equilibrium model for the constitutive equation of evaporation and/or condensation does not include condensate nucleation which requires local supersaturation of the vapor phase and depends upon surface energy effects. Extensive studies of nucleation phenomena in supersaturated vapor flow have been amply reported in the literature, e.g. Ref. [8]. In Ref. [8] it is also shown that "capillary superheating" of condensate droplets is significant only for very small droplets, $R < 10^{-5}$ in. The present model for the

constitutive equation of evaporation and/or condensation will be extended to include condensate nucleation and "capillary superheating" in a future publication.

1.3 Purpose of the Investigation

The purpose of this analysis is to develop a general constitutive equation for evaporation and/or condensation in a (non-nucleating) two-phase vapor film flow. The analysis combined with the results of Part I then complete the generalized dispersed two-phase film lubrication equation.

This two-phase Reynolds lubrication equation which is applicable for both dynamic and static film flows is then specialized to consider the steady-state evaporative strip film flow. This latter analysis clearly shows the major thermo-hydrodynamic parameters for vapor bearings and the influence these parameters, such as the inlet moisture fraction, the ratio of the film residence and droplet evaporation time, and the initial droplet superheating have upon an evaporative two-phase film flow.

Also the implications of this analysis on the dynamic behaviour of vapor bearings are discussed.

2. ANALYSIS

2.1 The Constitutive Equation of Evaporation and/or Condensation

The unique parameter in the general two-phase Reynolds' equation as obtained in Part I, is the net volumetric liquid mass formation rate, Γ_f. Consider therefore a dispersed two-phase fluid element of mass m which contains N liquid droplets entrained in the vapor phase and flowing in a thin film. The assumption of an entrained droplet flow, implies small droplets which have a short inertial relaxation time constant. Under these flow conditions, secondary droplet formation, due to collisions and shear fracture, is negligible so that the droplet number density in a fluid element, n = N/m, remains constant with time, and therefore

$$\Gamma_f/\rho = \frac{d}{dt}\left[\left(\frac{N}{m}\right)\left(\frac{4}{3}\right)\pi R^3\rho_f\right] = c_i \frac{d(R/R_i)^3}{dt} \tag{1}$$

and since the density of the mixture ρ, for mass concentrations $c \ll 1$ is approximately $\rho_g/1\text{-}c$, Γ_f from Equation (1) is given as

$$\Gamma_f = \rho_g \left(\frac{c_i}{1-c_i}\right) \frac{d(R/R_i)^3}{dt} \approx \rho_g c_i \frac{d(R/R_i)^3}{dt} \tag{2}$$

Equations (1) and (2) assume that the liquid droplet density ρ_f, is constant, and that R equals the volume weighted mean droplet radius.

Also it should be noted that a positive time rate of change of the normalized droplet mass $(R/R_i)^3$ signifies the occurrence of condensation, and a negative rate of change in droplet evaporation. In the following section the equation for the mean droplet radius as a function of the local film pressure is developed. This relationship in conjunction with Equation (2) will define the constitutive equation for a dispersed two-phase film flow.

2.2 Non-Equilibrium Droplet Dynamics

Liquid droplets of mean initial radius R_i are assumed to enter the film having a flat radial temperature profile at a temperature, $T_{fi} \geq T_{gi}$. When these droplets are transported into a region where $T_{fi} > T_s$, i.e. the local saturation temperature (T_s) as determined by the local static film pressure is less than the initial droplet temperature, the liquid surface of the droplets evaporates. Alternately when $T_s > T_{fi}$ the vapor phase condenses on the entrained droplets. The rate of evaporation and/or condensation is governed by the diffusion rate of thermal energy to the liquid-vapor interface and the latent heat of vaporization of the fluid. The liquid-vapor interface will be essentially at the local equilibrium pressure and temperature throughout the evaporation process, so that in the case of evaporation, thermal energy will difuse from both the liquid and bulk vapor phases as shown in Fig. I. The ratio of the liquid phase and vapor phase interface heat fluxes is proportional to $\left[(k\rho C_p)_f/(k\rho C_p)_g\right]^{1/2}$, which for most fluids is much greater than unity. Therefore this analysis only considers the diffusion of thermal energy within the liquid phase of the droplets to and from the vapor-liquid interface.

The non-equilibrium droplet evaporation and/or condensation model is thus reduced to finding the surface heat flux of a spherical liquid droplet having a time varying surface temperature equal to the local saturation temperature.

A mass and energy balance at the liquid droplet surface requires that

$$\phi = - \rho_f h_{fg} \dot{R} \tag{3}$$

where ϕ is the surface heat flux, ρ_f the droplet density, h_{fg} the latent heat of vaporization and $\dot{R}$ the time rate of change of the droplet radius.

With a spherical coordinate system fixed in a droplet, and assuming polar and azimuthal symmetry, the time dependent temperature field of a droplet being transported through the bearing film is given as

$$\frac{1}{r^2}\frac{\partial}{\partial r}\left[r^2\frac{\partial(T_{fi}-T_f)}{\partial r}\right]=\frac{1}{\alpha_f}\frac{\partial(T_{fi}-T_f)}{\partial t} \tag{4}$$

Integrating Equation (4) with respect to r gives

$$\phi=-k\left.\frac{\partial T_f}{\partial r}\right|_{r=R}=\frac{k_f}{\alpha_f R^2}\int_0^R r^2\frac{\partial(T_{fi}-T_f)}{\partial t}\,dr \tag{5}$$

Combining Equations (3) and (5) and using the boundary condition that the temperature of the droplet surface is equal to the local saturation temperature, one obtains

$$-\frac{\lambda}{3}\frac{dR^3}{dt}=\frac{d}{dt}\left\{\int_0^R (T_{fi}-T_f)\,r^2\right\}dr \tag{6}$$

where $\lambda \equiv \dfrac{h_{fg}-C_{pf}(T_{fi}-T_s)}{C_{pf}}$ is approximately $(h_g - C_{pf}T_{fi})/C_{pf}$ and essentially constant for many fluids since h_g for most vapors is a weak function of temperature. Integrating Equation (6) then gives

$$\frac{\lambda}{3}(R_i^3-R^3)=\int_0^R (T_{fi}-T_f)\,r^2\,dr \tag{7}$$

The asymptotic droplet evaporation can be readily obtained from Equation (7) by substituting the asymptotic saturation temperature for the droplet temperature (T_f) and integrating to obtain

$$\frac{R_i^3 - R_\infty^3}{R_\infty^3} = \frac{(T_{fi} - T_{s\infty})}{\lambda} \tag{8}$$

Thus $(R/R_i)_\infty^3 > \left[1 - \delta\right]$ where $\delta \equiv C_{pf} T_{fi}/h_{fg}$

In the case of saturated steam the ratio of the available and latent heat δ, is approximately 1/3 over a wide range of pressures so that the asymptotic unevaporated droplet mass fraction is greater than 2/3.

Following Von Karman's integral boundary layer method, an approximate solution of the heat-balance integral given by equation (7) can be obtained by prescribing a rational droplet temperature profile such as

$$T_{fi} - T_f \approx \begin{cases} (T_{fi} - T_s)\left(\frac{r-r'}{R-r'}\right) & ; \quad r' \leq r \leq R \\ 0 & ; \quad 0 \leq r < r' \end{cases} \tag{9a}$$

when $r'/R > 0$, and

$$T_{fi} - T_f \approx (T_{fi} - T_s)\left(\frac{r-r'}{R-r'}\right) \quad ; \quad 0 \leq r \leq R \tag{9b}$$

when $r'/R < 0$.

Note $(1-r'/R)$ defines the droplet thermal diffusion layer thickness.

Substituting Equations (9) into Equation (7) gives

$$\frac{\frac{4\lambda}{3}(R_i^3 - R^3)/R^3}{(T_{fi} - T_s)} \approx \begin{cases} (1-r'/R)\left[1 + \frac{2}{3}\left(\frac{r'}{R}\right) + \frac{1}{3}\left(\frac{r'}{R}\right)^2\right]; & r'/R > 0 \quad (10a) \\ \left[1 - \frac{1}{3}\left(\frac{r'/R}{1-r'/R}\right)\right] ; & r'/R < 0 \quad (10b) \end{cases}$$

Equations (10) are shown in Fig. 2.

Note that Equation (10b) is asymptotically correct, for when

$$r'/R \to \infty \ , \quad \frac{R_i^3 - R_\infty^3}{R_\infty^3} \to \frac{(T_{fi} - T_s)}{\lambda} \tag{11}$$

in agreement with Equation (8).

Also in accordance with Equation (10a) and (10b) when $(r'/R) = 0$ the evaporation process is approximately (3/4) completed since

$$\left(\frac{R_i^3 - R^3}{R^3}\right) = \frac{3}{4} \left(\frac{T_{fi} - T_s}{\lambda}\right) \tag{12}$$

To complete the solution of Equation (7), the droplet thermal diffusion layer thickness $(1-r'/R)$ must be defined in terms of the droplet radius and the thermal driving force, $(T_{fi} - T_s)$. This relationship can be obtained from the vapor-liquid mass-energy balance Equation (3), and the droplet surface temperature gradient obtained from Equations (9), giving

$$(1 - r'/R)\, R\dot{R} = - \frac{k_f}{\rho_f h_{fg}} (T_{fi} - T_s) \tag{13}$$

where $\dot{R} \equiv \frac{dR}{dt}$

Equation (13) combined with Equations (10) define the local dynamics of the droplet-vapor interface in the thermal potential field, $(T_{fi} - T_s)$. The resultant system of first order non-linear differential equations is complicated by the fact Equations (10a) and (10b) are discontinuous in the time domain. However a

good approximation for Equations (10a) and (10b) which is continuous over the entire range of $r'/R \leq 1$ is given as

$$1 - r'/R = \frac{\theta/2}{1-(\theta/\frac{4}{3})^2} \tag{14}$$

where $\theta \equiv \frac{4\lambda(1-R^{*3})/3R^{*3}}{(T_{fi} - T_s)}$

and the normalized droplet radius R^*, is defined by the ratio of instantaneous droplet radius R, and the initial radius R_i, of the droplet as it enters the film.

A comparison of Equations (10) and (14) is shown in Fig. 2.

Combining Equations (13) and (14) gives the following first order non-linear differential equation for the normalized droplet radius

$$\tau_D R^{*5} \frac{d}{dt}\left(\frac{1-R^{*3}}{R^{*3}}\right)^2 + \left(\frac{1-R^{*3}}{R^{*3}}\right)^2 = F(T^*) \tag{15}$$

where the characteristic droplet evaporation-condensation time, $\tau_D \equiv \frac{(R_i/3)^2/\alpha_f}{1-\delta(1-T_i^*)}$,

the thermal driving potential $F(T^*) \equiv \left[\frac{\delta(1-T^*)}{1-\delta(1-T_i^*)}\right]^2$, and $T^* \equiv \frac{T_s}{T_{fi}}$.

The product of the characteristic droplet evaporation-condensation time and the normalized droplet radius raised to the fifth power $\tau_D R^{*5}$, defines a first order time lag for variations of the quadratic droplet mass fraction. The asymptotic droplet mass fraction $\left(\frac{1-R_\infty^{*3}}{R_\infty^{*3}}\right)$, as given by Equation (15) is $\sqrt{F(T_\infty^*)}$ which

equals $\left(\frac{\delta(1-T_\infty^*)}{1-\delta(1-T_i^*)}\right)$. Thus the asymptotic evaporation fraction given by Equation (15) is exact and agrees therefore with Equation (8).

The forcing function $F(T^*)$ is determined by the thermal driving potential which is determined by the initial droplet temperature T_{fi} and the local saturation temperature T_s. It should also be noted that the droplet evaporation-condensation model includes the effect of introducing droplets which are initially superheated or subcooled into the vapor film. This is clearly shown in the thermal forcing function which in the case of evaporation equals the ratio of the specific heat available for evaporation, and the specific latent heat of the droplets reduced by their initial specific superheat.

The Clapeyron equation gives the relationship between the local saturation temperature and the film pressure so that

$$\frac{1-T^*}{T^*} = \frac{1-T_i^*}{T_i^*} - N_T \ln P \tag{16}$$

where the Trouton number N_T equals $\mathcal{R}T_{fi}/Jh_{fg}$ and $P \equiv p/p_i$.

In obtaining Equation (16) it is assumed that the latent heat is essentially constant, the specific volume of the vapor is much greater than that of the liquid phase, and the vapor phase behaves as an ideal gas.

Also the initial condition for Equation (16), i.e. $P = 1$ is defined by the initial fractional droplet superheat ratio $(1-T_i^*)/T_i^*$.

Combining and rearranging Equations (15) and (16) gives

$$\tau_D R^{*5} \frac{d}{dt}\left[\frac{1-R^{*3}}{R^{*3}}\right]^2 + \left[\frac{1-R^{*3}}{R^{*3}}\right]^2 = F(P) \tag{17}$$

where $F(P) \equiv \left(\frac{\delta}{1-\delta(1-T_i^*)}\right)^2 \left[1 - \frac{T_i^*}{1-N_T \ell nP}\right]^2$

In accordance with Equation (8), $1 \geq R^{*5} > (1-\delta)^{5/3}$ and when $\delta << 1$ Equation (17) is approximately linear in the variable $\Psi \equiv \left[\frac{1-R^{*3}}{R^{*3}}\right]^2$. In the case of steam $1 \geq R^{*5} > .5$.

Linearizing Equation (17) then gives

$$\tau_D \frac{d\Psi}{dt} + \Psi = F(P) \tag{18}$$

Integrating Equation (18) one obtains

$$R^{*3}(t,P) = \left\{1 + \left[\int_0^t F(P) \exp\left(-\frac{t-\zeta}{\tau_D}\right) d\zeta\right]^{1/2}\right\}^{-1} \tag{19}$$

Combining Equation (19) and Equation (2) one obtains the <u>general constitutive equation</u> for evaporation and/or condensation in a dispersed two-phase film flow

$$\Gamma_f = \frac{pc_i}{RT_{vi}} \frac{D}{Dt} \left\{1 + \left[\int_0^t F(P) \exp\left[-\frac{t-\zeta}{\tau_D}\right] d\zeta\right]^{1/2}\right\}^{-1} \tag{20}$$

where $\frac{D}{Dt} \equiv$ substantial derivative.

2.3 Steady State Evaporative Film Flow

Formally Euqation (20) combined with Equation (39) in Part I of this report completes the dispersed two-phase Reynolds' film flow equation. This equation describes both the static and dynamic film pressure profiles and flow rates of a dispersed two-phase film flow including the effects of a non-equilibrium change of phase.

As a first step toward obtaining an understanding of non-equilibrium two-phase film flow phenomena, the preceding general equations have been used to analyze steady state, one dimensional, evaporative two-phase film flow. Besides lending clarity and tractability to the analysis, the simple film flow geometry considered in this study, Fig. I (semi-infinite strip bearing), can also be used to synthesize the steam journal bearing test configuration of Ref. [4].

The general two-phase Reynolds' equation as obtained in Part I, for the case of a strip bearing configuration without relative motion between the boundaries, under steady state conditions reduces to

$$\frac{d}{dx}\left\{\frac{h^3}{12\mu}\ p\ \frac{dp}{dx}\right\} = \mathcal{R}T_{vi}\ h\ \left\langle \Gamma_f \right\rangle \tag{21}$$

In a steady state dispersed two-phase film flow the thermodynamic forcing function $F(T^*)$ is always positive, i.e. $(T_{fi} - T_s) \geq 0$. Therefore the liquid droplets evaporate as they traverse the film, and in accordance with Equation (2) Γ_f averaged across the film under steady flow conditions is given as

$$\left\langle \Gamma_f \right\rangle = \frac{1}{h}\left\{\int_0^h \rho\, c_i\, u\ \frac{dR^{*3}}{dx}\right\} dy \tag{22}$$

Since $u = 6(\frac{y}{h})(1 - \frac{y}{h})\ \frac{Q}{\rho h}$ where Q is the mass flow rate per unit width of the bearing film, Equation (22) becomes

$$\left\langle \Gamma_f \right\rangle = c_i \left(\frac{Q}{h}\right) \frac{d\left\langle R^{*3} \right\rangle}{dx} \tag{23}$$

where

$$\left\langle R^{*3} \right\rangle = \frac{\int_0^1 R^{*3}\ (y/h)(1-y/h)d(y/h)}{\int_0^1 (y/h)(1-y/h)d(y/h)} \tag{24}$$

Combining Equations (21) and (24) gives

$$\frac{d^2 p^2}{dx^2} = C_1 c_i \frac{d\left\langle R^{*3} \right\rangle}{dx} \tag{25}$$

where $C_1 \equiv \frac{24\mu Q \mathcal{R} T_{gi}}{h^3}$

Integrating Equation (25) and requiring that the negative gradient of the quadralic pressure distribution for a dry film equals C_1, gives

$$\frac{dp^2}{dx} = - C_1 \left[1 - c_i \left\langle R^{*3} \right\rangle\right] \tag{26}$$

Since the instantaneous mean droplet mass fraction $\left\langle R^{*3} \right\rangle$, equals $\left\langle \frac{1}{1+\Psi^{1/2}} \right\rangle$ equation (26) becomes

$$\frac{dp^2}{dx} = - C_1 \left[1 - \left\langle \frac{c_i}{1+\Psi^{1/2}} \right\rangle \right] \tag{27}$$

The quadratic evaporation fraction Ψ, is determined from Equation (18) which for steady flow conditions becomes

$$\tau_D \, u \, \frac{d\Psi}{dx} + \Psi = F(P) \tag{28}$$

Equations (27) and (28) define the steady state film pressure profile, and flow rate.

To solve Equations (27) and (28) it is most convenient to first eliminate the spatial coordinate and solve for the quadratic evaporation fraction Ψ, as a function of pressure, and the transverse coordinate of the film, y. Dividing these equations one obtains

$$- 3 \left(\frac{\tau_D}{\tau_f(y)} \right) \frac{d\Psi}{dP^3} + \Psi = F(P) \tag{29}$$

where the y dependent film transit time $\tau_f(y)$, is defined as $\frac{p_i h L}{6(y/h)(1-y/h)Q\mathcal{R}T_{gi}}$, and $c_i << 1$.

The ratio of the droplet time constant τ_D and the characteristic film transit time $\tau_f(y)$ defines a local evaporation relaxation parameter. If the evaporation relaxation parameter is much less than unity this implies that the asymototic evaporation rate will be established near the inlet region of the film. In the case of a relaxation parameter much greater than unity only a small amount of evaporation will occur within the film.

Rearranging Equation (29) one obtains

$$\frac{d}{dP^3}\left\{\Psi \exp\left[-\frac{P^3}{3\gamma(y)}\right]\right\} = F(P)\ \frac{d}{dP^3}\left\{\exp\left[-\frac{P^3}{3\gamma(y)}\right]\right\} \tag{30}$$

where $\gamma(y) \equiv \tau_D/\tau_f(y)$

Integrating Equation (30) by parts, one obtains the approximation

$$\Psi(P,y) \approx F(P)\left\{1 - \frac{F(1)}{F(P)} \exp\left[-\frac{(1-P^3)}{3\gamma(y)}\right]\right\} \tag{31}$$

Thus

$$\Psi^{1/2}(P,y) \approx \eta\left(1 - \frac{T_i^*}{1-N_T \ell nP}\right)\left\{1 - \left(\frac{1-T_i^*}{1-\frac{T_i^*}{1-N_T \ell nP}}\right)^2 \exp\left[-\frac{(1-P^3)}{3\gamma(y)}\right]\right\}^{1/2} \tag{32}$$

where $\eta \equiv \frac{\delta}{1-\delta(1-T_i^*)}$

The normalized droplet evaporation fraction $\Psi^{1/2}/\eta$, is shown in Fig. 3 as a function of the local film pressure ratio P, the evaporation relaxation constant γ, and the initial fractional superheating of the liquid droplets, $(1-T_i^*)$. The Trouton number for steam ($N_T \approx 1/10$) was used in these calculations.

Combining Equations (27) and (32) one obtains the film pressure profile by quadratures, such that

$$1 - P^2 \approx \left(\frac{C_1 x}{p_i^2}\right) + 2\int_1^P \left\langle \frac{c_i}{1+\Psi^{1/2}} \right\rangle PdP \tag{33}$$

For equal mass flow rates the wet film pressure drop is less than that of a dry film. Moisture fractions much less than unity do not significantly influence the pressure profile when the evaporation relaxation constant γ_{av}, is either much greater or much less than unity. A large value of γ_{av} implies that the majority of the evaporation process occurs at the exit region of the film whereas γ_{av} much less than unity causes the entrained droplets to rapidly attain the asymptotic evaporation rate at the inlet region of the film.

As noted previously, the droplet evaporation time is proportional to (R_i^2/α_f), thus the initial droplet size is critical in the determination of γ_{av} which is proportional to the ratio of the droplet evaporation time constant, τ_D, and the film residence time, τ_f. The experiments and analysis reported in Ref. 7 allow a rough determination of the mean-maximum droplet radius. The atomization of liquid droplets in two component spray nozzles of various configurations showed that the fineness of a low-viscosity liquid droplet spray is approximately inversely proportional to the kinetic energy of the gas phase relative to the droplets, thus

$$R_i \leq 3\sigma_f \Big/ \frac{\rho_g V_{rel}^2}{2g_o} \tag{37}$$

Equation (37) is based on a critical Weber number, $\frac{2\rho_g R_c V_{rel}^2}{g_o \sigma_f}$ for stable droplets equal to 12.

Combining this result with the definitions of τ_{fav} and τ_D one can show the ratio of the droplet evaporation time constant and the average film transit time is proportional to $(2g_o\rho_g\sigma_f)^2 \Big/ \alpha_f \rho_g G^3$ where σ_f is the liquid phase surface tension and G is the mass flux of the film. In the case of the externally pressurized steam journal bearing tests, Refs. [3, 4], $1/10 < \gamma_{av} < 1$.

Figure 3 shows the strong effect the evaporation relaxation number γ, and the initial droplet superheat fraction $(1-T_i^*)$ has on the evaporation process. As γ decreases the rate of evaporation increases due to the reduced thermal inertia

where $c_i << 1$ and, in accordance with the averaging operator defined by Equation (24), Equation (33) becomes

$$1-P^2 \approx \left(\frac{C_1 x}{p_i^2}\right) - 12 \int_P^1 \int_0^1 \left\{(y/h)(1-y/h)\left(\frac{c_i P}{1+\Psi^{1/2}}\right)\right\} d(y/h)\, dP \qquad (34)$$

A comparison of wet and dry film pressure profiles obtained from Equation (34) are shown in Fig. 4, for a range of inlet moisture fractions c_i, and film pressure ratios, P_a. The mean evaporation relaxation constant γ_{av} indicated in Fig. 4 equals τ_D/τ_{fav} where the average film transit time τ_{fav} is defined as $p_i hL/Q\mathcal{R}T_{gi}$.

From Equation (33) it should be noted that

$$(1+c_i)\left[1 - \left(\frac{p_a}{p_i}\right)^2\right] > \frac{C_1 L}{p_i^2} \qquad (35)$$

The right hand side of the inequality (35) equals $\left(\frac{p_{i\ Dry}}{p_{i\ Wet}}\right)^2 \left[1 - \left(\frac{p_a}{p_i}\right)^2_{Dry}\right]$

where $p_{i_{Dry}}$ and $p_{i_{Wet}}$ are respectively the dry film inlet pressure and wet film inlet pressure for equal film mass flow rates. Then for practical film pressure ratios $(p_i/p_a)^2 >> 1$, one obtains the relationship

$$1 < \left(\frac{p_{i\ Dry}}{p_{i\ Wet}}\right)^2 < 1 + c_i \qquad (36)$$

3. DISCUSSION

3.1 The Constitutive Equation for a Non-Equilibrium Change of Phase

A general constitutive equation for evaporation and/or condensation in a two-phase vapor film has been obtained, in a convective (Lagrangian) coordinate system. The dynamic behavior of the constitutive equation is governed by the time rate of change of the mean droplet mass. The temporal behavior of the quadratic droplet mass fraction whether evaporating or condensing is described by a first order time delay equation with a time constant proportional to the ratio of the initial droplet surface area and thermal diffusivity. The forcing function for the droplet evaporation and/or condensation is determined by the thermal driving potential between the internal droplet temperature and a time varying surface saturation temperature.

The heat-balance integral method, Ref. 9, is the basis of the non-equilibrium droplet dynamic analysis. While not exact the tractability of the method strongly recommends itself for this complex phase-change problem.

Formally, the constitutive equation as obtained here when combined with the results of Part I gives the complete equation for a dispersed two-phase Reynolds' film flow. As a first step toward applying these analysis, a steady state evaporative strip film flow was considered. This idealized configuration is particularly useful for synthesizing the pressure-flow characteristics of externally pressurized vapor lubricated journal bearings.

3.2 Important Parameters

The results of these steady state analysis clearly show that the total vapor film pressure drop is only slightly modified by the presence of a small inlet film moisture fraction. On the other hand the presence of condensate can dramatically effect the dynamics of a two-phase film flow. These dynamic effects are discussed in the following section.

For equal mass flow rates the wet film pressure drop is less than that of a dry film. Moisture fractions much less than unity do not significantly influence the pressure profile when the evaporation relaxation constant γ_{av}, is either much greater or much less than unity. A large value of γ_{av} implies that the majority of the evaporation process occurs at the exit region of the film whereas γ_{av} much less than unity causes the entrained droplets to rapidly attain the asymotic evaporation rate at the inlet region of the film.

As noted previously, the droplet evaporation time is proportional to (R_i^2/α_ℓ), thus the initial droplet size is critical in the determination of γ_{av} which is proportional to the ratio of the droplet evaporation time constant, τ_D, and the film residence time, τ_f. The experiments and analysis reported in Ref. 7 allow a rough determination of the mean-maximum droplet radius. The atomization of liquid droplets in two component spray nozzles of various configurations showed that the fineness of a low-viscosity liquid droplet spray is approximately inversely proportional to the kinetic energy of the gas phase relative to the droplets, thus

$$R_i \leq 3\sigma_f \Big/ \frac{\rho_g V_{rel}^2}{2g_o} \tag{37}$$

Equation (37) is based on a critical Weber number, $\frac{2\rho_g R_c V_{rel}^2}{g_o \sigma_f}$ for stable droplets equal to 12.

Combining this result with the definitions of τ_{fav} and τ_D one can show the ratio of the droplet evaporation time constant and the average film transit time to $(2g_o\rho_g\sigma_f)^2 / \alpha_f \rho_g G^3$ where σ_f is the liquid phase surface tension and G is the mass flux of the film. In the case of the externally pressurized steam journal bearing tests, Refs. [3, 4], $1/10 < \gamma_{av} < 1$.

Figure 3 shows the strong effect the evaporation relaxation number γ, and the droplet superheat fraction $(1-T_i^*)$ has on the evaporation process. As γ decreases the rate of evaporation increases due to the reduced thermal inertia

of smaller droplets. When $(1-T_i^*)$ increases, the degree of droplet superheating at the inlet to the film increases which also causes a more rapid evaporation of the droplets. Droplet superheating can be obtained by rapidly throttling the wet vapor before it is fed into the film. Under these conditions the droplets will typically retain their initial temperature during the expansion (droplet transit time $<< \tau_D$), and thereby are superheated with respect to the saturation temperature of the throttled pressure at the inlet to the evaporative film. Externally pressurized vapor bearings traditionally use fed hole throttling to obtain bearing stiffness (compensation). At optimum design stiffness the ratio of the film inlet pressure and bearing supply pressure is typically 3/4. In the case of an externally pressurized steam lubricated bearing T_i^*, for the above pressure ratio is approximately .95 over a wide range of supply pressures (3-25 atm.).

3.3 Dynamic Effects

Of the three major wet-vapor film flow parameters;

a) inlet moisture fraction (c_i)
b) evaporation relaxation constant (γ_{av})
c) droplet superheat fraction ($1-T_i^*$)

The latter two parameters are the most sensitive to dynamic film flow effects. The inlet moisture fraction is typically fixed by the vapor supply conditions and independent of the vapor film flow. An exception to this situation was noted in Ref. 5 where it was shown that environmental temperature of the film inlet can cause local condensation of the vapor being supplied to the film. It should be noted though, that the magnitude of the dynamic flow effects reflect the level of the inlet moisture fraction.

It has been shown that the initial droplet size is influenced by the film flow rate and that the evaporation constant γ_{av} is inversely proportional to the cube of the film mass flux, therefore the droplet evaporation rate and the mass storage in the film will be sensitive to variations in the film flow.

A varying flow rate in a bearing film will also modify the compensation pressure ratio and thereby change the initial droplet superheat fraction ($1-T_i^*$). This dynamic effect will also change the film mass storage rate.

The damping and stability of a vapor bearing depend upon the dynamics of the film mass storage. If the time constant is too large to store vapor and increase the mean film pressure as the compensated film inlet pressure is increased, the bearing will be poorly damped or unstable. Since an increasing inlet film pressure will decrease the droplet superheat fraction and retard droplet evaporation the mean film pressure will build more slowly than in a dry film. This dynamic mass storage effect in conjunction with the dynamic effects of the evaporation relaxation number causes a wet-vapor bearing to have a unique stability boundary compared to that of non-condensing gas bearings.

Thus, the above steady-state evaporative film analysis is but a first step toward a dynamic analysis of vapor films and the evaluation of vapor bearing stability maps. In this regard, Equations (39) of Part I and (20) of Part II form the basis of a dynamic evaporative film analysis.

4. CONCLUSIONS

1. A non-equilibrium two-phase film flow model has been developed. The model postulates that evaporation and/or condensation of liquid droplets entrained in a vapor film flow is determined by the thermal driving potential of the internal droplet temperature and the local time varying surface saturation temperature of the droplets. The model is applicable to the analysis of steam lubricated bearings.

2. A constitutive equation of condensation and/or evaporation was obtained for a two-phase film flow including the effects of a non-equilibrium change of phase. This constitutive equation combined with the field equations of a two-phase Reynolds' film flow developed in Part I complete the equation for the static and dynamic film pressure profiles and flow rates.

3. The steady state, one-dimensional evaporative film flow was analyzed. This analysis identified three major thermo-hydrodynamic parameters of a wet vapor film flow: a) the inlet moisture fraction, b) the evaporation relaxation constant, c) the initial droplet superheat fraction. This analysis showed the influence of these parameters upon the droplet evaporation fraction, and the film pressure profile.

4. Finally the dynamic effects of the inlet liquid droplet Weber number and, the above thermo-hydrodynamic parameters on a wet vapor lubrication film were discussed.

5. REFERENCES

1. Unterberg, W., and Ausman, J.S., "Condensing Vapor Lubrication of Self-Acting Long Journal Bearings", Jour. of Basic Engineering, Trans. ASME, Series D, No. 1,March, 1966.

2. Dougherty, D.E. and Pan, C.H.T., "Process Fluid Lubrication", AD-641369, for Office of Naval Research, (1967).

3. Dougherty, D.E. and Orcutt, F.K., "Exploratory Investigation of Externally-Pressurized Steam-Lubricated Journal Bearing Instabilities", MTI-66TR37, Contract Nonr-3731(00)FBM, (1966).

4. Orcutt, F.K., Dougherty, D.E., Malanoski, S.B., "Steam Lubrication Studies, Part I - Experimental Investigation of a Steam Lubricated Journal Bearing", MTI-67TR76, Contract N00014-66-C0214, Office of Naval Research, November, 1967.

5. Hsing, F. and Dougherty, D.E., "Steam Lubrication Studies, Part II, Thermal Environmental Analysis of an Externally Pressurized Steam Bearing", MTI-67TR77, Contract N00014-66-C0214, (1967).

6. Zuber, N., "On the Atomization and Entrainment of Liquid Films in Shear Flow", Rt. No. 62GL153, General Electric Co., Sept., (1962).

7. Kutateladze, S.S. and Stysikovich, M.A., Hydraulics of Gas-Liquid Systems, Chapter 8, Moscow (1958), Translation NP-TR-550, Tech. Info. Center, MCLTD, Wright-Patterson Air Force Base, 1960.

8. Gyarmathy, G., "Foundations of a Theory of the Wet-Steam Turbine", FTD-TT-63-785, Translation Div. Wright-Patterson Air Force Base, April, (1964).

9. Goodman, T.R., "Application of Integral Methods to Transient Non-Linear Heat Transfer", Advances in Heat Transfer (Academic Press Inc., New York, 1964), Vol. 1, pp. 51-122.

NOMENCLATURE

Units M,L,T,θ

c = Mass concentration of the liquid $[-]$
C_p = Heat capacity $[L^2\ T^{-2}\ \theta^{-1}]$
D_H = Hydraulic diameter $[L]$
h = Film thickness $[L]$
h_{fg} = Latent heat of evaporation $[L^2\ T^{-2}]$
J = The mechanical equivalent of heat $[-]$
k = Thermal conductivity $[MLT^{-3}\ \theta^{-1}]$
L = *Length of the strip film* $[L]$
N_T = Trouton number, Eq. (16), $[-]$
n = Droplet number density $[M^{-1}]$
p = Film pressure $[ML^{-1}\ T^{-2}]$
P = Normalized film pressure, Eq. (16), $[-]$
Q = Vapor-liquid mass flow rate per unit width of film $[MT^{-1}\ L^{-1}]$
r = Radial coordinate in liquid droplets $[L]$
R = Radius of a liquid droplet $[L]$
$\mathcal{R}$ = Vapor phase gas constant
t = Time $[T]$
T = Temperature $[\theta]$
u = The x component of *the local film velocity* $[LT^{-1}]$
V = Mean velocity of the vapor in the film supply region $[LT^{-1}]$
y = Transverse film coordinate $[L]$

Greek letters

α = Thermal diffusivity $[L^2\ T^{-1}]$
δ = Ratio of stored and latent heat, following Eq. (8), $[-]$
η = Ratio of stored and net heat of vaporization, following Eq. (32) $[-]$
γ = Evaporation relaxation parameter, Eq. (30), $[-]$
Γ_f = Volumetric liquid-phase source generation rate $[ML^{-3}\ T^{-1}]$
ζ = Dummy variable $[-]$

$1/\lambda$ = η/T_{fi} $[\theta^{-1}]$

μ = Vapor viscosity $[ML^{-1}\ T^{-1}]$

ρ = Density of liquid-vapor mixture $[ML^{-3}]$

σ = Surface tension $[MT^{-2}]$

τ_D = Droplet time constant $[T]$

τ_f = Film residence time $[T]$

ϕ = Heat flux $[MT^{-3}]$

Ψ = The quadratic evaporation fraction $[-]$

Superscript

. denotes total derivative with respect to time

* denotes dimensionless quantities

Subscripts

av denotes average quantity

f denotes liquid phase

g denotes vapor phase

i denotes initial value

rel denotes relative to the liquid-droplet phase

s denotes saturation value

∞ denotes asymptotic value

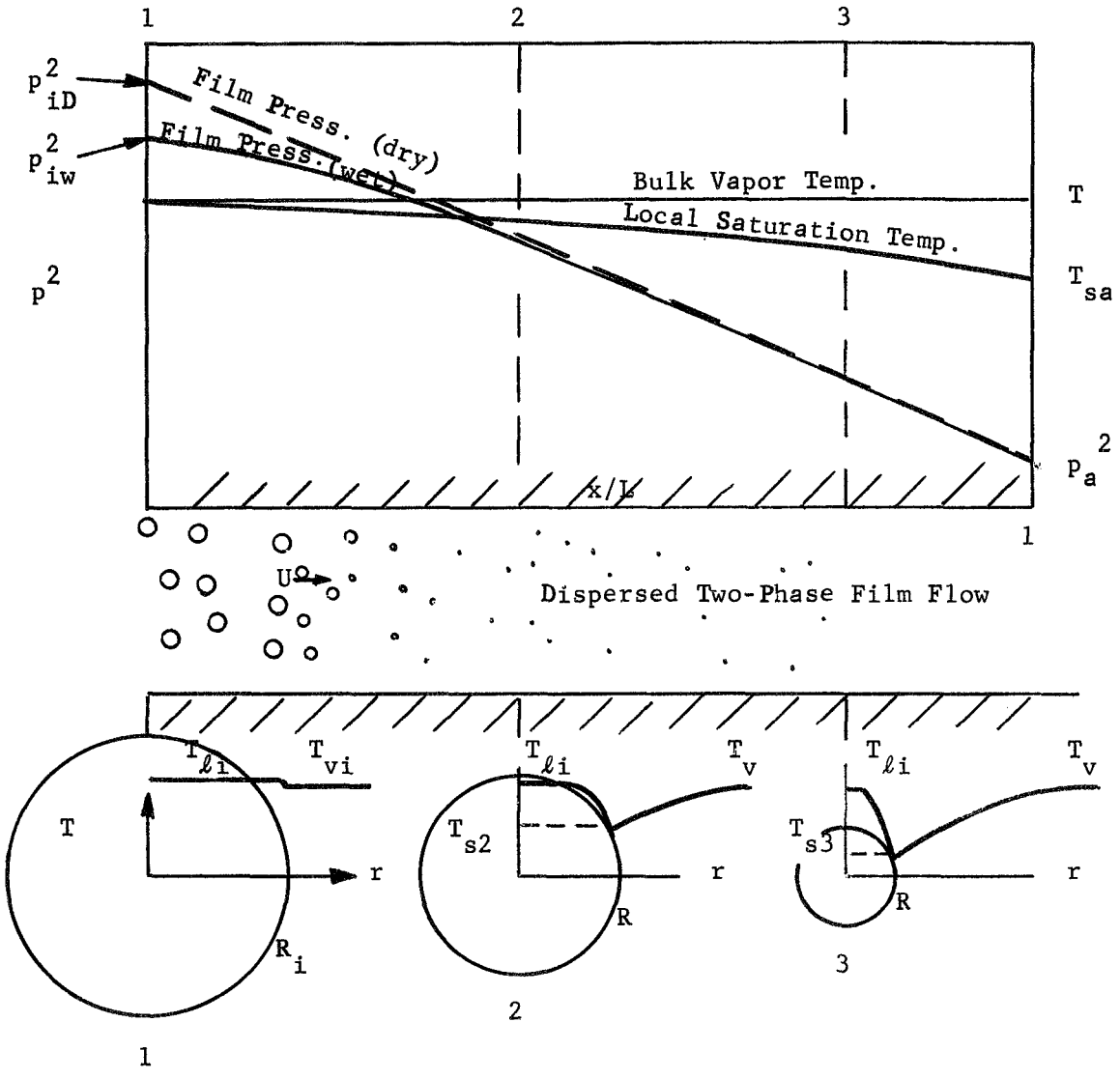

Fig. I Phenomenological Processes in Dispersed Two-Phase Evaporative Film Flow

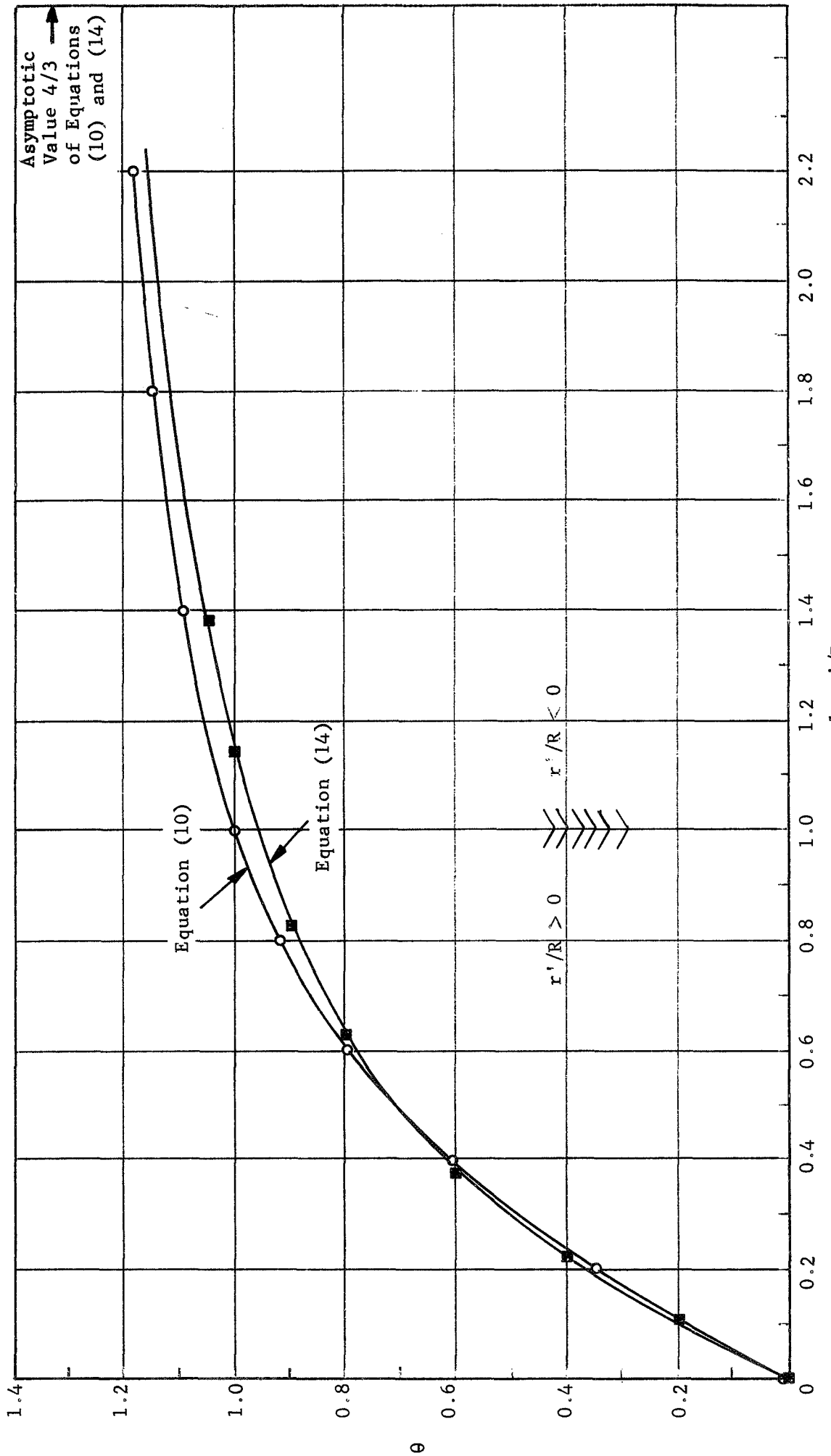

Fig. 2 The Thermal Diffusion Layer Approximations

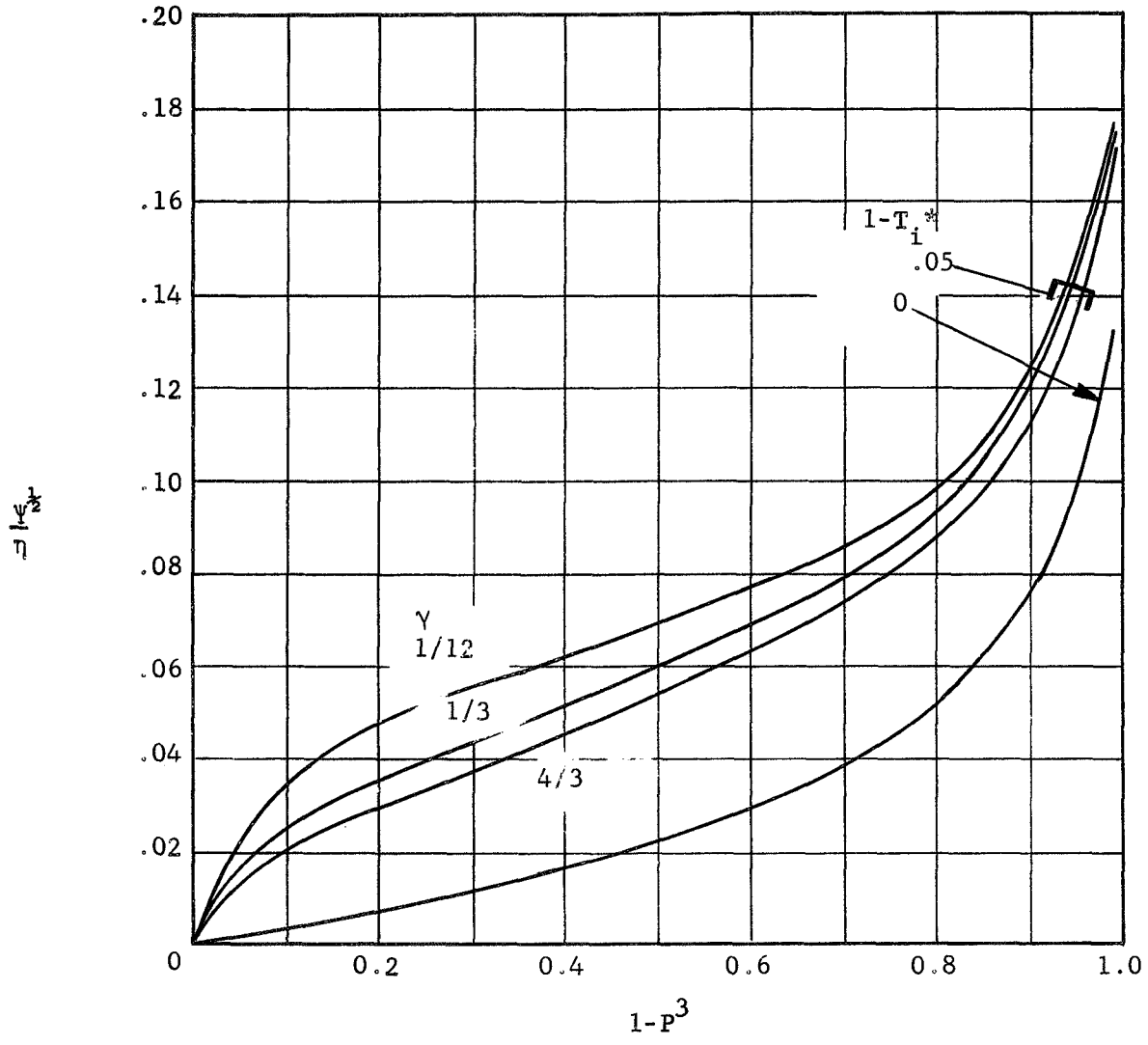

Fig. 3 The Evaporation Fraction versus the Film Pressure Ratio

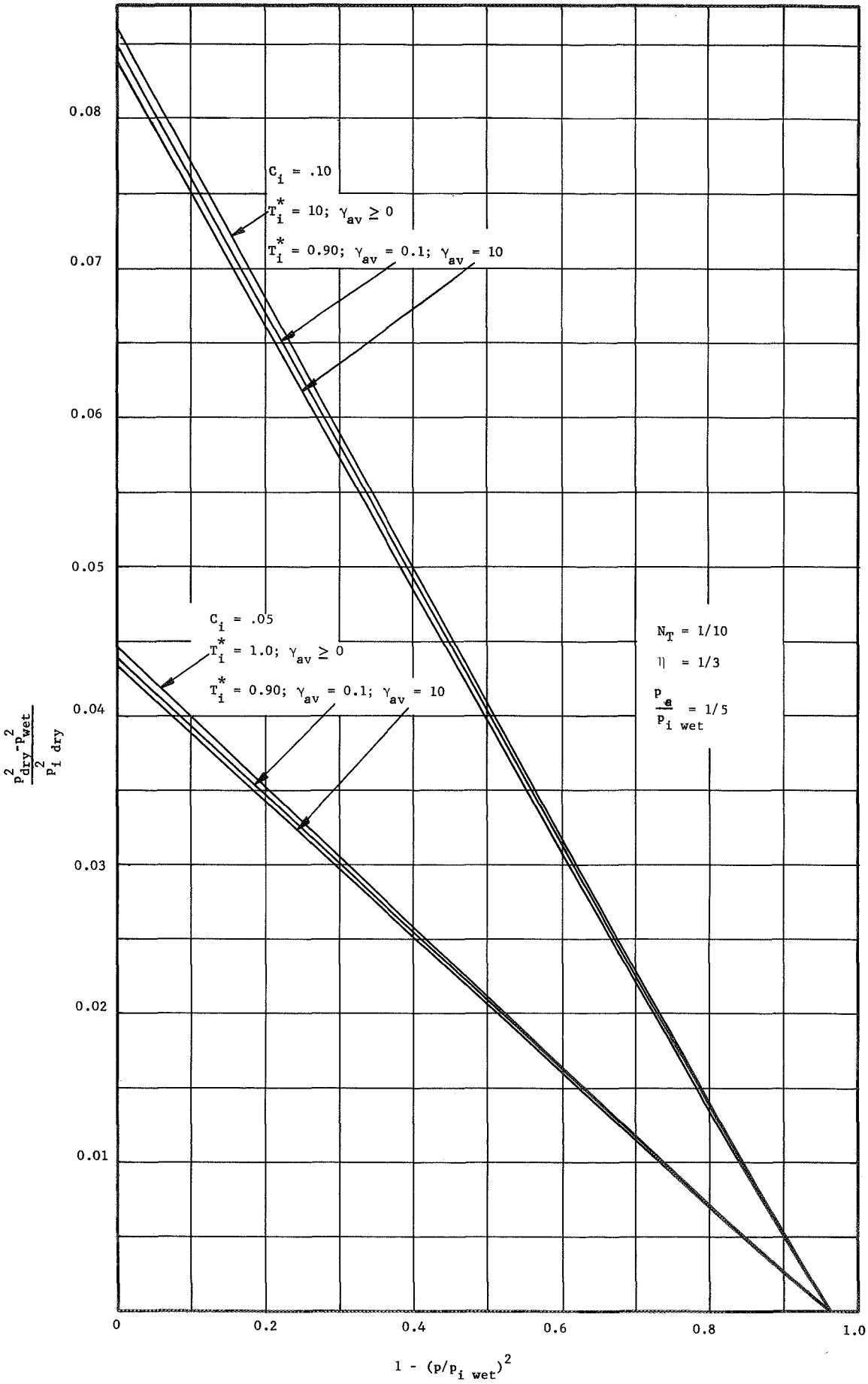

FIG. 4a A COMPARISON OF WET AND DRY VAPOR FILM PRESSURE PROFILES

MTI-5387

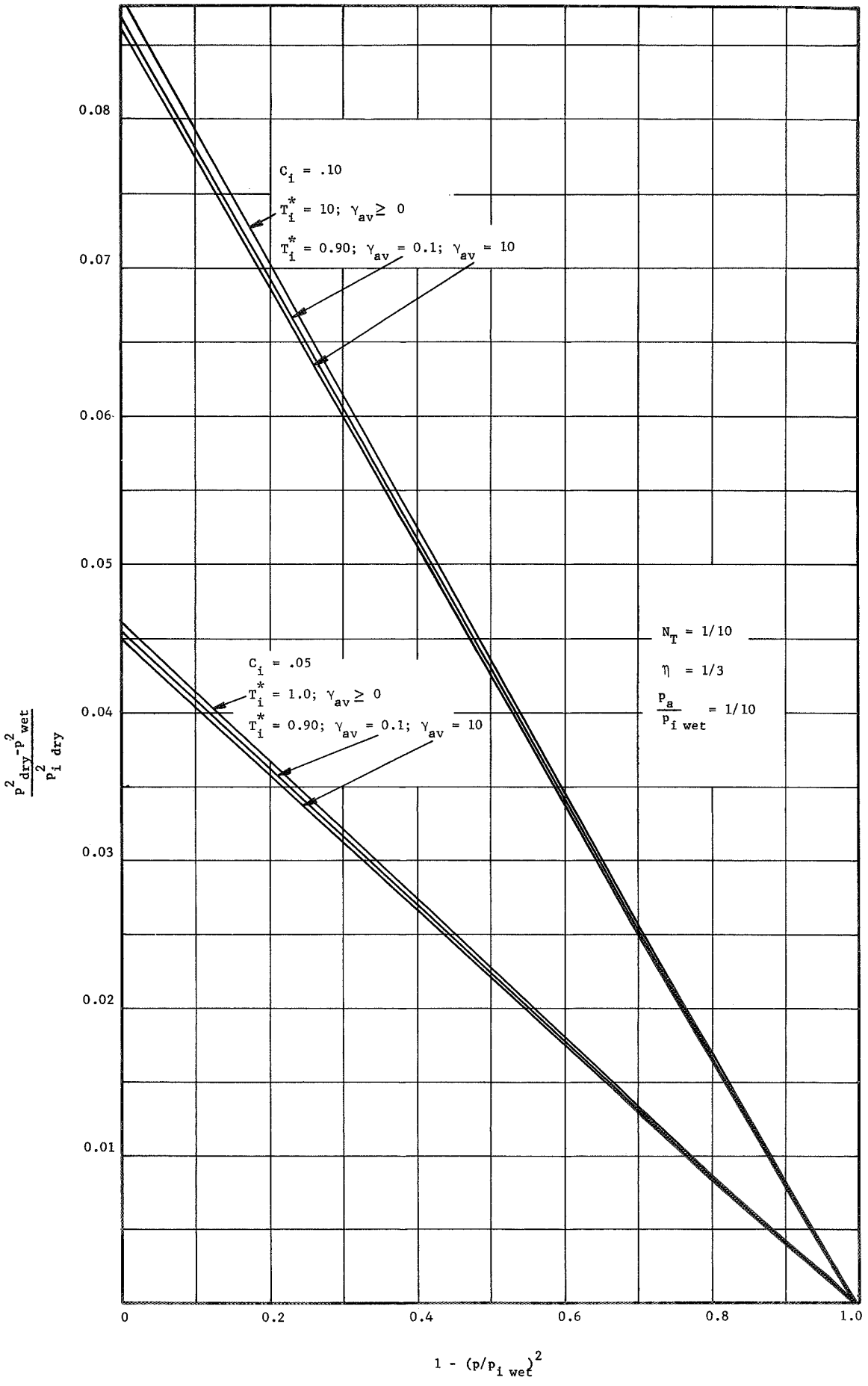

FIG. 4b A COMPARISON OF WET AND DRY VAPOR FILM PRESSURE PROFILES

MTI-5386

APPENDIX III

ENERGY EQUATION FOR VAPOR BUBBLE

Consider the vapor bubble shown in the sketch below

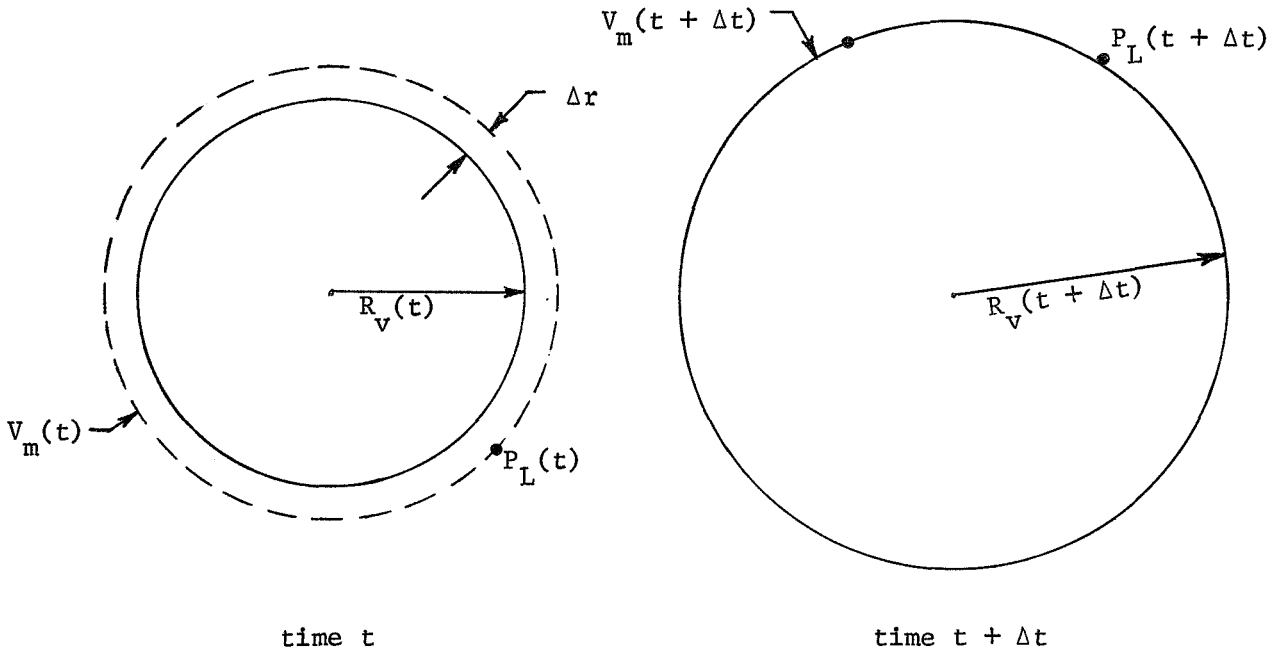

We consider as our thermodynamic system the vapor bubble at time t plus a layer of liquid around the bubble of infinitesimal thickness Δr which contains the volume of liquid $V_L = \Delta r\ 4\pi R_v^2$ which will vaporize into the bubble in the time interval from $t + \Delta t$. Thus, we are taking as our control system a material volume V_m which always contains the same mass of fluid. Applying conservation of energy to this material volume, neglecting kinetic and potential energy, we have

$$\frac{dU_m}{dt} + \frac{1}{J} P_L \, d V_m + \frac{d E_\sigma}{dt} = \frac{dQ}{dt} \qquad \text{(C-1)}$$

where U_m is the internal energy of the material volume V_m, P_L is the pressure at the outer surface of the volume, $\frac{dQ}{dt}$ is the heat transfer into the volume, and

E_σ represents the energy stored in the surface tension of the vapor bubble. The term $d E_\sigma/dt$ can be expressed as

$$\frac{d E_\sigma}{dt} = \frac{1}{J} (P_v - P_L) \frac{dV}{dt} \tag{C-2}$$

where V represents the volume of the bubble specifically. Noting that

$$\frac{d V_m}{dt} = \frac{d V}{dt} + \frac{d V_L}{dt} \tag{C-3}$$

and using Eq. (C-2) we can write Eq. (C-1) as

$$\frac{dU}{dt} + \frac{P_L}{J} \frac{d V_L}{dt} + \frac{P_v}{dt} = \frac{dQ}{dt} \tag{C-4}$$

The change in internal energy in the material volume can be divided as follows:

$$\frac{dU}{dt} = \frac{dU_v}{dt} + \frac{dU_L}{dt} \tag{C-5}$$

where U_v and U_L are the internal energies of all the vapor and liquid respectively inside the material volume. dU_L/dt can be written as

$$\frac{dU_L}{dt} = - u_L \dot{m} \tag{C-6}$$

where u_L is the specific internal energy of the liquid and $\dot{m}$ is the mass rate of change of vapor contained within the bubble. dV_L/dt may be written as

$$\frac{dV_L}{dt} = - \frac{1}{\rho_L} \dot{m} \tag{C-7}$$

Substituting Eqs. (C-6) and (C-7) into Eq. C-4) we obtain Eq. (12) of the text

$$\frac{dU_v}{dt} + \frac{P_v}{J}\frac{dV}{dt} = \frac{dQ}{dt} + u_L \dot{m} + \frac{1}{J}\frac{P_L}{\rho_L}\dot{m} \tag{C-8}$$

By neglecting certain terms, Eq. (C-8) can be greatly simplified. First, we can write

$$\frac{dU_v}{dt} + \frac{P_v}{J}\frac{dV}{dt} = \frac{dH_v}{dt} - \frac{V}{J}\frac{dP_v}{dt} \tag{C-9}$$

where H_v is the total enthalpy of the vapor. Similarly we can write

$$\left(u_L + \frac{P_L}{\rho_L}\right)\dot{m} = h_L \dot{m} \tag{C-10}$$

We can express $\frac{dH_v}{dt}$ as

$$\frac{dH_v}{dt} = \frac{d(h_v\, m)}{dt} = h_v \dot{m} + m\frac{dh_v}{dt} \tag{C-11}$$

where m is the mass of vapor contained in the bubble. $\dot{m}$ may be written as

$$\dot{m} = \frac{d}{dt}\left(\frac{4}{3}\rho_v \pi R_v^3\right) = 4\pi\rho_v R_v^2 \frac{dR_v}{dt} + \frac{4}{3}\pi R_v^3 \frac{d\rho_v}{dt} \tag{C-12}$$

Now, h_L is the specific enthalpy of the liquid just outside the bubble. If we assume that the temperature of the liquid just outside the bubble is the same as the temperature of the vapor inside the bubble, then we can write

$$h_v - h_L = h_{fg} \tag{C-13}$$

where h_{fg} is the latent heat of vaporization.

Combining Eq. (C-8) through (C-13) we obtain

$$\frac{dQ}{dt} = h_{fg}\, 4\pi \rho_v R_v^2 \frac{dR_v}{dt} + \frac{4\pi R_v^3}{3}\left[h_{fg}\frac{d\rho_v}{dt} + \rho_v \frac{dh_v}{dt} - \frac{1}{J}\frac{dP_v}{dt}\right] \qquad (C\text{-}14)$$

Now we make the important simplifying assumption that the terms within the brackets on the right hand side of Eq. (C-14) are negligible compared to the first terms on the right hand side. With this assumption, we obtain

$$\frac{dQ}{dt} \cong h_{fg}\, 4\pi \rho_v R_v^2 \frac{dR_v}{dt} \qquad (C\text{-}15)$$

which is Eq. (13) in the test.

We can note here that the validity of neglecting the terms in the brackets in Eq. (C-14) can be checked a Posteriori once the solution for bubble growth rate is obtained. This check does not provide absolute assurance that the terms are negligible but at least does provide a check on the self-consistency of the analysis.

Distribution List For Reports
Study of Thermo-Hydraulic Oscillations in Boiling
Systems Employing Liquid Metal Working Fluids
Contract No. NASW-1705
Mechanical Technology Incorporated
968 Albany-Shaker Road
Latham, New York 12110

ADDRESSEE	NUMBER OF COPIES
Jet Propulsion Laboratory 4800 Oak Grove Drive Pasadena, California 91103 Attn: G.M. Kikin, Mail Stop 122-103	1
General Electric Company Knolls Atomic Power Laboratory Schenectady, New York Attn: G. Halsey	1
General Electric Company Knolls Atomic Power Laboratory Schenectady, New York Attn: J. Carr	1
General Electric Company Knolls Atomic Power Laboratory Schenectady, New York Attn: Library	1
General Electric Company Missiles and Space Power Section Cincinnati, Ohio 45215 Attn: M.A. Zipkin	1
General Electric Company Missiles and Space Power Section Cincinnati, Ohio 45215 Attn: J.R. Peterson	2
General Electric Company 175 Courtner Avenue San Jose, California 95125 Attn: S. Levy	2
General Electric Company 175 Courtner Avenue San Jose, California 95125 Attn: F.E. Tippets	1
General Electric Company 175 Courtner Avenue San Jose, California 95125 Attn: K. Cohen, Manager APO	1
General Electric Company 310 DeGuigne Drive Sunnyvale, California 95125 Attn: W.G. Meinhardt	1
AiResearch Manufacturing Company 402 South 36 Street Phoenix, Arizona 85034 Attn: R. Gruntz	1
AiResearch Manufacturing Company 402 South 36 Street Phoenix, Arizona 85034 Attn: Library	2
Geoscience Ltd. 410 South Cedros Avenue Solana Beach, California 92075 Attn: H.F. Poppendiek	2
TRW Systems Group One Space Park Redondo Beach, California 90278 Attn: S.M. Zivi	1
TRW Systems Group One Space Park Redondo Beach, California 90278 Attn: L.G. Neal	1

ADDRESSEE	NUMBER OF COPIES
Aerojet-General Corporation Von Karman Center P.O. Box 296 Azusa, California 91702 Attn: Librarian	2
University of Michigan Department of Chemical and Metallurgical Engineering Ann Arbor, Michigan 48105 Attn: R.E. Balzhieser	2
Massachusetts Institute of Technology Cambridge, Massachusetts 02139 Attn: W.M. Rohsenow	2
New York University Dept. of Mechanical Engineering New York, New York 10003 Attn: N. Zuber	10
New York University Dept. of Mechanical Engineering New York, New York 10003 Attn: Library	2
Department of the Air Force Air Force Aero Propulsion Laboratory Wright-Patterson Air Force Base, Dayton, Ohio 45433 Attn: C.H. Armbruster	1
Department of the Air Force Air Force Aero Propulsion Laboratory Wright-Patterson Air Force Base, Dayton, Ohio 45433 Attn: J.W. Zmurk	1
A. Research Manufacturing Company 9851 Sepulveda Boulevard Los Angeles, California 90009 Attn: F.E. Carroll	2
A. Research Manufacturing Company 9851 Sepulveda Boulevard Los Angeles, California 90009 Attn: P.J. Berenson	1
Columbia University Department of Chemical Engineering New York, New York 10027 Attn: C.F. Bonilla	2
NASA Scientific & Technical Information Facility P.O. Box 33 College Park, Maryland 20740	Reproducible Copy
M.J. SAMES, LIBRARIAN NEW DEPARTURE-HYATT BEARINGS DIV. 2509 HAYES AVE. SANDUSKY, OHIO 44870	
General Electric Company Knolls Atomic Power Laboratory Schenectady, New York 12305 Attn: O. Jones	1
NASA Lewis Research Center 21000 Brookpark Road Cleveland, Ohio 44135 Attn: M. Gutstein Mail Stop 500-201	1

Study of Thermo-Hydraulic Oscillations in Boiling
Systems Employing Liquid Metal Working Fluids
Contract No. NASW-1705
Mechanical Technology Incorporated
968 Albany-Shaker Road
Latham, New York 12110

ADDRESSEE	NUMBER OF COPIES
NASA Headquarters Code RNP Washington, D.C. 20546 Attn: S.V. Manson	2
NASA Headquarters Code RNP Washington, D.C. 20546 Attn: J.J. Lynch	1
NASA Headquarters Code RNP Washington, D.C. 20546 Attn: F. Schulman	1
NASA Lewis Research Center 21000 Brookpark Road Cleveland, Ohio 44135 Attn: B. Lubarsky, Mail Stop 9200	1
NASA Lewis Research Center 21000 Brookpark Road Cleveland, Ohio 44135 Attn: R.E. English, Mail Stop 9200	1
NASA Lewis Research Center 21000 Brookpark Road Cleveland, Ohio 44135 Attn: T.A. Moss, Mail Stop 9220	1
NASA Lewis Research Center 21000 Brookpark Road Cleveland, Ohio 44135 Attn: R.N. Weltmann, Mail Stop 9232	2
U.S. Atomic Energy Commission Washington, D.C. 20545 Attn: N. Grossman, Code DRD&T	1
U.S. Atomic Energy Commission Washington, D.C. 20545 Attn: C. Johnson, Code SNS	1
U.S. Atomic Energy Commission Washington, D.C. 20545 Attn: G. Leighton, Code SNS	1
U.S. Atomic Energy Commission Washington, D.C. 20545 Attn: R. Scroggins, Code DRD&T	1
U.S. Atomic Energy Commission Washington, D.C. 20545 Attn: S. Salewitz, Code SNPO	1
Brookhaven National Laboratory Upton, New York 11973 Attn: D.H. Gurinsky	1
Brookhaven National Laboratory Upton, New York 11973 Attn: O.E. Dwyer	1
Brookhaven National Laboratory Upton, New York 11973 Attn: J.C. Chen	1
Brookhaven National Laboratory Upton, New York 11973 Attn: L.M. Shotkin	1

ADDRESSEE	NUMBER OF COPIES
NASA Lewis Research Center 21000 Brookpark Road Cleveland, Ohio 44135 Attn: U.H. Von Glahn, Mail Stop 2120	1
NASA Lewis Research Center 21000 Brookpark Road Cleveland, Ohio 44135 Attn: R.G. Dorsch, Mail Stop 2123	4
NASA Lewis Research Center 21000 Brookpark Road Cleveland, Ohio 44135 Attn: J.P. Lewis, Mail Stop 2121	1
NASA Lewis Research Center 21000 Brookpark Road Cleveland, Ohio 44135 Attn: R.W. Graham, Mail Stop 2142	1
NASA Lewis Research Center 21000 Brookpark Road Cleveland, Ohio 44135 Attn: Y. Hsu, Mail Stop 2142	1
NASA Lewis Research Center 21000 Brookpark Road Cleveland, Ohio 44135 Attn: V.H. Gray, Mail Stop 2121	1
Argonne National Laboratory Argonne, Illinois 60439 Attn: Library Services, Department 203-CE125 Report Section	3
Oak Ridge National Laboratory Oak Ridge, Tennessee 37830 Attn: A.P. Fraas	1
Oak Ridge National Laboratory Oak Ridge, Tennessee 37830 Attn: W.H. Hoffman	1
Oak Ridge National Laboratory Oak Ridge, Tennessee 37830 Attn: Library	1
Los Alamos Scientific Laboratory Los Alamos, New Mexico 87544 Attn: R.S. Thurston	2
Los Alamos Scientific Laboratory Los Alamos, New Mexico 87544 Attn: Library	1
Jet Propulsion Laboratory 4800 Oak Grove Drive Pasadena, California 91103 Attn: D.R. Bartz, Section 383	1
Jet Propulsion Laboratory 4800 Oak Grove Drive Pasadena, California 91103 Attn: J.P. Davis, Section 383	1